# NASA TECHNICAL MEMORANDUM

NASA TM X-73,164

NASA TM X-73,164

WIND-TUNNEL INVESTIGATION OF A LARGE-SCALE MODEL OF A LIFT/CRUISE FAN V/STOL AIRCRAFT WITH EXTENDED LIFT/CRUISE NACELLES

Bruno J. Gambucci, Kiyoshi Aoyagi, and L. Stewart Rolls

Ames Research Center
Moffett Field, California 94035

August 1976

1. Report No. NASA TM X-73,164	2. Government Accession No.	3. Recipient's Catalog No.
4. Title and Subtitle WIND-TUNNEL INVESTIGATION OF A LARGE-SCALE MODEL OF A LIFT/CRUISE FAN V/STOL AIRCRAFT WITH EXTENDED LIFT/CRUISE NACELLES		5. Report Date
		6. Performing Organization Code
7. Author(s) Bruno J. Gambucci, Kiyoshi Aoyagi, and L. Stewart Rolls		8. Performing Organization Report No A-6727
		10. Work Unit No. 505-10-35
9. Performing Organization Name and Address Ames Research Center Moffett Field, California 94035		11. Contract or Grant No.
		13. Type of Report and Period Covered Technical Memorandum
12. Sponsoring Agency Name and Address National Aeronautics and Space Administration Washington, D. C. 20546		14. Sponsoring Agency Code

15. Supplementary Notes

16. Abstract

An investigation was conducted in the Ames 40- by 80-Foot Wind Tunnel to determine the aerodynamic characteristics of a large-scale model of a lift/cruise fan V/STOL aircraft. The model was equipped with three fans, one mounted in the forward section of the fuselage in a lift mode, and two mounted on top of the wing adjacent to the fuselage in a lift/cruise mode.

The data that were obtained include longitudinal and lateral-directional characteristics of the model, with the horizontal tail on and off, for both the powered-lift and cruise configurations. Lateral-directional characteristics were obtained with the horizontal and vertical tail sections removed. Powered-lift data were obtained at several wind-tunnel velocities and at several lift/cruise fan thrust vector angles by varying the position of the hooded deflectors from 0° (the cruise condition) to 90°.

17. Key Words (Suggested by Author(s)) Lift/cruise fan V/STOL Powered lift	18. Distribution Statement Unlimited STAR Category - 02		
19. Security Classif. (of this report) Unclassified	20. Security Classif. (of this page) Unclassified	21. No. of Pages 95	22. Price* $4.75

*For sale by the National Technical Information Service, Springfield, Virginia 22161

b wing span, m (ft)

C_D drag coefficient about the wind axis, $\dfrac{D}{qS}$

$C_{D_{ram}}$ ram drag coefficient about the body axis, $\dfrac{WV_o}{gqS}$

C_ℓ rolling-moment coefficient about the stability axis, $\dfrac{\ell}{qSb}$

C_L lift coefficient about the wind axis, $\dfrac{L}{qS}$

C_m pitching-moment coefficient about the stability axis at $0.25\bar{c}$, $\dfrac{m}{qS\bar{c}}$

C_n yawing-moment coefficient about the stability axis, $\dfrac{n}{qSb}$

C_y side-force coefficient about the stability axis, $\dfrac{y}{qS}$

c wing-chord parallel to the plane of symmetry, m (ft)

$\bar{c}$ mean aerodynamic chord, $\dfrac{2}{S}\displaystyle\int_o^{b/2} c^2\, dy$, m (ft)

D drag, N (lb)

F_A static axial force, N (lb)

F_g gross thrust with $\delta_{cn} = 0°$, N (lb)

F_N static normal force, N (lb)

g acceleration of gravity, 9.81 m/sec^2 (32.2 ft/sec^2)

i_t horizontal tail incidence angle, deg

L total lift on the model, N (lb)

ℓ rolling moment, N·m (ft-lb)

m pitching moment, N·m (ft-lb)

n yawing moment, N·m (ft-lb)

P_o standard absolute pressure, 101352.9 N/m^2 (14.7 psi)

P_s free-stream static pressure, N/m^2 (lb/ft^2)

q	free-stream dynamic pressure, N/m^2 (lb/ft^2)
$rpm/\sqrt{\theta}$	corrected fan rotational speed
S	wing area, m^2 (ft^2)
T	fan thrust with forward speed, N (lb)
T_S	fan static thrust, N (lb)
V_o	free-stream velocity, m/sec (ft/sec)
V_j	fan exit velocity, m/sec (ft/sec)
W	fan inlet weight rate of flow, kg/sec (lb/sec)
X	chordwise distance from wing leading edge, %c
y	side force, N (lb)
Y_L	lower surface distance from wing chord plane, %c
Y_U	upper surface distance from wing chord plane, %c
α	angle of attack, deg
β	angle of sideslip, deg
β_v	lift fan exit louver deflection angle, deg
δ	relative static pressure, $\dfrac{P_s}{P_o}$
δ_{ail}	aileron deflection, deg
δ_{cn}	lift/cruise fan exhaust duct geometric angle, deg
δ_f	trailing-edge flap deflection, deg
δ_j	fan exhaust flow static turning angle, $\tan^{-1}\left(\dfrac{F_N}{F_A}\right)$, deg
δ_R	rudder deflection, deg
η	percent of wing semispan or static turning efficiency, $\dfrac{\sqrt{F_N^2 + F_A^2}}{F_g}$
θ	ratio of ambient temperature to standard temperature (519° R)
θ_j	lift/cruise fan exhaust flow static turning angle, deg

Subscripts

ail   aileron

j   fan exit

R   rudder

S   static conditions

u   uncorrected data

WIND-TUNNEL INVESTIGATION OF A LARGE-SCALE MODEL OF A LIFT/CRUISE

FAN V/STOL AIRCRAFT WITH EXTENDED LIFT/CRUISE NACELLES

Bruno J. Gambucci, Kiyoshi Aoyagi, and L. Stewart Rolls

Ames Research Center

SUMMARY

An investigation was conducted in the Ames 40- by 80-Foot Wind Tunnel to determine the aerodynamic characteristics of a large-scale model of a lift/cruise fan V/STOL aircraft. The model was equipped with three fans, one mounted in the forward section of the fuselane in a lift mode, and two mounted on top of a wing adjacent to the fuselage in a lift/cruise mode.

The data that were obtained include longitudinal and lateral-directional characteristics of the model, with the horizontal tail on and off, for both the powered-lift and cruise configurations. Lateral-directional characteristics were obtained with the horizontal and vertical tail sections removed. Powered-lift data were obtained at several wind-tunnel velocities and at several lift/cruise fan thrust vector angles by varying the position of the hooded deflectors from 0° (the cruise condition) to 90°.

INTRODUCTION

The NASA/Navy Lift/Cruise Fan Aircraft Technology Program is a cooperative effort between NASA and the Navy; its purpose is to establish a firm technology base for the design of lift/cruise fan V/STOL multimission aircraft for both military and civilian applications. The program may include the design, fabrication, and flight test of a research and technology aircraft that uses a lift/cruise fan propulsion system. Currently underway are design studies (refs. 1 and 2), wind-tunnel tests of small- and large-scale models (ref. 3), and systems evaluation tests and simulation to develop the base required for the design of a research and technology aircraft. This report contains the results of a large-scale wind-tunnel test of a lift/cruise fan aircraft model typical of one of several configurations being investigated as candidate configurations for a research and technology aircraft. The tests were conducted in the Ames Research Center 40- by 80-Foot Wind Tunnel.

The large-scale lift/cruise fan V/STOL model used in this test was a modification of a model used in the test reported in reference 3. The model lift/cruise nacelles of the previous tests were modified tc simulate the length requirement for a typical lift/cruise mechanical drive propulsion system. The model was powered by three lift fans, each of which was driven by a gas generator. Data were obtained for two modes of operation, powered lift and cruise. For the cruise-mode operation, only the two generators over the wing-mounted

lift/cruise fans were powered; the forward fan was covered. Static tests
planned for the hover mode will be the subject of a separate report.

The longitudinal force and moment characteristics of the model, as well
as its lateral-directional characteristics, are presented for both modes of
operation. Results for powered lift were obtained at a constant fan speed
over a range of wind-tunnel velocities; the cruise configuration were run at
three lift/cruise fan exit velocities and at constant wind-tunnel speed. In
the interest of an expedient release of the accumulated data, the test data
are not analyzed here; their analyses will be the subject of future reports.

MODEL DESCRIPTION

Photographs of the model mounted in the Ames 40- by 80-Foot Wind Tunnel
are shown in figure 1. Geometric details and pertinent dimensions are
presented in figure 2. The model was equipped with adjustable flaps, ailerons,
horizontal stabilizer, and rudder. The horizontal and vertical tail sections
are removable. The ailerons and horizontal tail were remotely controlled.

Lift/Cruise Fan Nacelles

The lift/cruise fan nacelles of the model described in : ference 3 were
extended forward to simulate a lift/cruise fan mechanical drive propulsion
system (i.e., the gas generator mounted in line and directly aft of the fan,
thus necessitating a long nacelle). A cross-sectional view of the nacelle is
shown in figure 2(c). For expediency, the lift/cruise fan gas generator
inlets were not altered when the fan nacelles were extended (see fig. 2(a) and
fig. 3). The nacelles were extended approximately 1.25 m (4.2 ft) for the
test reported herein.

Wing

The wing aspect ratio was 4.5, the taper ratio was 0.30, and '- sweep
along the quarter chord line was 25°. An NACA 4416 airfoil sect   s the
basic wing section at the exposed root. This became a modified   ritical
airfoil with wing station (0.442η) and tip having a thickness-to-c   . ratio
of 0.14 and 0.08, respectively. The wing incidence was 3.23° at r   exposed
root and -2.77° at the theoretical tip; this resulted in a wing twist of 6°.
Wing airfoil ordinates are presented in table 1.

Flaps and Ailerons

The wing control surfaces consisted of plain flaps and ailerons, both
hinged at the wing 75 percent chord line and with a constant percent chord
radius. A typical cross section of the control surfaces is shown in fig-
ure 2(d). Although the flaps and ailerons had a built-in seal, the gap

2

betwern them and the shroud was taped for all runs except the aileron sweeps which required remote aileron operation. The flaps could be set at discrete deflection positions, but for this investigation, the only deflection used was 15°. The ailerons had a deflection range of ±25°.

Empennage

The horizontal tail was an NACA 64A0 series airfoil section with a thickness-to-chord ratio at the root of 0.10 and of 0.08 at the tip. The all-movable horizontal tail could be remotely actuated and had an incidence range of ±20°.

The vertical tail had an NACA 65A010 airfoil section and was equipped with a movable rudder. For most tail-off tests, only the horizontal tail was removed. A limited amount of testing was conducted with both the horizontal and vertical sections removed.

Propulsion System

The model was equipped with three 36-in. diam. General Electric X-376 turbo-tip fans with a design pressure ratio of 1.1. As shown in figure 2(a), one lift fan was mounted in the forward fuselage section with the thrust axis tilted 15° forward with respect to the horizontal plane. Two lift/cruise fans were mounted in nacelles on the upper surface of the wing adjacent to the fuselage. Each of these fans was powered by a modified T58-8B gas generator. The relationship between the fans and gas generators is shown by the schematic in figure 3.

Thrust vectoring of the forward fan was obtained by a cascade of 14 0.102-m (0.333 ft) chord plain louvers that were mounted at the duct exit as shown in figure 2(b). These louvers were remotely operated and varied from 103° to complete closure (0°). Two yaw vectoring vanes were located below the louvers and 0.235 m (0.771 ft) symmetrically off the model centerline. The vanes had a chord of 0.298 m (0.978 ft) and could be deflected ±20°. For the cruise configuration ($\delta_{cn} = 0°$), the inlet and the exit of the forward lift fan were covered for most cases with the exit louvers and yaw vanes removed.

Thrust vectoring of the lift/cruise fans was obtained by using the same hooded deflectors and cruise nozzle (0°) of reference 4. Geometric angles of 90°, 71°, 56°, and 38° were obtained by removing or adding circular sections as shown in figure 2(c). Two yaw vectoring vanes were located at the hooded deflector exit and could be deflected ±20° as shown in figure 2(b). The nozzle geometric area of the hooded deflector was 0.7678 m^2 (1190 in.^{2}). When the cruise nozzle was used, the nozzle geometric area was 0.6937 m^2 (1075 in.^{2}).

For the cruise configuration, the nozzle with the 0° geometric angle was used. This nozzle configuration was used without the yaw vanes.

3

TESTS AND PROCEDURE

Longitudinal force and moment data were obtained at discrete lift/cruise fan exit nozzle deflections for model angle of attack and wind-tunnel speed ranges with the horizontal tail on and off. Lateral-directional data were obtained for a range of sideslip angles at model angles of attack of $0°$, $8°$, and $16°$. A summary of the principal test variables for the powered-lift configuration is presented as follows:

q	67.032 to 952.817 N/m^2 (1.4 to 19.9 psf)
δ_{cn}	$90°$ to $38°$
α_u	$-4°$ to $24°$
β	$-12°$ to $4°$
i_t	$-10°$ to $20°$
Fan rpm/$\sqrt{\theta}$	3600 (nominal)

Similar data were obtained for the cruise configuration. A summary of the variables for this mode of operation is presented below:

q	1699.749 N/m^2 (35.5 psf)
δ_{cn}	$0°$
α_u	$-4°$ to $32°$
β	$-12°$ to $4°$
i_t	$-10°$ to $20°$
Fan rpm/$\sqrt{\theta}$	2700 to 1600 (nominal)

When either the angle of attack or angle of sideslip was varied in the data acquisition process, the fan rpm, wind-tunnel dynamic pressure, flap deflection, and fan exit nozzle deflection were held constant. In the cruise configuration, data were obtained with the forward fan inlet and exit covered. All the data were obtained with the nose gear extended.

CORRECTIONS

Force and moment data with the lift fans windmilling (power off) were corrected for wind-tunnel wall constraints in the following manner:

$$\alpha = \alpha_u + 0.410 C_{L_u}$$

$$C_D = C_{D_u} + 0.0071(C_{L_u})^2$$

$$C_m = C_{m_u} + 0.0112 C_{L_u} \quad \text{(only with the horizontal tail on)}$$

4

None of the power-on data (i.e., lift fans driven by the gas generators) was corrected for wind-tunnel wall constraints. Corrections have not been applied for the effects of the exposed tips on the model support struts or for ram drag.

PRESENTATION OF DATA

Static fan performance (i.e., at wind-tunnel free-stream dynamic pressure of zero q = 0 psf) for the lift/cruise and forward fans is presented in figures 4 through 6. Lift/cruise fan deflector static turning and turning efficiency are presented in figure 7. In figure 8, the variation of jet velocity ratio with wind-tunnel velocity is presented for the three fans. The variation of jet velocity ratio with the angle of attack and fan rpm for the cruise configuration is presented in figure 9. Windmilling characteristics of the lift/cruise fans at various thrust vector angles and for the forward lift fan are presented in figure 10. The variation of fan thrust at forward speed to static fan thrust ratio with angle of attack at several jet velocity ratios is presented in figure 11. Variation of ram drag coefficient with angle of attack at several jet velocity ratios for each fan (three fans) is presented in figure 12. The variation of lift, drag, and pitching moment coefficients with jet velocity ratio of 0° angle of attack are presented in figure 13 for three fan and lift/cruise fan operations.

An index to all the figures presenting the basic aerodynamic data is given in table 2. For ease of presentation, the aerodynamic data have been divided into two parts: namely, powered lift and cruise. The longitudinal aerodynamic characteristics of the model in the powered-lift mode, with the horizontal tail on and off the model, are presented in figures 14 and 15. The aerodynamic characteristics of the model with the rudder deflected 23° are presented in figure 16. The effect of differential aileron deflection on the model longitudinal and lateral characteristics is presented in figure 17. The lateral-directional characteristics of the model with sideslip are presented in figure 18 with the horizontal tail off and in figure 19 with the horizontal and vertical tails off. Horizontal tail sweep effects on the model longitudinal aerodynamic characteristics are presented in figures 20, 21, 22, and 23. Other data, such as the effect of total differential aileron deflection and lift/cruise fan exit nozzles with the forward fan covered and its exit louvers closed ($\beta_v = 0°$), are presented in figures 24 and 25.

Longitudinal characteristics for the cruise with the horizontal tail on and off are presented in figures 26 and 27. Also presented are the model longitudinal and lateral characteristics with a sideslip of 8° in figure 28. Cruise-mode model longitudinal characteristics with the flaps and ailerons deflected are presented in figure 29. The variation of side force, yawing-moment, and rolling-moment coefficients with sideslip are presented in figure 30.

5

REFERENCES

1. Design Definition Study of a Lift/Cruise Fan Technology V/STOL Aircraft-Vol. I. NASA CR-137678, 1975.

2. Zabinsky, J. M.; and Higgins, H. C.: Design Definition Study of a Lift/Cruise Fan Technology V/STOL Airplane — Summary. NASA CR-137749, 1975.

3. Gambucci, Bruno J.; Aoyagi, Kiyoshi; and Rolls, L. Stewart: Wind Tunnel Investigation of a Large-Scale Model of a Lift/Cruise Fan V/STOL Aircraft. NASA TM X-73,139, 1976.

4. Atencio, Adolph, Jr.; Hall, Leo P.; and Kirk, Jerry V.: Low Speed Wind Tunnel Investigation of a Large-Scale Lift Fan STOL Transport Model. NASA TM X-62,231, 1973.

TABLE 1 - LARGE SCALE LIFT/CRUISE FAN AIRCRAFT MODEL AIRFOIL ORDINATES

STATION	EXPOSED ROOT (0.221η) NACA 4416		WING STATION (0.442η) MODIFIED, SUPERCRITICAL, t = 14%c		THEORETICAL TIP (0.941η) MODIFIED, SUPERCRITICAL, t = 8%c	
X, %c	Y_U, %c	Y_L, %c	Y_U, %c	Y_L, %c	Y_U, %c	Y_L, %c
0	0	0	0	0	0	0
1.25	3.275	-1.909	2.471	-2.467	1.422	-1.435
2.5	4.448	-2.645	3.233	-3.218	1.836	-1.840
5.0	6.123	-3.486	4.126	-4.069	2.307	-2.334
7.5	7.371	-3.957	4.729	-4.653	2.641	-2.678
10.0	8.363	-4.245	5.208	-5.099	2.902	-2.944
15.0	9.888	-4.459	5.945	-5.756	3.293	-3.335
20.0	10.933	-4.427	6.481	-6.177	3.569	-3.598
25.0	11.648	-4.245	6.876	-6.433	3.768	-3.766
30.0	12.000	-4.000	7.165	-6.560	3.904	-3.682
40.0	12.000	-3.467	7.478	-6.435	4.029	-3.837
50.0	11.232	-2.901	7.494	-5.753	3.988	-3.531
60.0	9.920	-2.283	7.229	-4.503	3.788	-2.766
70.0	8.139	-1.653	6.662	-2.786	3.420	-1.465
80.0	5.920	-1.099	5.685	-1.091	2.829	-0.084
90.0	3.285	-0.608	3.980	-0.194	1.843	+0.496
95.0	1.781	-0.384	2.616	-0.210	1.090	+0.42
100.0	0.171	-0.171	0.496	-0.447	0.108	-0.214
L.E. RADIUS, % c	2.822		3.041		1.154	
CHORD LENGTH, m (ft)	2.409 (8.231)		2.049 (6.723)		0.891 (2.922)	
INCIDENCE, deg	3.23		2.49		-2.77	

7

TABLE 2 - LIST OF BASIC DATA FIGURES

Run No.	Figure	q		α_u, deg	δ_f, deg	δ_{ail}, deg	δ_{cn}, deg	β_v, deg	i_t, deg	δ_R, deg	β, deg	Fan RPM/$\sqrt{\theta}$		Remarks
		psf	N/m²									Fwd. Fan	Wing Fans	
4	14(a)	3.23	154.7	-4 to 20	15	10	90	90	0	0	0	3600	3600	Longitudinal data
5		7.09	339.5									3602	3602	
7		7.13	341.4									Windmilling	Windmilling	
3	14(b)	1.28	61.3									3590	3590	
36	14(c)	3.21	153.7				71	55				3619	3619	
37		7.05	337.6									3612	3612	
39		7.04	337.1									Windmilling	Windmilling	
35	14(d)	1.27	60.8									3609	3609	
24	14(e)	3.15	150.8				56	43				3595	3595	
25		6.94	332.3									3606	3606	
22		12.12	580.3									3598	3598	
27		12.12	580.3									Windmilling	Windmilling	
47	14(f)	7.12	340.9				38					3601	3601	
48		12.33	590.4									3612	3612	
49		19.39	923.6									3615	3615	
51		19.20	919.3									Windmilling	Windmilling	
101	15(a)	3.39	162.3	-4 to 16			90	90	OFF			3620	3620	Horizontal tail off
102		7.13	341.4									3614	3614	
103		7.24	346.7									Windmilling	Windmilling	
100	15(b)	1.35	64.6									3604	3604	
104	15(c)	3.32	159.0	-4 to 20			56	43				3606	3606	
105		7.09	339.5									3616	3616	
106		12.30	588.9									3619	3619	
107		12.30	588.9									Windmilling	Windmilling	
63	16(a)	7.22	345.7	0 to 24			38		0	23		3607	3607	Longitudinal data
64		12.31	589.4									3619	3619	
65		19.25	921.7	0 to 16								3609	3609	
66		19.24	921.2	0 to 24								Windmilling	Windmilling	

8

TABLE 2 - LIST OF BASIC DATA FIGURES -- CONTINUED

Run No.	Figure	q psf	q N/m²	α_u, deg	δ_f, deg	δ_{ail}, deg	δ_{cn}, deg	β_v, deg	i_t, deg	δ_R, deg	β, deg	Fan RPM/$\sqrt{\theta}$ Fwd. Fan	Fan RPM/$\sqrt{\theta}$ Wing Fans	Remarks
63	16(b)	7.22	345.7	0 to 24	15	10	38	43	0	23	0	3607	3607	Lateral data
64		12.31	589.4									3619	3619	
65		19.25	921.2	0 to 16								3609	3609	
66		19.24	921.2	0 to 24								Windmilling		
60	17(a)	6.96	333.2			−25/25				0		3607	3607	Differential Aileron
62		12.22	585.1									3606	3606	
60	17(b)	6.96	333.2									3607	3607	
62		12.22	585.1									3606	3606	
11	18(a)	1.21	57.9	0		10	90	90			4 to −12	3598	3598	Sideslip
12		3.27	156.6									3602	3602	
13		7.09	339.5									3607	3607	
14		7.14	341.9									Windmilling		
42	18(b)	1.17	56.0				71	55				3611	3611	
33	18(c)	3.25	155.6				56	43				3605	3605	
32		12.19	583.7									3599	3599	
34		12.32	589.9									Windmilling		
52	18(d)	7.30	349.5				38					3604	3604	
53		12.31	589.4									3610	3610	
54		19.26	922.2									3610	3610	
55		19.24	921.2									Windmilling		
108	19	3.22	159.0				56		OFF	OFF		3604	3604	Horizontal and Vertical tail off
109		7.09	339.5									3611	3611	
110		12.30	588.9									3608	3608	
9	20(a)	3.23	154.7				90	90	−10 to 20	0	0	3601	3601	Tail Sweeps
10		7.09	339.5									3610	3610	
8	20(b)	1.32	63.2									3590	3590	
9	20(c)	3.19	152.7	8								3596	3596	
10		6.94	332.3									3611	3611	

TABLE 2 - LIST OF BASIC DATA FIGURES - CONTINUED

Run No.	Figure	q (psf)	q (N/m²)	α_u, deg	δ_f, deg	δ_{ail}, deg	δ_{cn}, deg	β_v, deg	i_t, deg	δ_R, deg	β, deg	Fan RPM/√θ Fwd. Fan	Fan RPM/√θ Wing Fans	Remarks
8	20(d)	1.29	61.8	8	15	10	90	90	-10 to 20	0	0	3589	3589	Tail Sweeps
9 / 10	20(e)	3.14 / 7.02	150.3 / 336.1	16								3596 / 3604	3596 / 3604	
8	20(f)	1.29	61.8									3609	3609	
41	21(a)	3.11 / 6.87	149.0 / 328.9	0			71	55				3609 / 3614	3609 / 3614	
41	21(b)	1.14	54.7									3616	3616	
28 / 29 / 30	22(a)	3.15 / 6.98 / 12.16	150.8 / 334.2 / 582.2				56	43				3595 / 3605 / 3600	3595 / 3605 / 3600	
28 / 29 / 30	22(b)	3.14 / 7.00 / 12.15	150.3 / 335.2 / 581.7	8								3601 / 3605 / 3606	3601 / 3605 / 3606	
28 / 29 / 30	22(c)	3.13 / 6.93 / 12.08	149.9 / 331.8 / 578.4	16								3598 / 3602 / 3606	3598 / 3602 / 3606	
58 / 59 / 50	23	7.12 / 12.32 / 19.28	340.9 / 589.9 / 923.1	0			38					3598 / 3600 / 3620	3598 / 3600 / 3620	
60 / 62	24(a)	6.96 / 12.22	333.2 / 585.1			25,/-25 co -25/25			0			3607 / 3606	3607 / 3606	Differential Aileron
60 / 62	24(b)	6.96 / 12.22	333.2 / 585.1									3607 / 3606	3607 / 3606	
19 / 43 / 45	25(a)	3.26 / 3.01 / 7.18	156.1 / 144.1 / 343.8	-4 to 20		10	56 / 7i / 38	0				Inlet Covered	3610 / 3619 / 3623	Forward Fan Inlet Covered Variable δ_{cn}
16	25(b)	1.32	63.0				90						3599	

10

TABLE 2 - LIST OF BASIC DATA FIGURES - CONCLUDED

Run No.	Figure	q		α_u, deg	δ_f, deg	δ_{ail}, deg	δ_{cn}, deg	β_v, deg	i_t, deg	δ_R, deg	β, deg	Fan RPM/$\sqrt{\theta}$		Remarks
		psf	N/m²									Fwd. Fan	Wing Fans	
80	26(a)	34.22	1638.5	0 to 32	0	0	0	Removed	-20	0	0	Covered	2717	Cruise Mode
83		↓	↓	↓					-10				↓	Forward Fan Inlet
77				-4 to 32					0					and Exit Covered
87				0 to 32					10					
81	26(b)	34.21	1638.0	↓					-20				2158	
85									-10				↓	
78		↓	↓	-4 to 32					0					
88				0 to 32					10					
84	26(c)	34.18	1636.5						-20				1599	
86									-10				↓	
79		↓	↓	-4 to 32					0					
89				0 to 32					10					
97	27	34.21	1638.0	-4 to 32				OFF					2709	Horizontal tail off
99		↓	↓	↓				↓					2157	
98													1592	
95	28(a)	34.23	1638.9	4 to 32					0		8		2713	Sideslip
														Forward Fan Inlet
														and Exit Covered
95	28(b)	↓	↓	↓	↓	↓		↓			↓		↓	
70	29	34.24	1639.5	-4 to 32	15	-		0			0		2695	Forward Fan Inlet
71		↓	↓	-4 to 20				↓			↓		1591	Covered
90	30(a)	34.26	1640.4	0	0	0		Removed			4 to -12		2712	Sideslip
91				8									↓	Forward Fan Inlet
93		↓	↓	16										and Exit Covered
90	30(b)	34.19	1637.0	0	0	0							1615	
92		34.09	1632.2	8										
94		34.18	1636.5	16	↓	↓	↓	↓	↓	↓	↓	↓	↓	

11

(a) Three-quarters front view.

Figure 1.- Photograph of the model mounted in the A 40- by 80-Foot
Wind Tunnel.
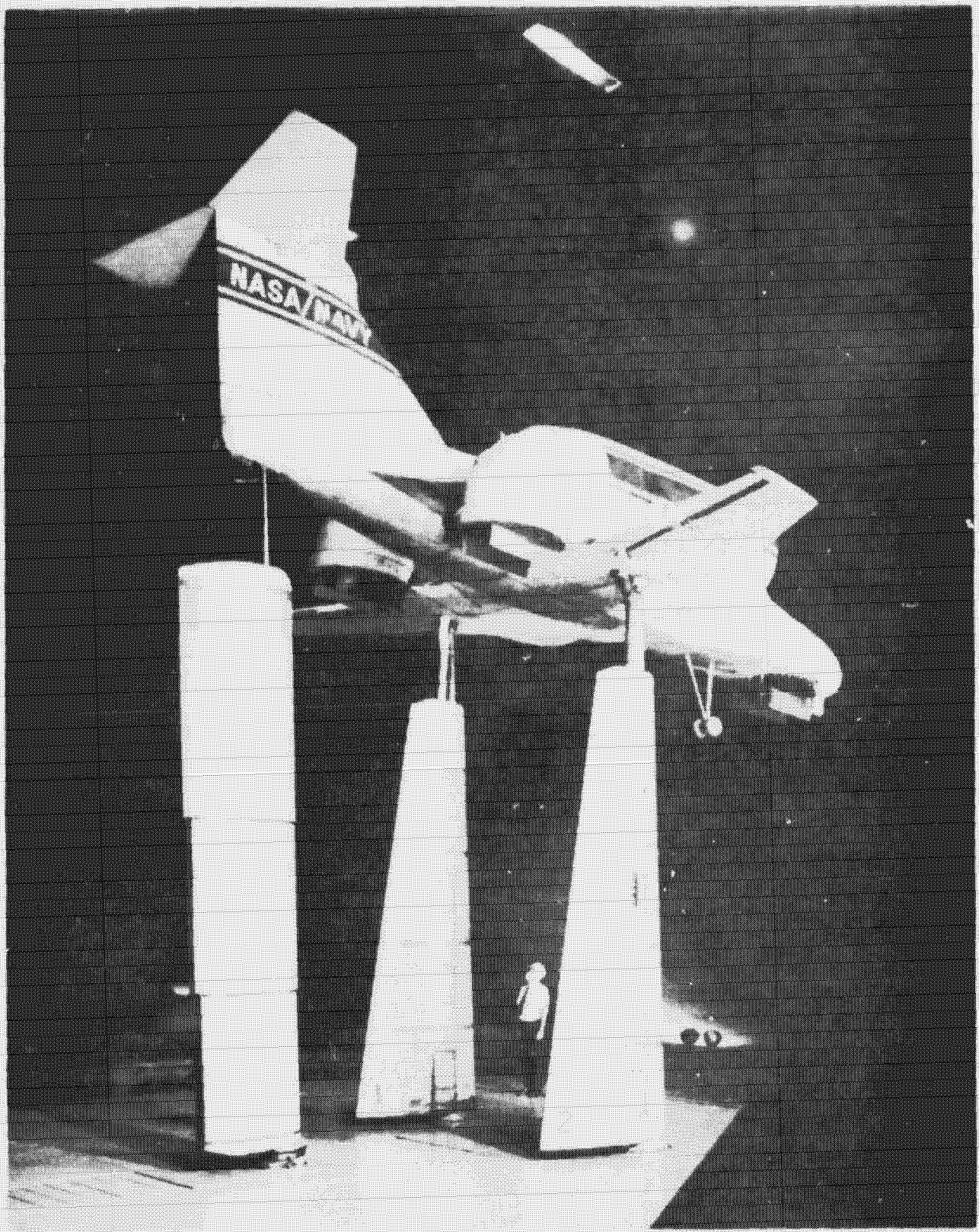
(b) Three-quarters rear view.

Figure 1.- Concluded.

13

14

	WING	HORIZONTAL TAIL	VERTICAL TAIL
AREA, m^2 (FT^2)	16.572 (180.32)	4.006 (43.12)	3.096 (33.32)
ASPECT RATIO	4.500	3.665	0.688
TAPER RATIO	0.300	0.405	0.433
b, m (FT.)	8.682 (28.49)	3.832 (12.57)	1.459 (4.787)
c_{root}, m (FT.)	2.968 (9.738)	1.488 (4.882)	2.96 (5.711)
c_{tip}, m (FT.)	0.890 (2.920)	0.603 (1.987)	1.282 (4.206)
$\bar{c}$ m (FT.)	2.116 (6.942)	1.108 (3.635)	2.232 (7.323)
Λ'— c/4	25.00°	25.2°	45.50°

5.25 (17.22)

0.84 (2.75)

1.92 (6.30)

$\frac{c}{4}$

$\bar{c}$

$\frac{c}{4}$

0.82 (2.69)

1.77 (5.82)

4.07 (13.36)

2.94 9.63

NOTE: ALL DIMENSIONS IN METERS (FEET) EXCEPT AS NOTED

1.30 (4.27)

4.34 (14.25)

0.26 (0.84)

15°

7°

10°

3.41 (11.20)

$\bar{c}$

0.50 (1.64)

2.28 (7.49)

9.76 (32.03)

FUSELAGE 0 STATION (0)

1.25 (4.10)

4.16 (13.61)

10.31 (33.83)
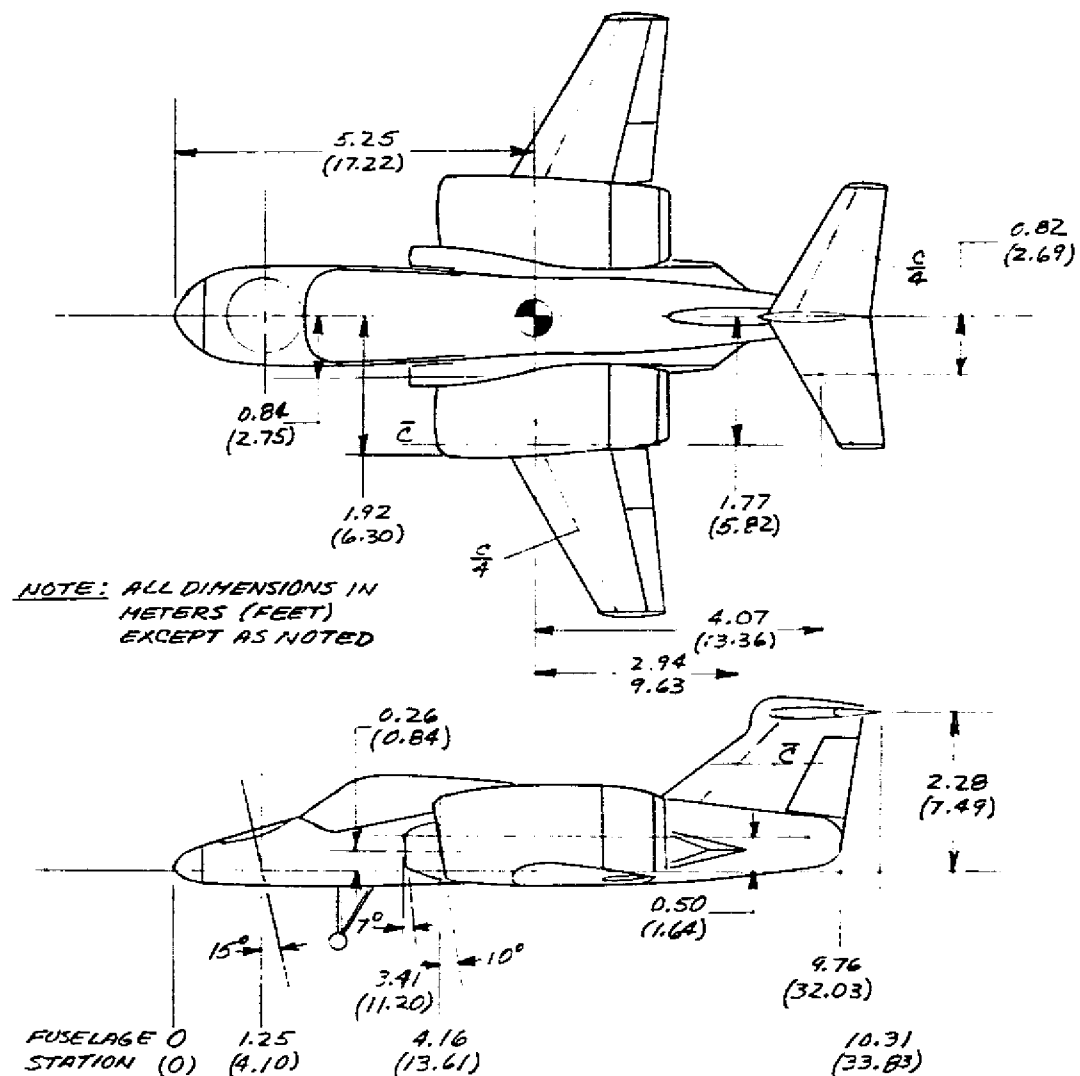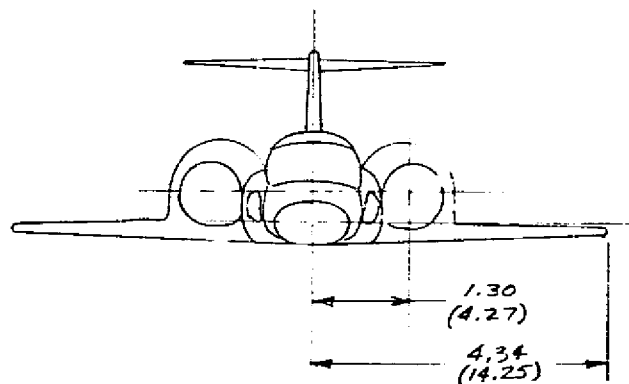
(a) Overall dimensions and geometry

Figure 2.— Geometric details of the model.

0.5715 (1.875)R

0.656R (2.15)R

15°

X 376 FAN

LOUVERS

YAW VANE
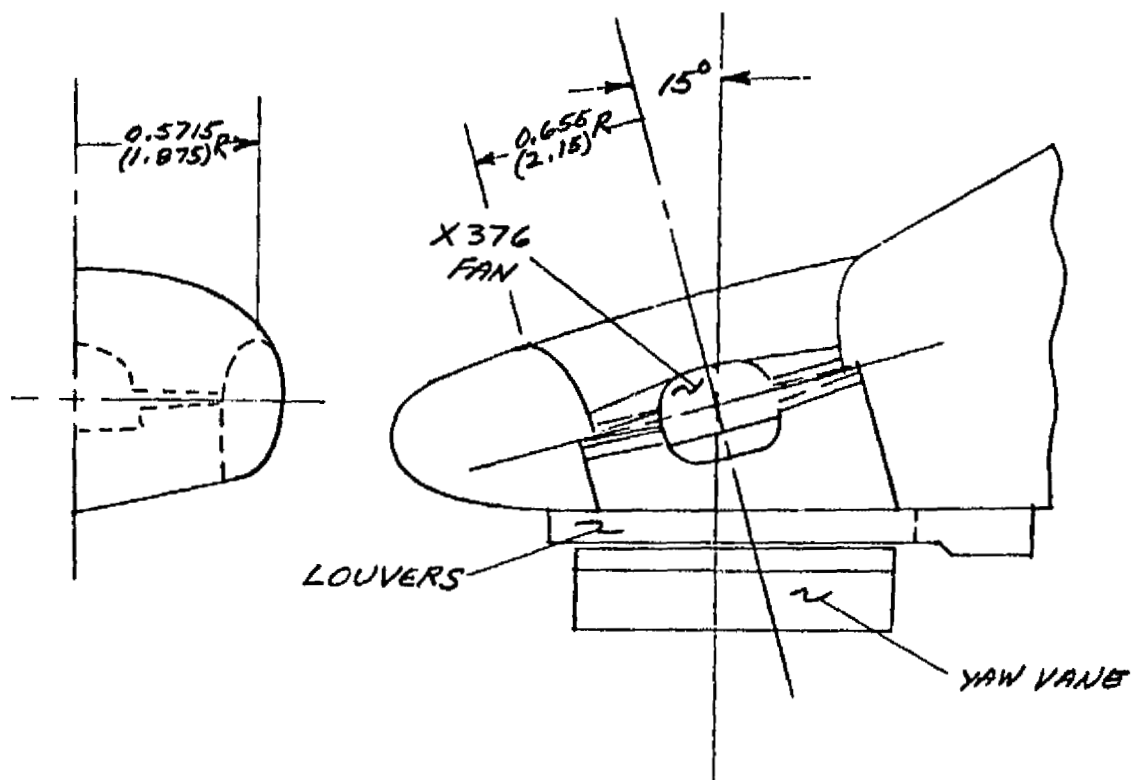
DIMENSIONS IN METERS (FEET) EXCEPT AS NOTED

(b) Forward fan details.

Figure 2.- Continued.

15
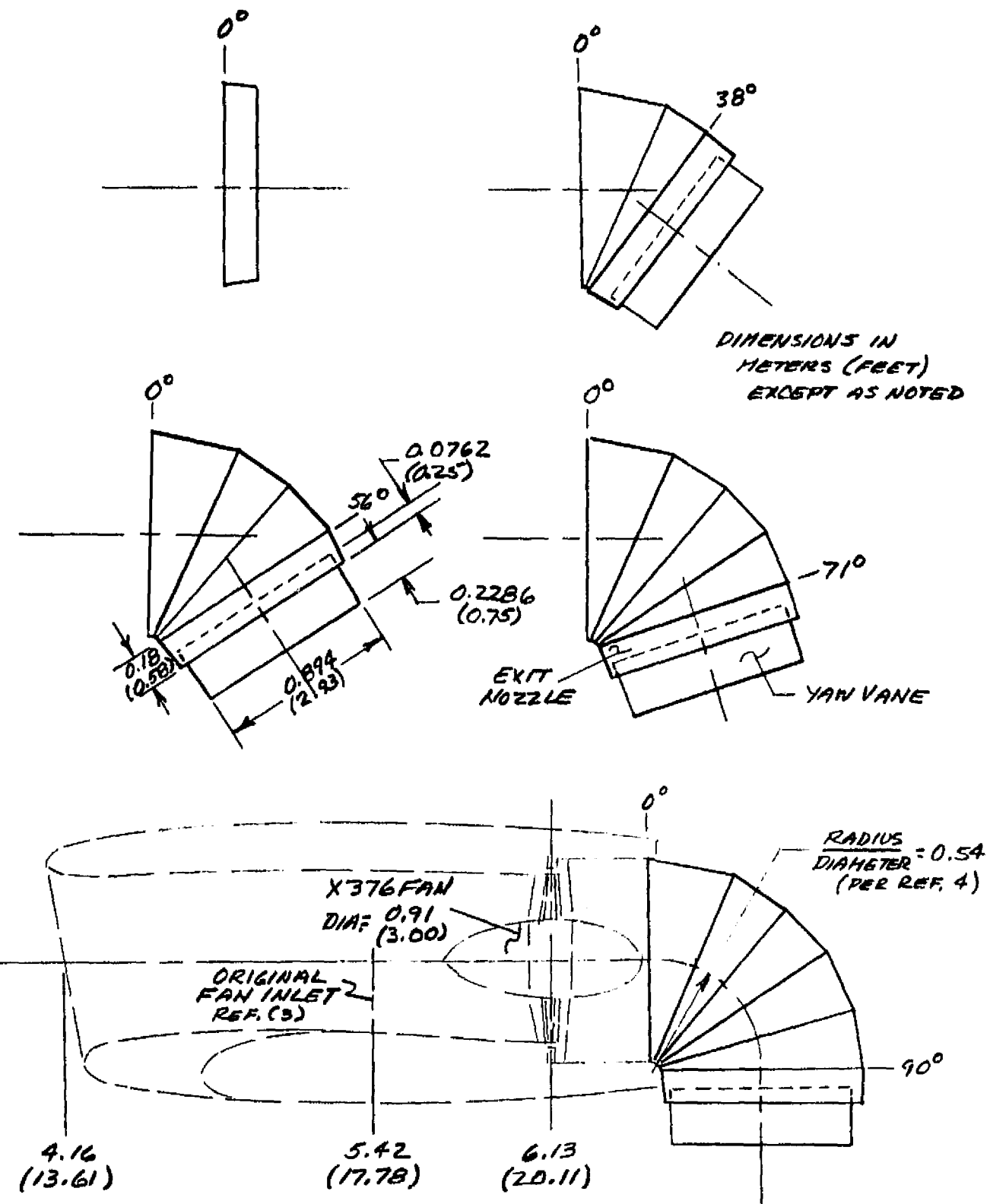
(c) Lift/cruise fan details.

Figure 2.- Continued.

16

NOTE: NOT TO SCALE.
FLAP AND AILERON ORDINATES
IN TABLE I.
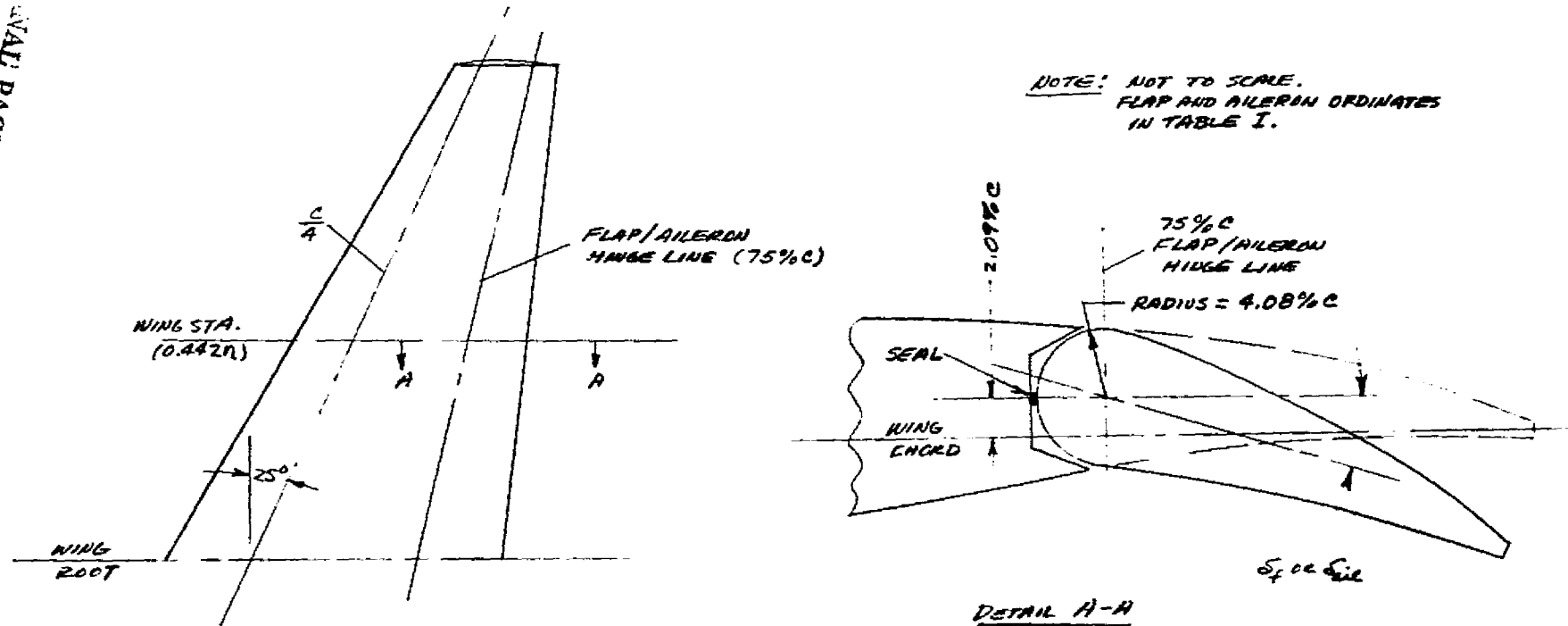
(d) Details of a typical plain flap/aileron section.

Figure 2.- Concluded.

L/C FAN INLET

T58 GAS GENERATOR

LIFT FAN INLET

LIFT FAN VECTORING LOUVERS

AUXILIARY INLET FOR THIRD ENGINE

L/C VECTORING NOZZLE
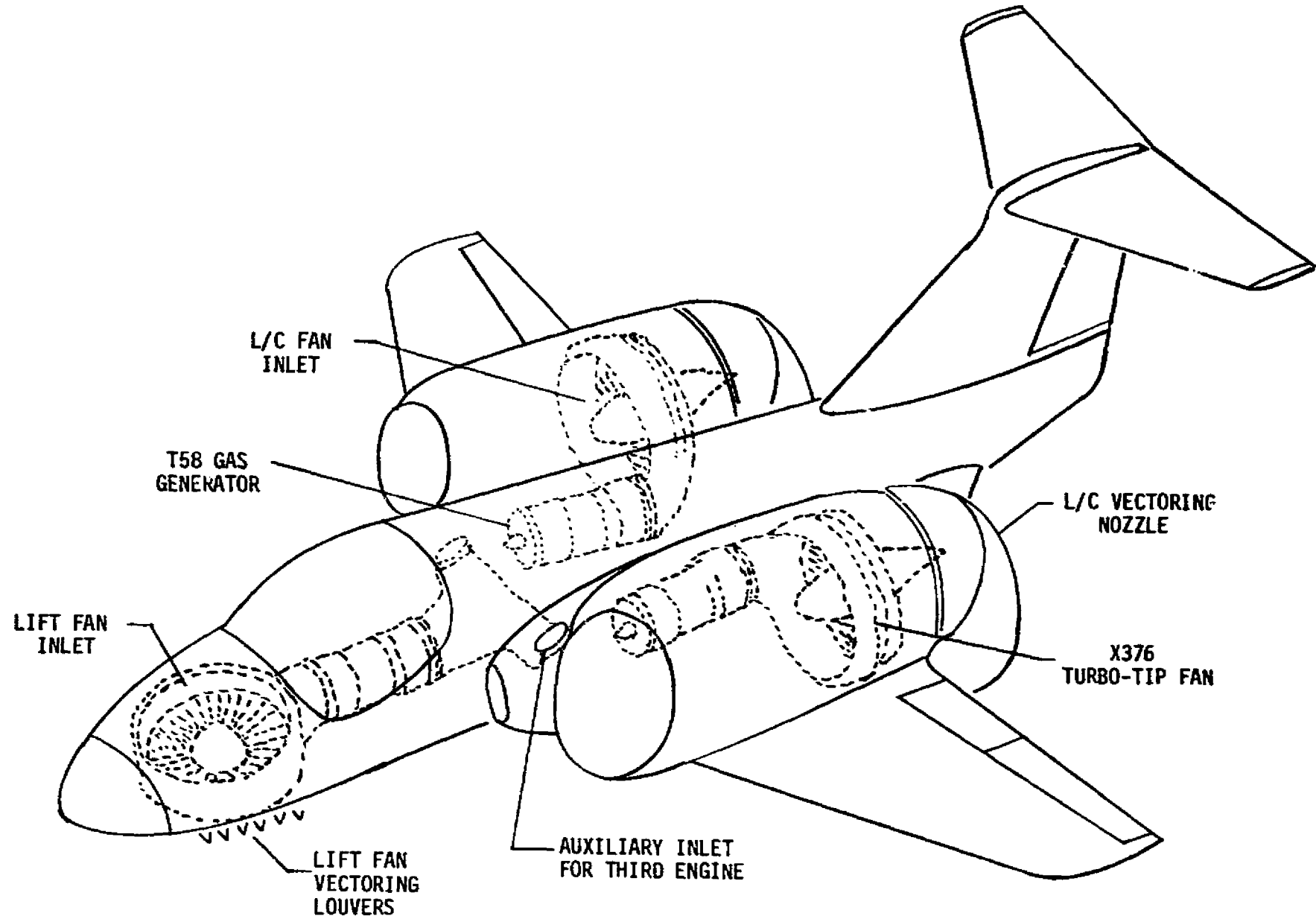
X376 TURBO-TIP FAN

Figure 3.- Schematic of the model showing gas generator and turbo-tip fan relationship.
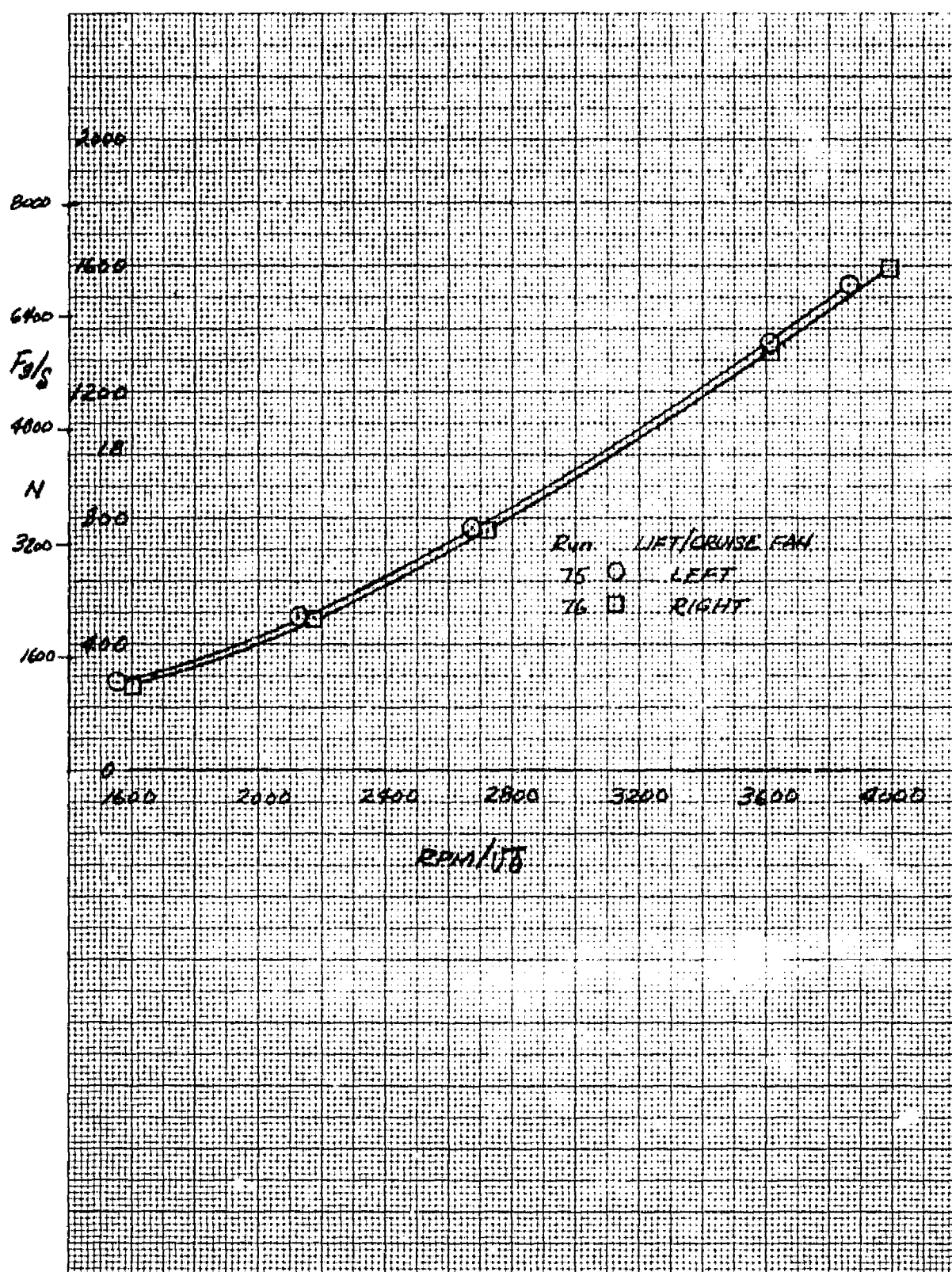
Figure 4.- Variation of static thrust with lift/cruise fan rpm; $\delta_{cn} = 0°$, $\alpha_u = 0°$, q = 0 N/m² (psf).
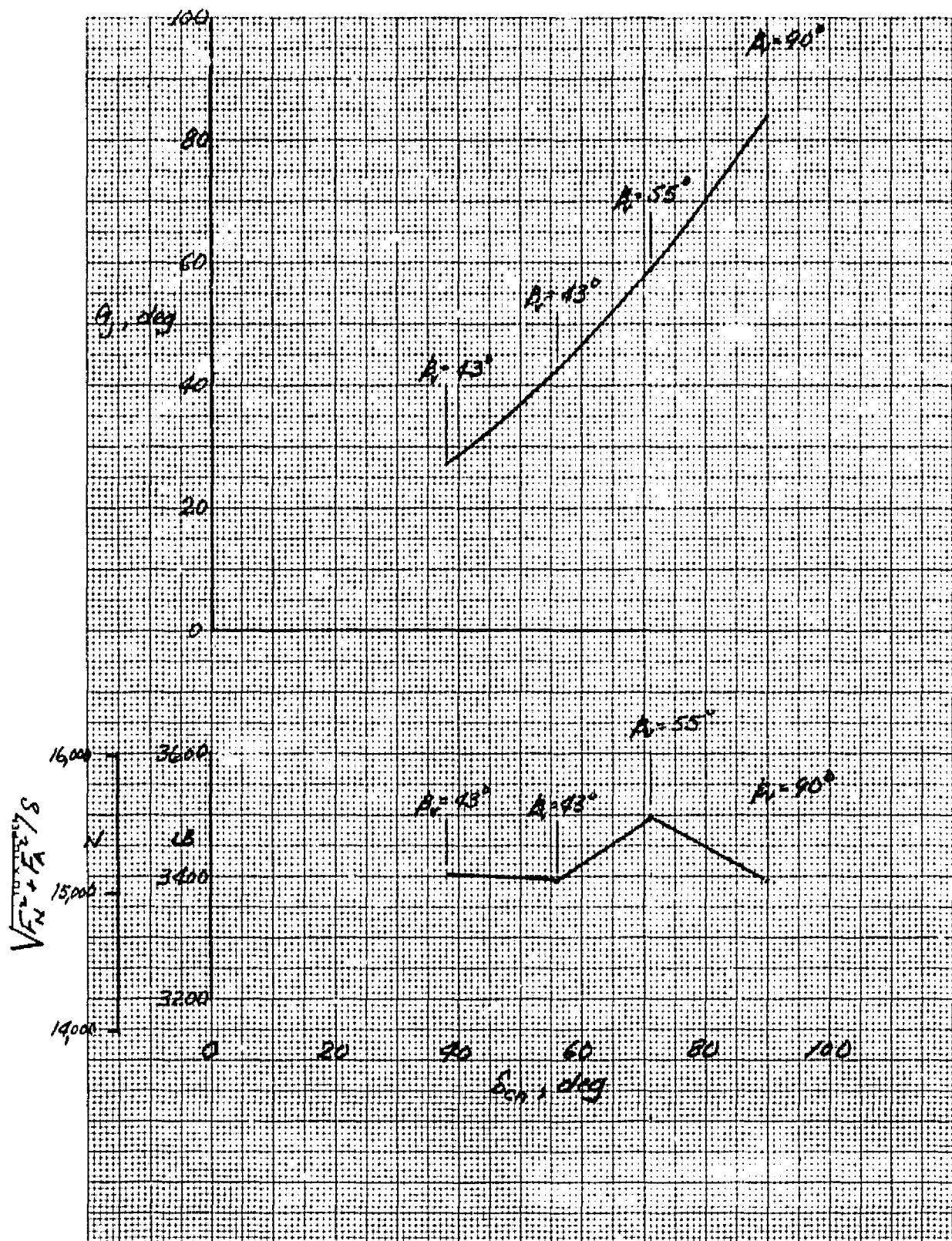
Figure 5.- Resultant static thrust and static turning angle with combined lift/cruise fan and forward fan operation; nominal rpm/$\sqrt{\theta}$ = 3600, α_u = 0°, q = 0 N/m² (psf).
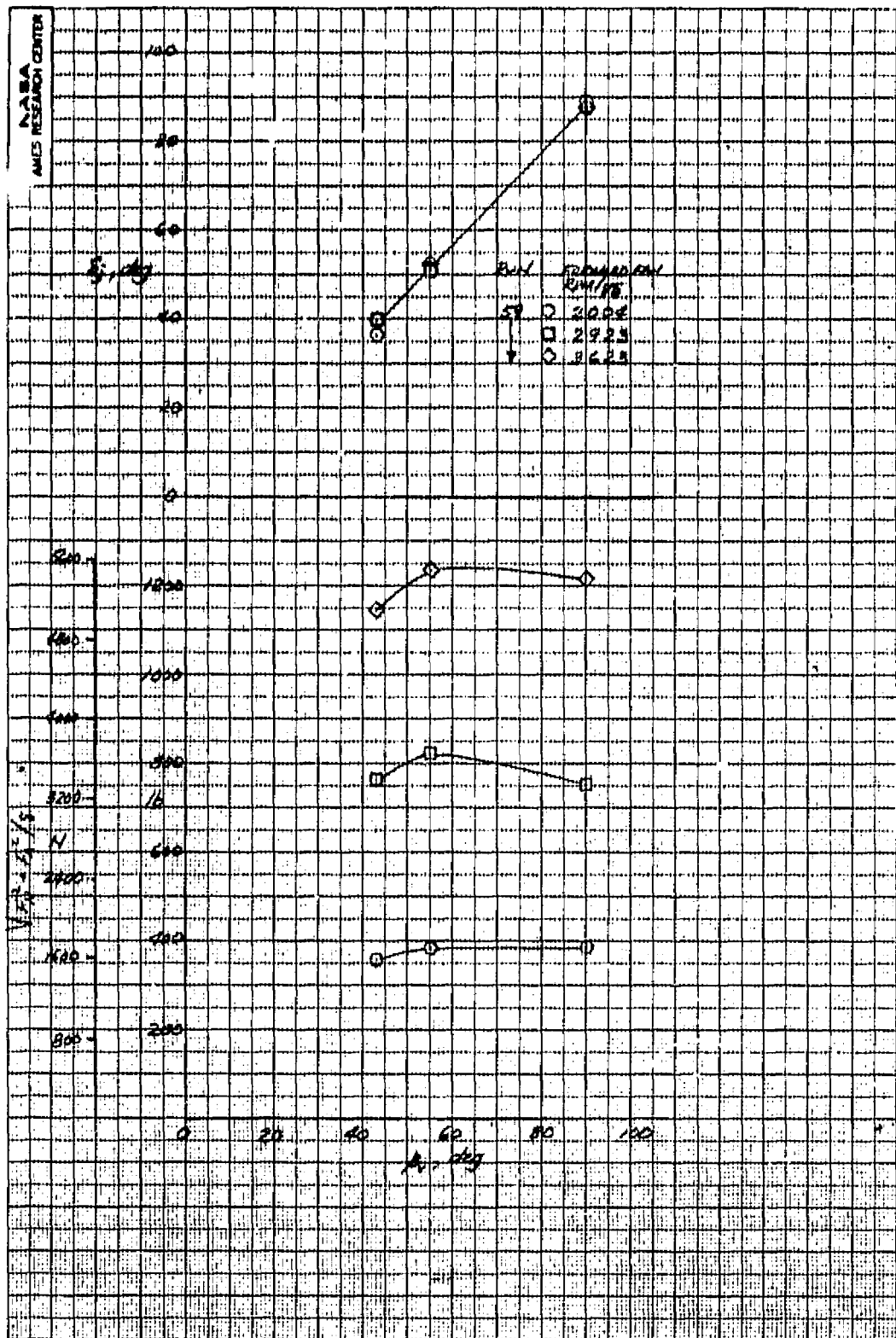
Figure 6.- Variation of resultant static thrust and static turning angle with forward fan β_v; $\alpha_u = 0°$.
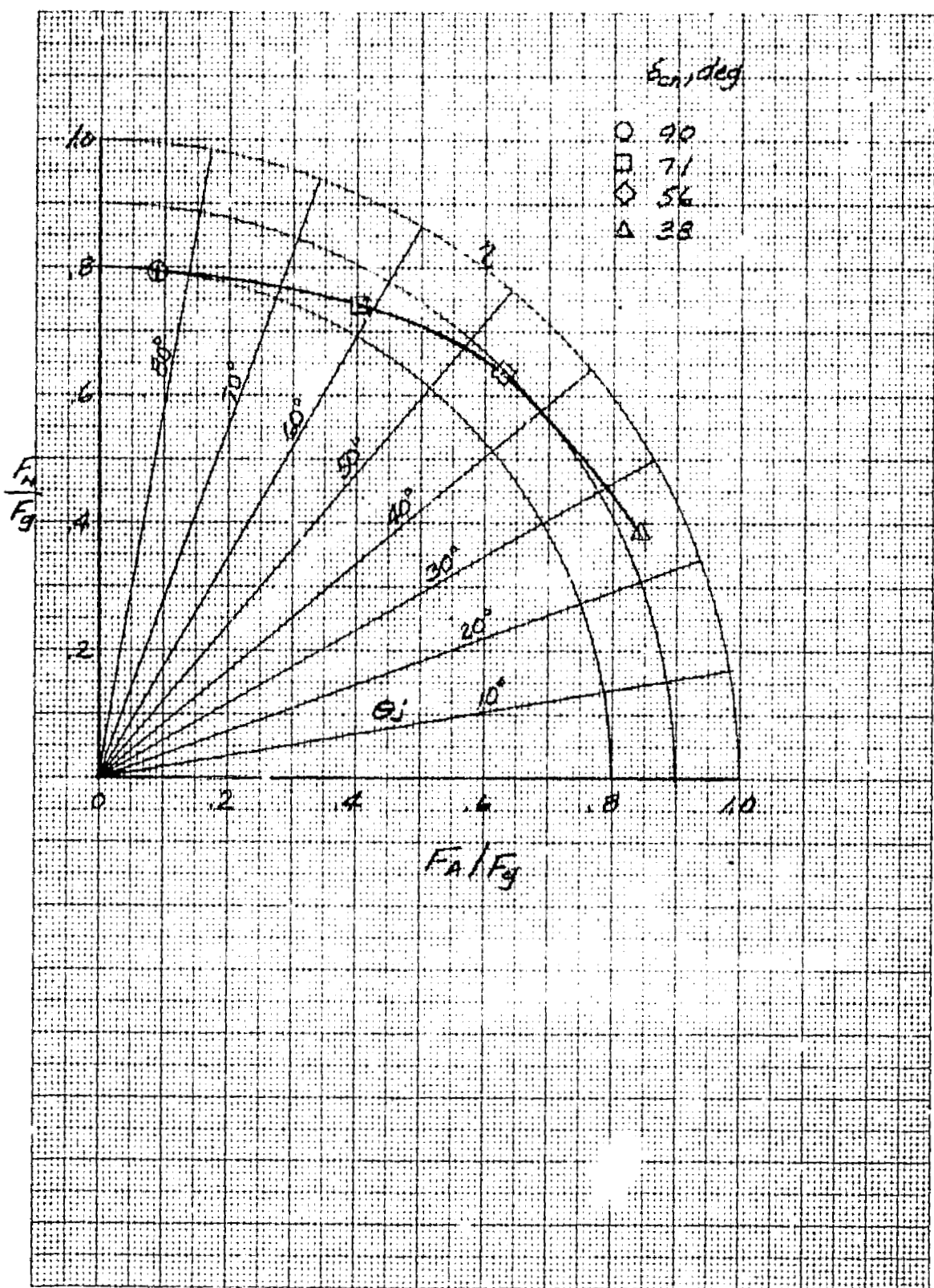
Figure 7.- Lift/cruise fan deflector static turning efficiency; $\alpha_u = 0°$.

22
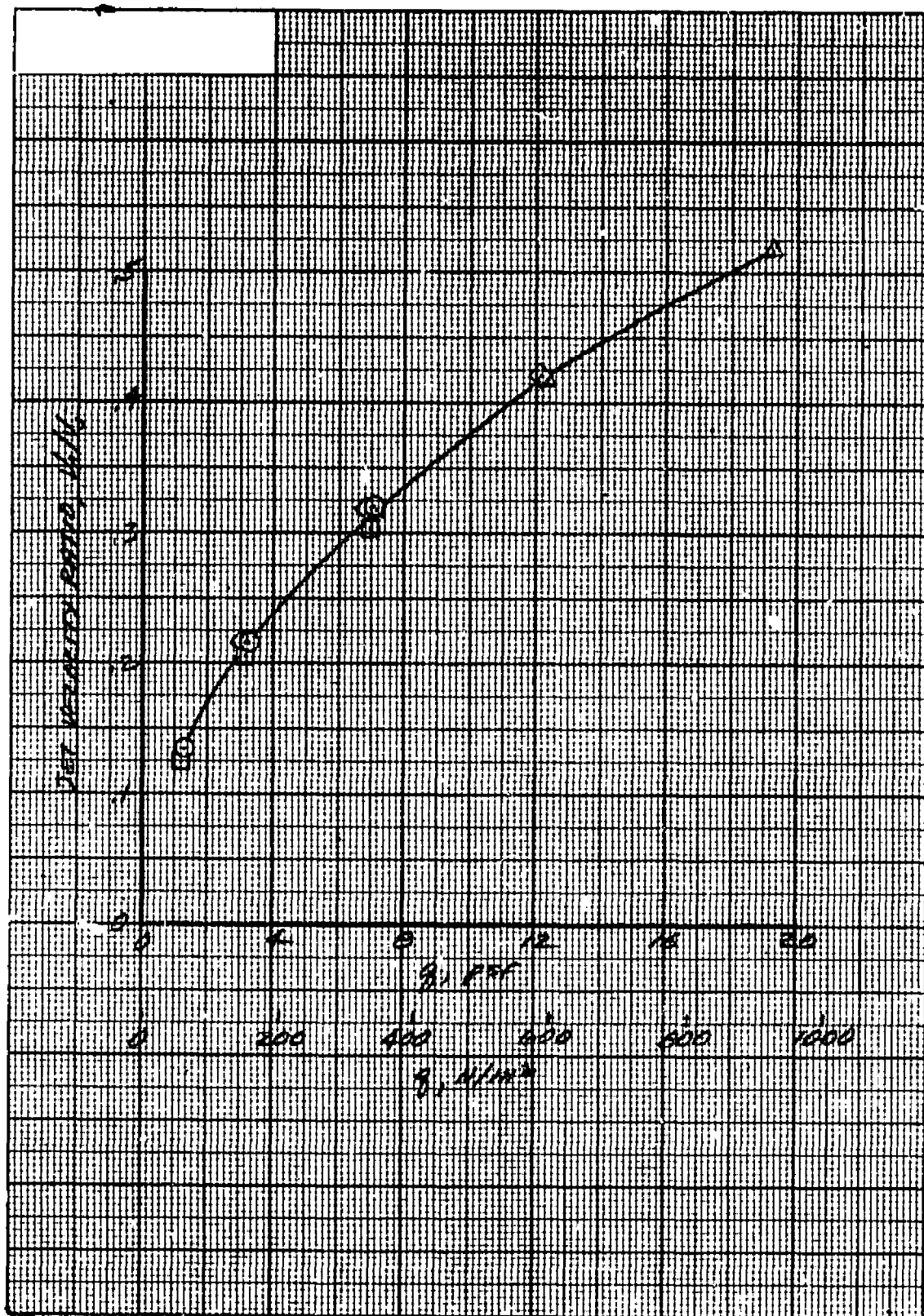
(a) Forward lift fan.

Figure 8.- The variation of jet velocity ratio with wind-tunnel dynamic pressure for the powered-lift model configuration; nominal fan rpm/$\sqrt{\theta}$ = 3600.

23
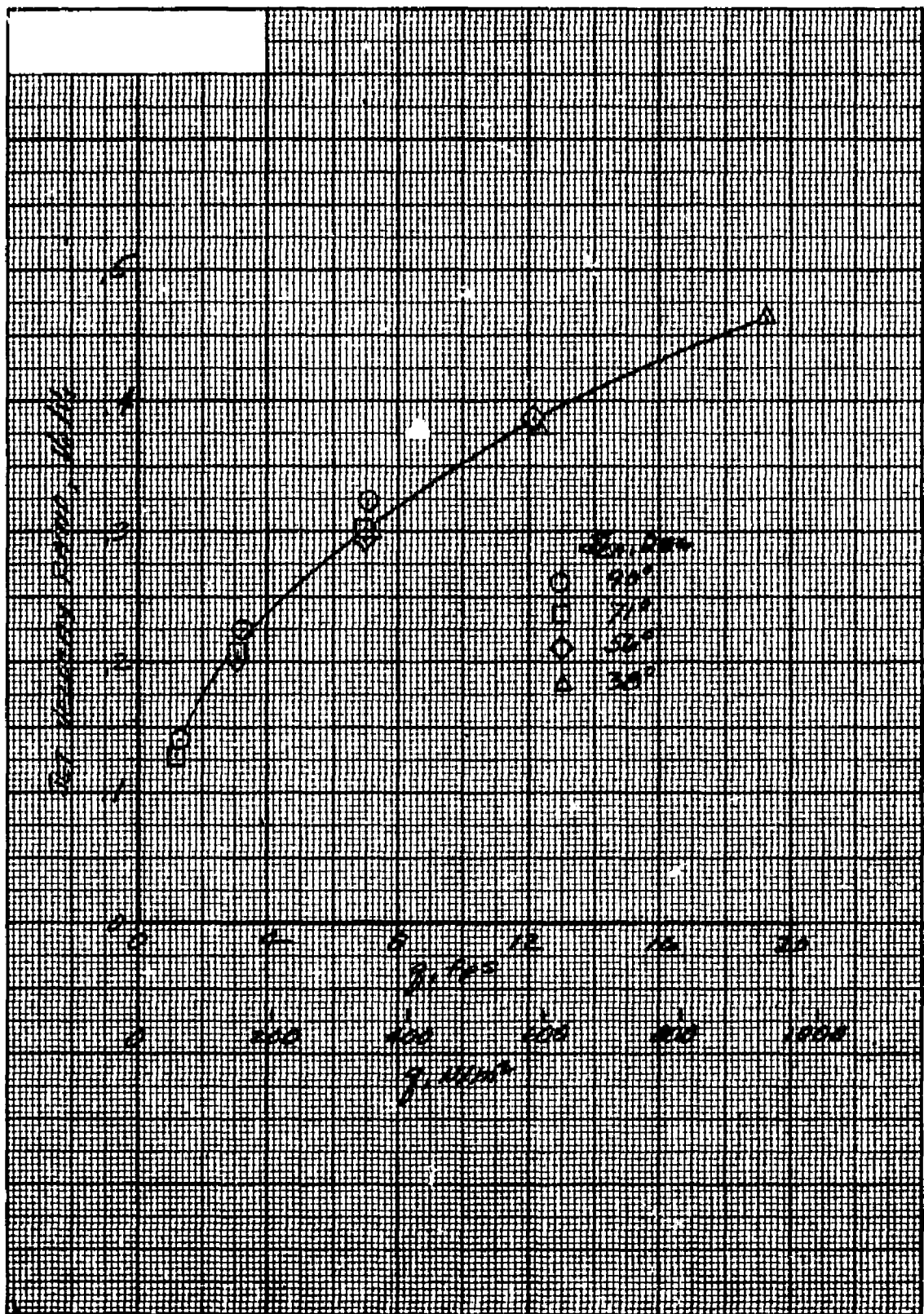
(b) L/H lift/cruise fan.

Figure 8.- Continued.
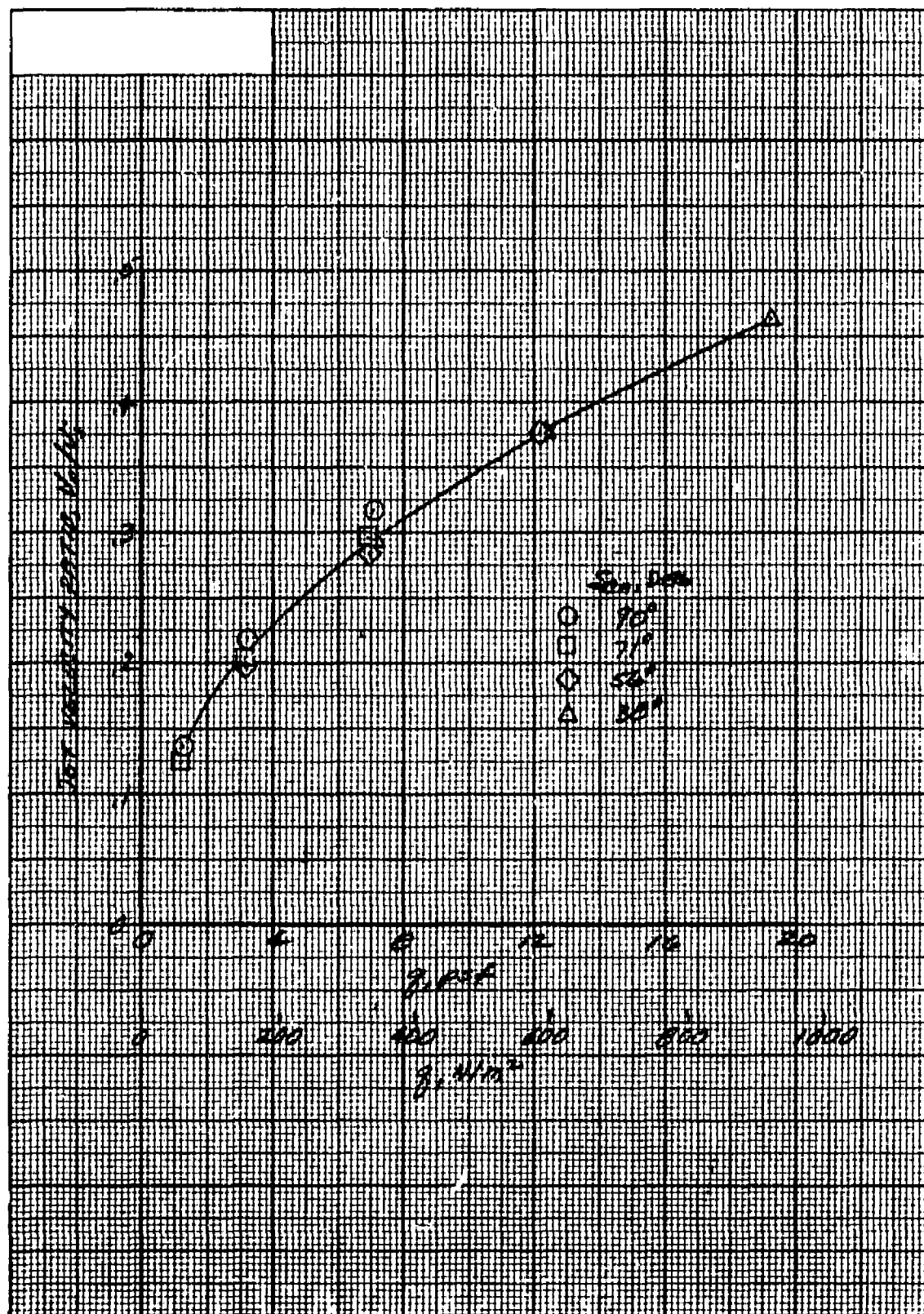
(c) R/H lift/cruise fan.

Figure 8.- Concluded.
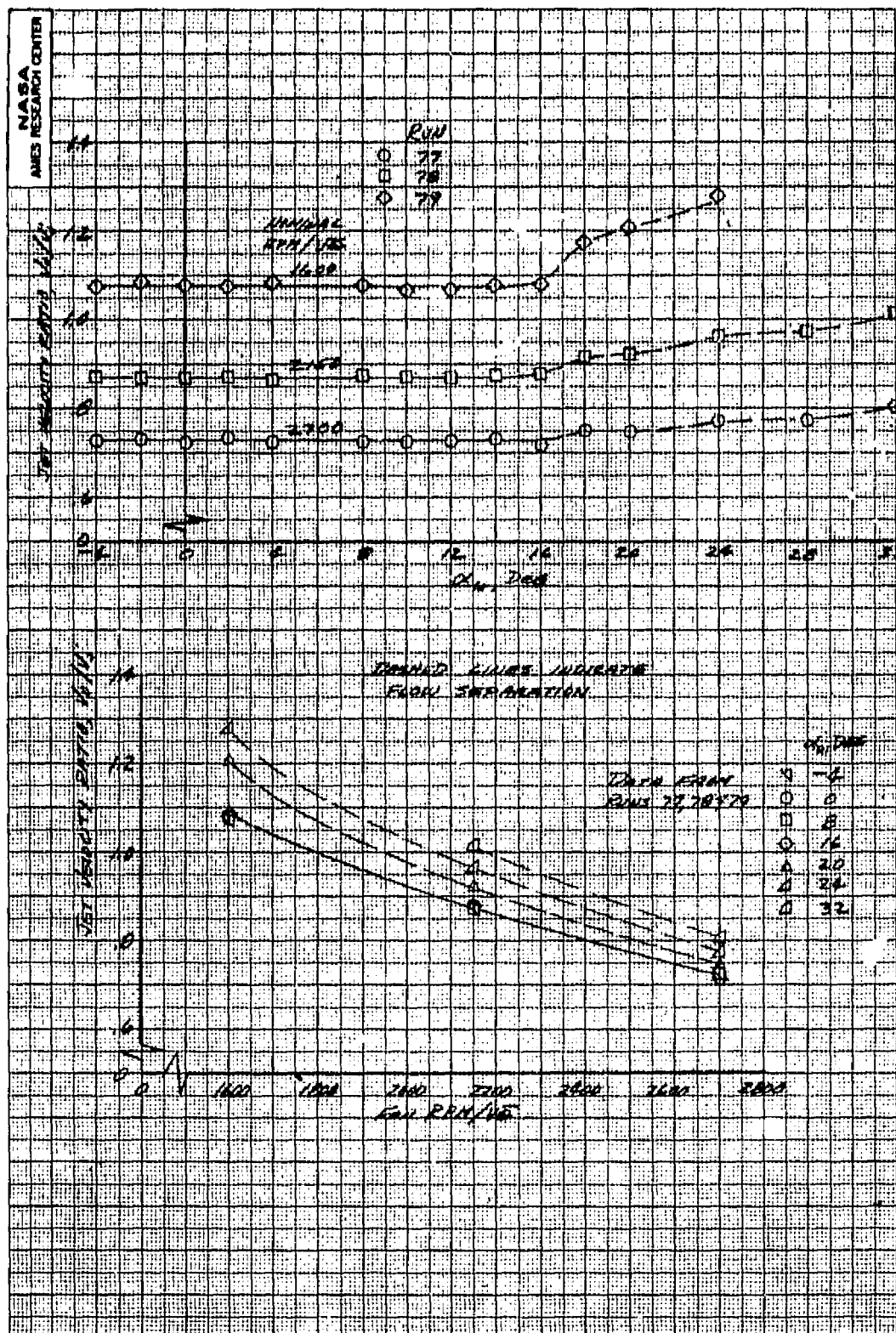
(a) L/H lift/cruise fan.

Figure 9.- Variation of jet velocity ratio with corrected fan rpm and model angle of attack, cruise configuration; nominal $q = 1699.7$ N/m^2 (35.5 psf), $\beta = 0°$, $\delta_{ail} = 0°$, $\delta_f = 0°$.

26
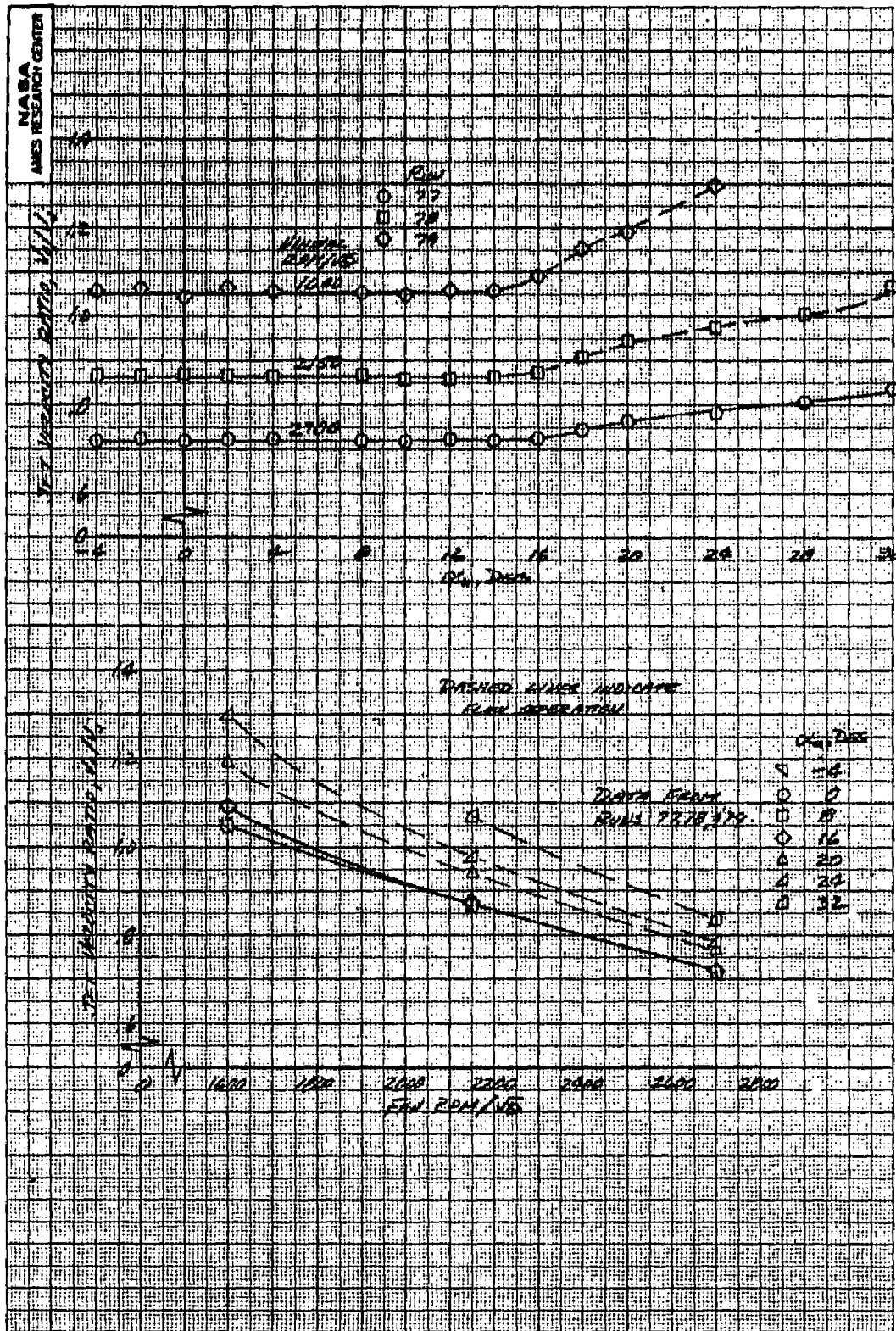
(b) R/H lift/cruise fan.

Figure 9.- Concluded.

27
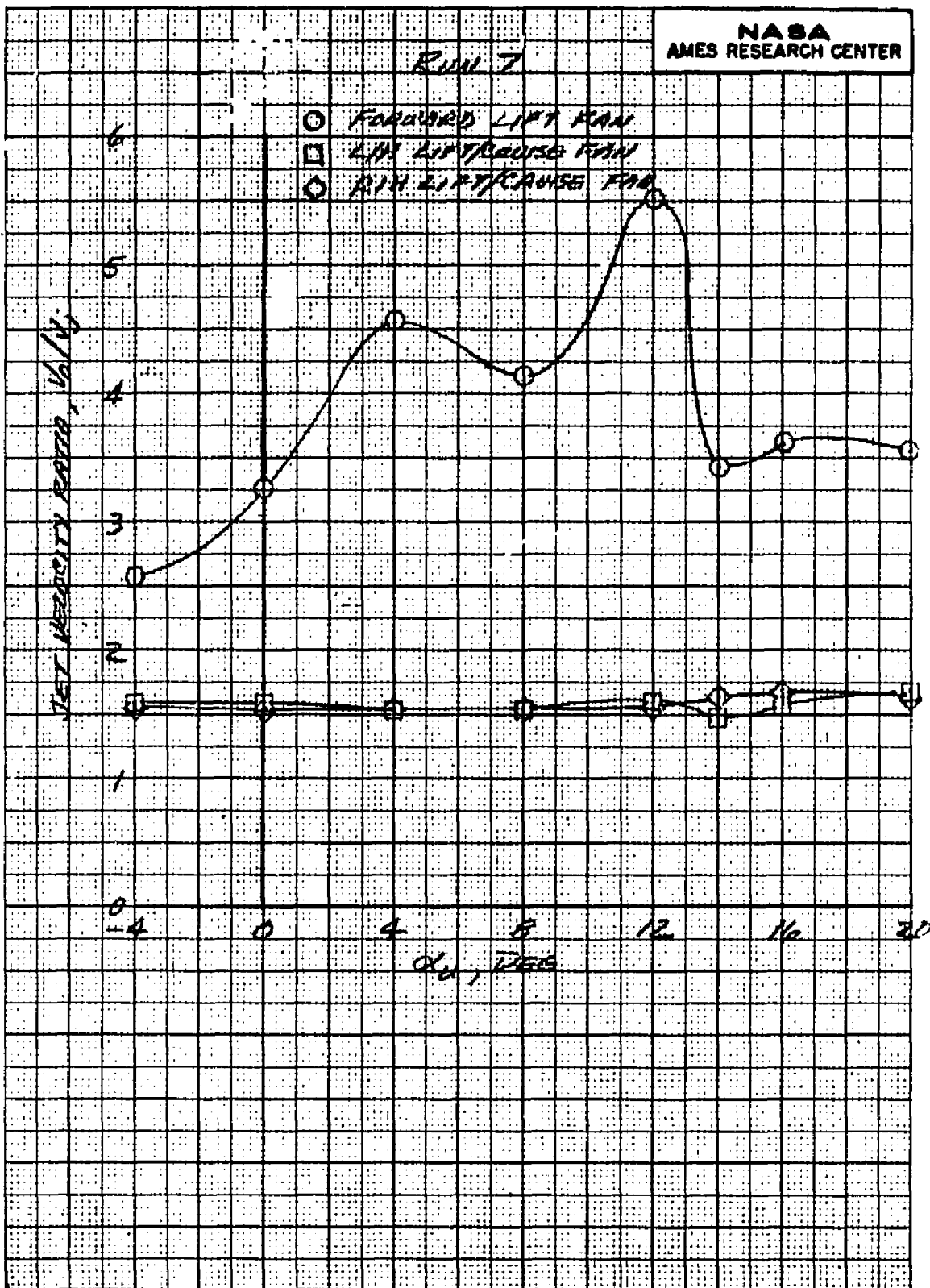
(a) $\delta_{cn} = ^r j^\circ$, $\beta_v = 90^\circ$, q = 341.4 N/m^2 (7.13 psf).

Figure 10.- Windmilling characteristics of the model fans.
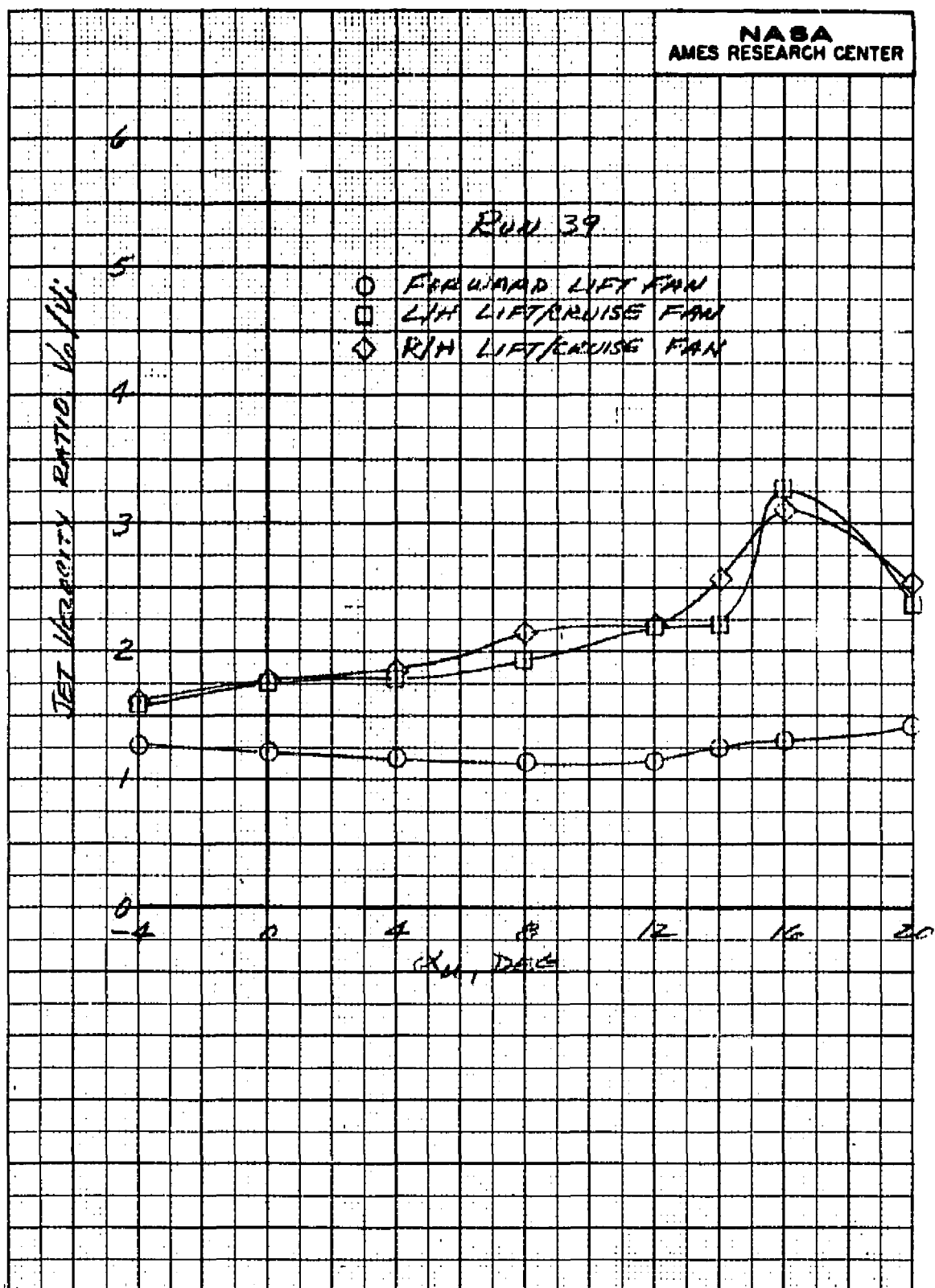
(b) $\delta_{cn} = 71°$, $\beta_v = 55°$, $q = 337.1$ N/m^2 (7.04 psf).

Figure 10.- Continued.
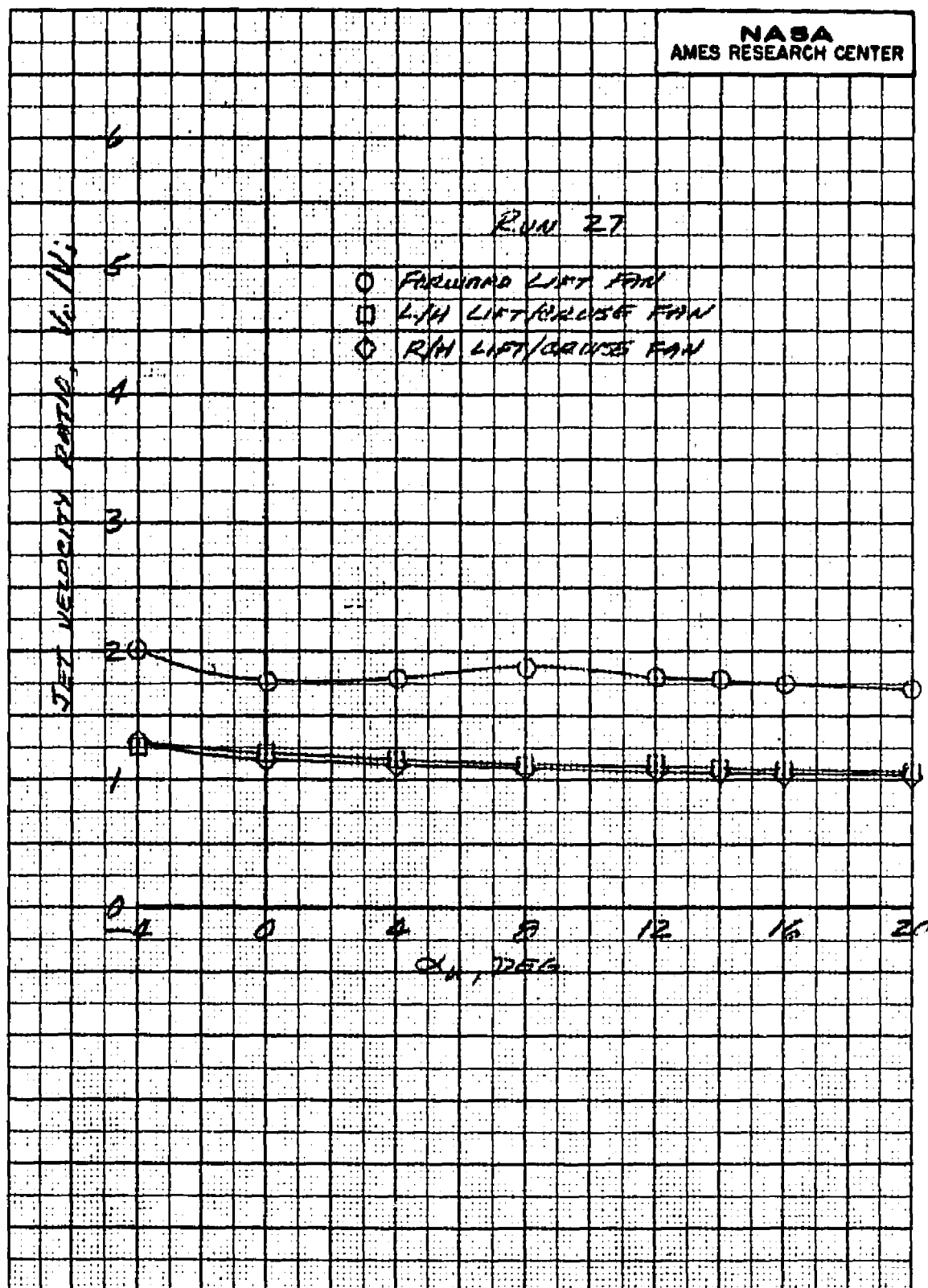
(c) δ_{cn} = 56°, β_v = 43°, q = 580.3 N/m^2 (12.12 psf).

Figure 10.- Continued.
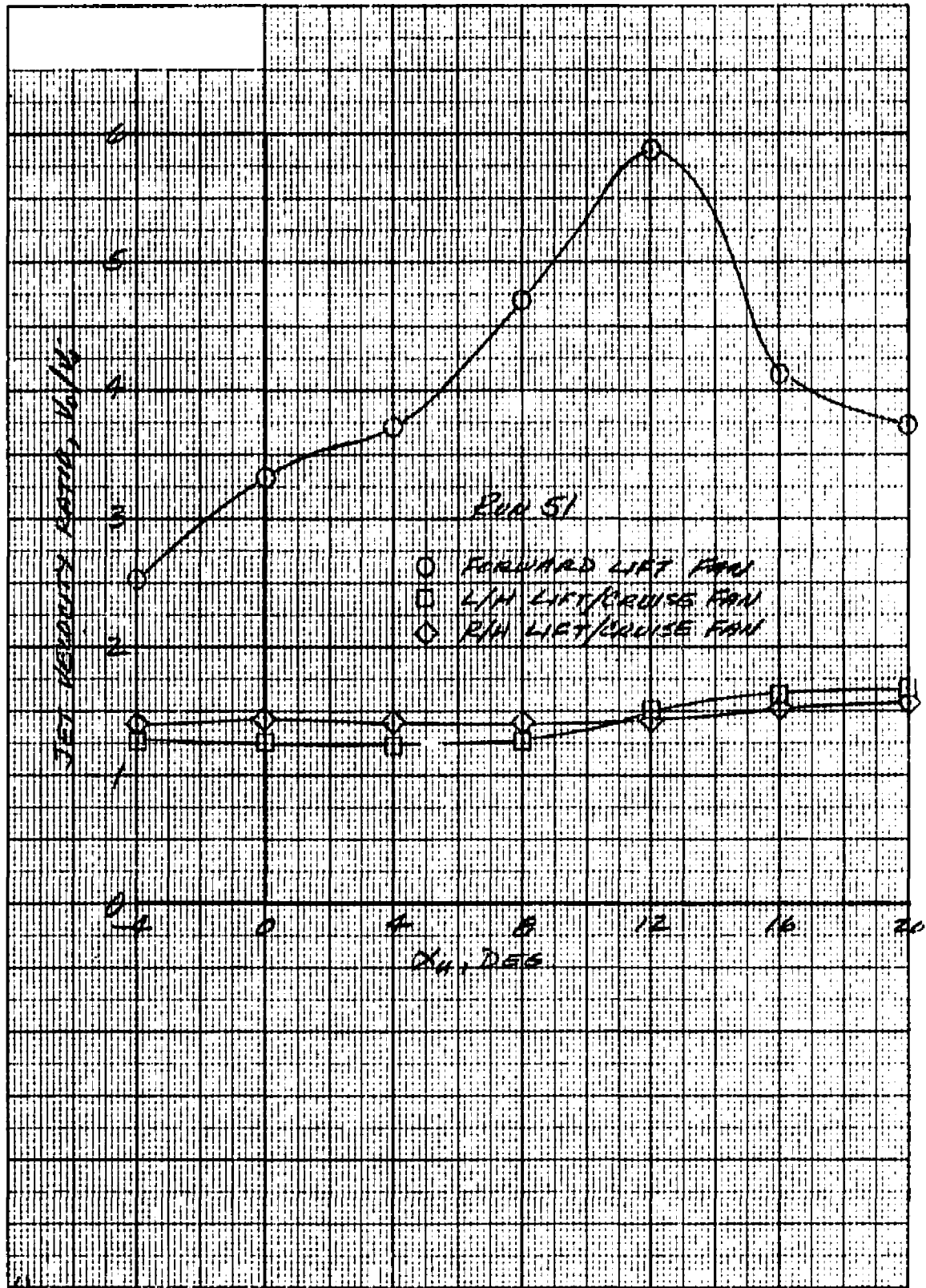
(d) δ_{cn} = 38°, β_v = 43°, q = 919.3 N/m^2 (19.20 psf)

Figure 10.- Concluded.

31
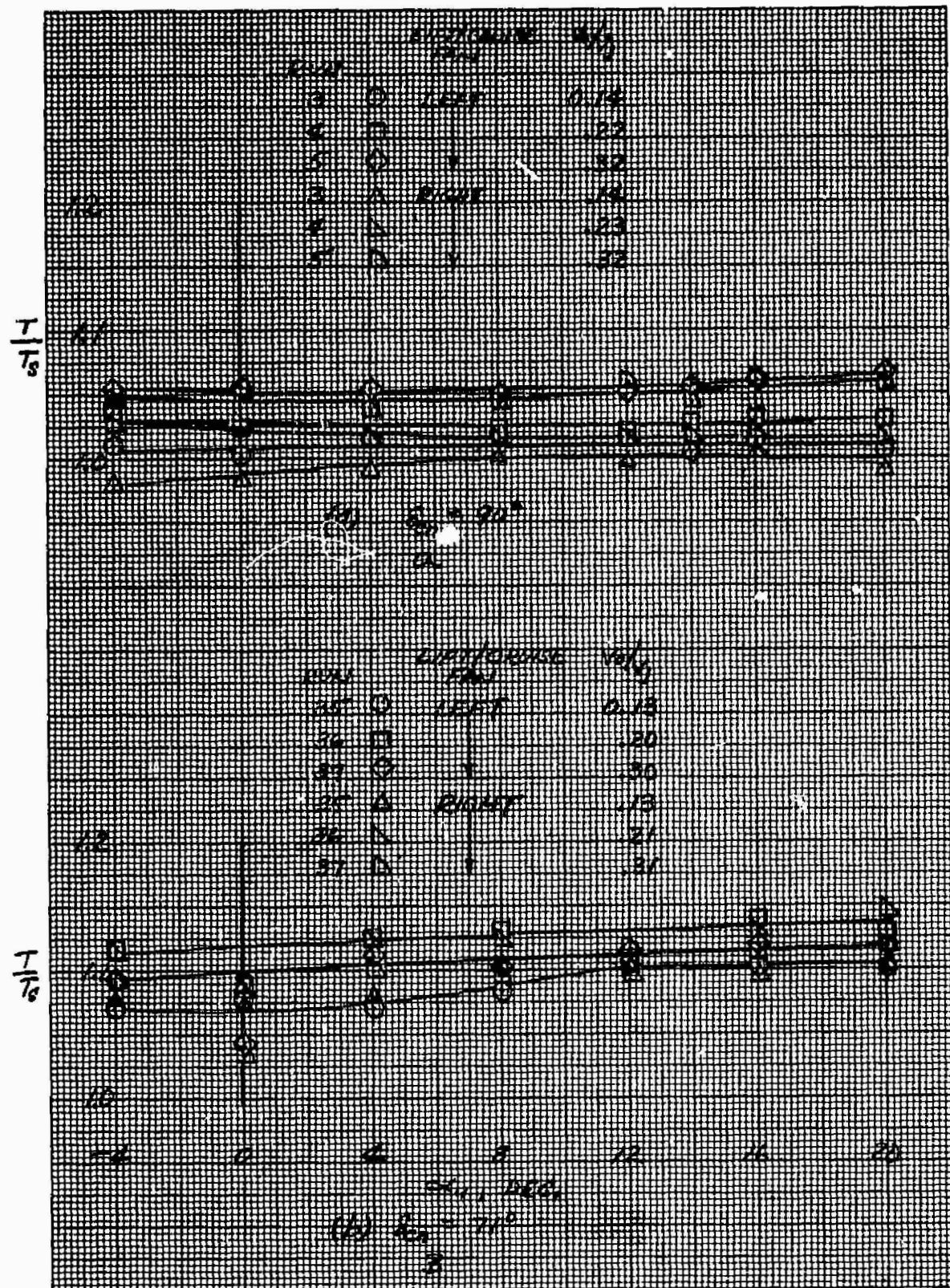
(a) $\delta_{cn} = 90°$

(b) $\delta_{cn} = 71°$

Figure 11.- Variation of fan resultant thrust to static resultant thrust ratio
with angle of attack.
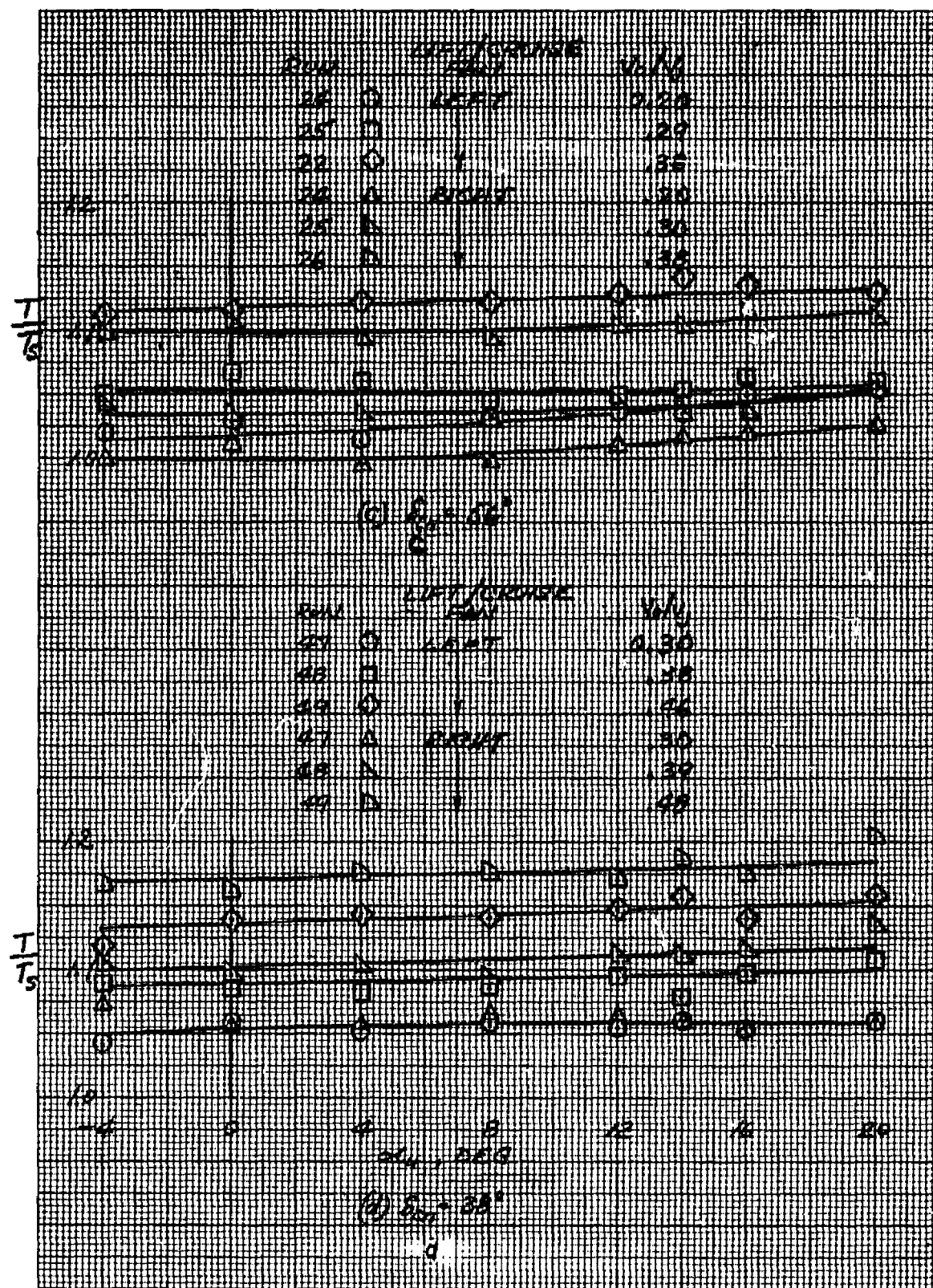
(c) $\delta_{cn} = 56°$

(d) $\delta_{cn} = 38°$

Figure 11.- Continued.

33
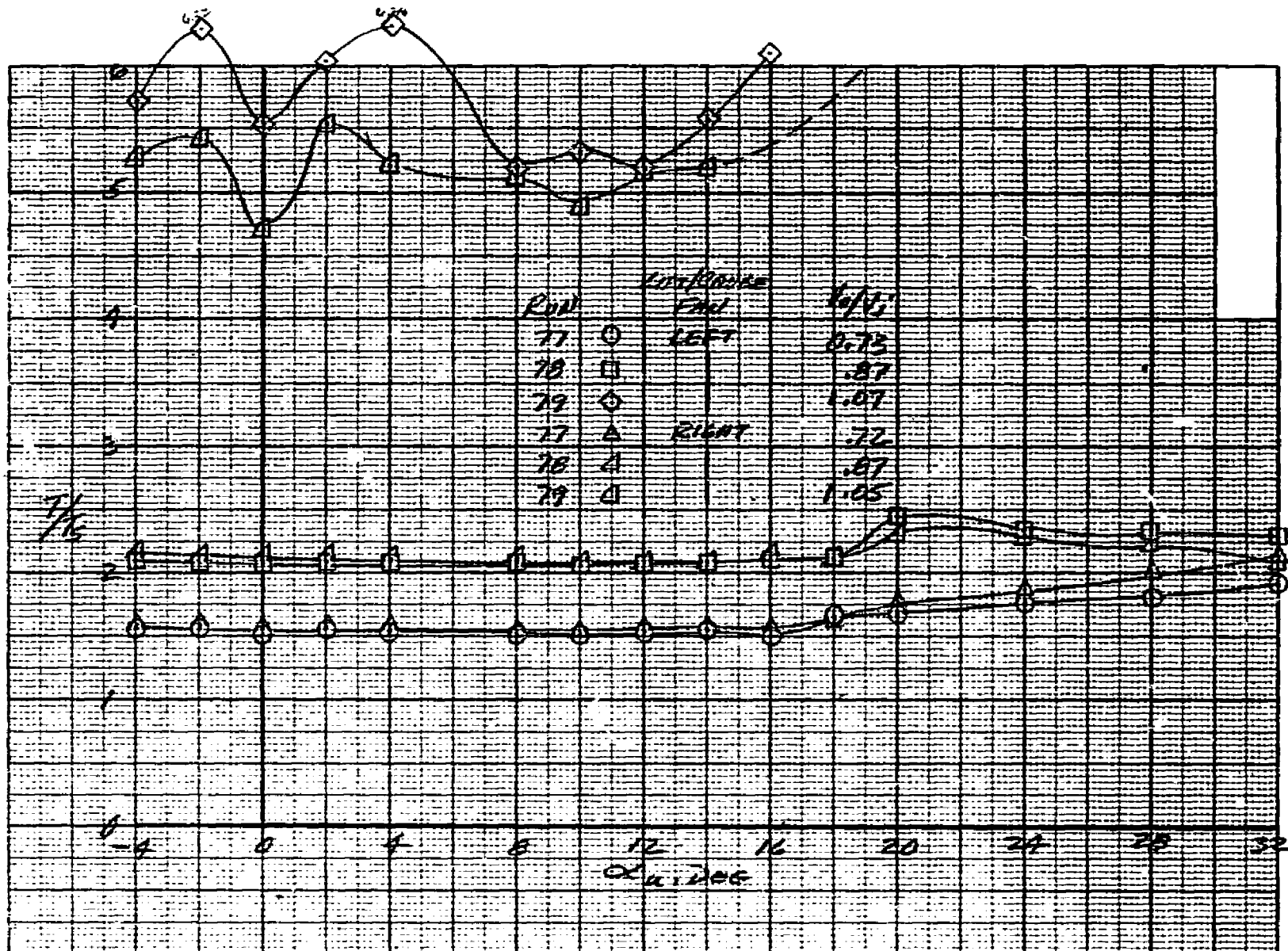
(e) $\delta_{cn} = 0°$

Figure 11.- Continued.

34
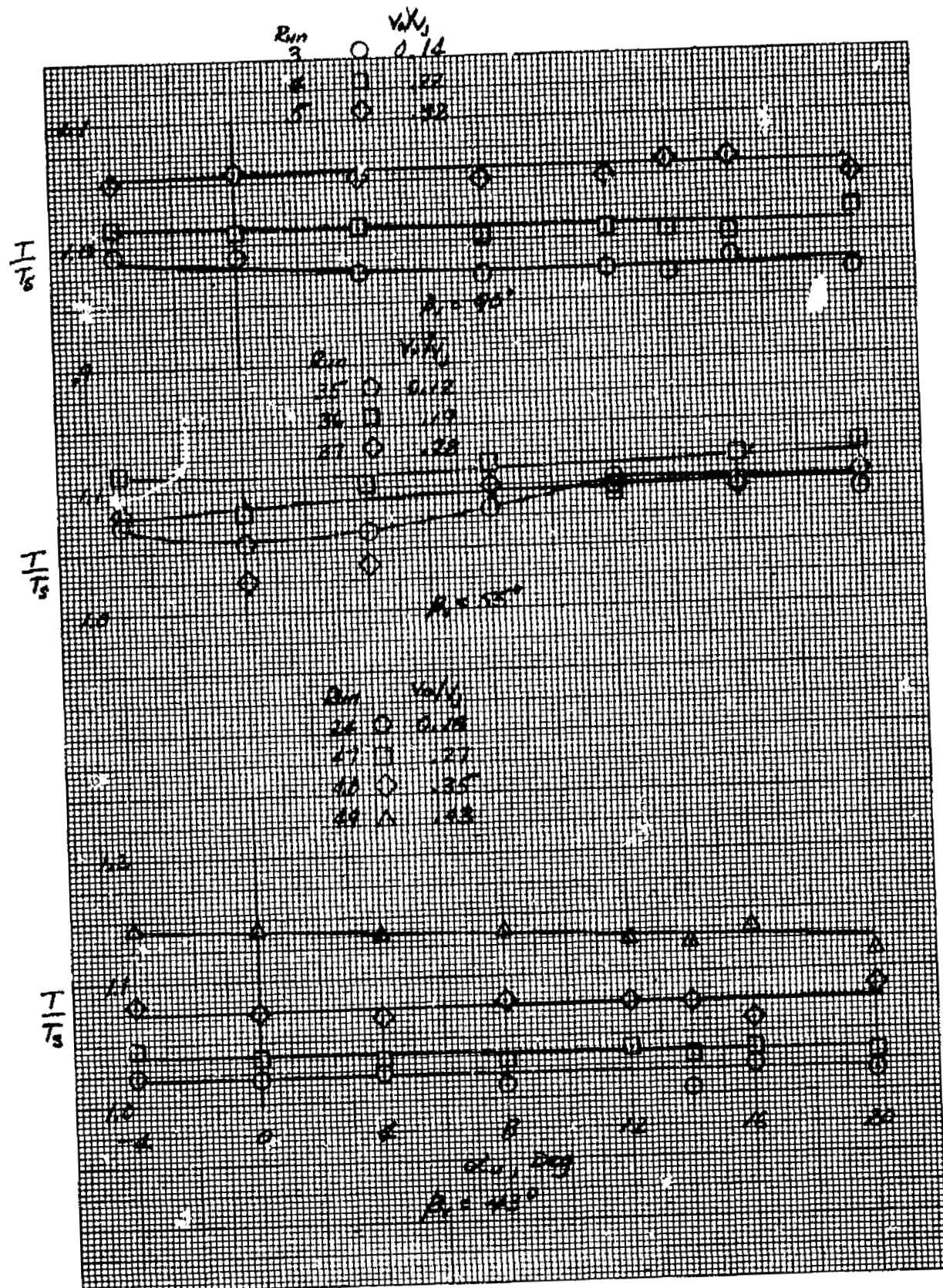
(f) Forward fan

Figure 11.- Concluded.
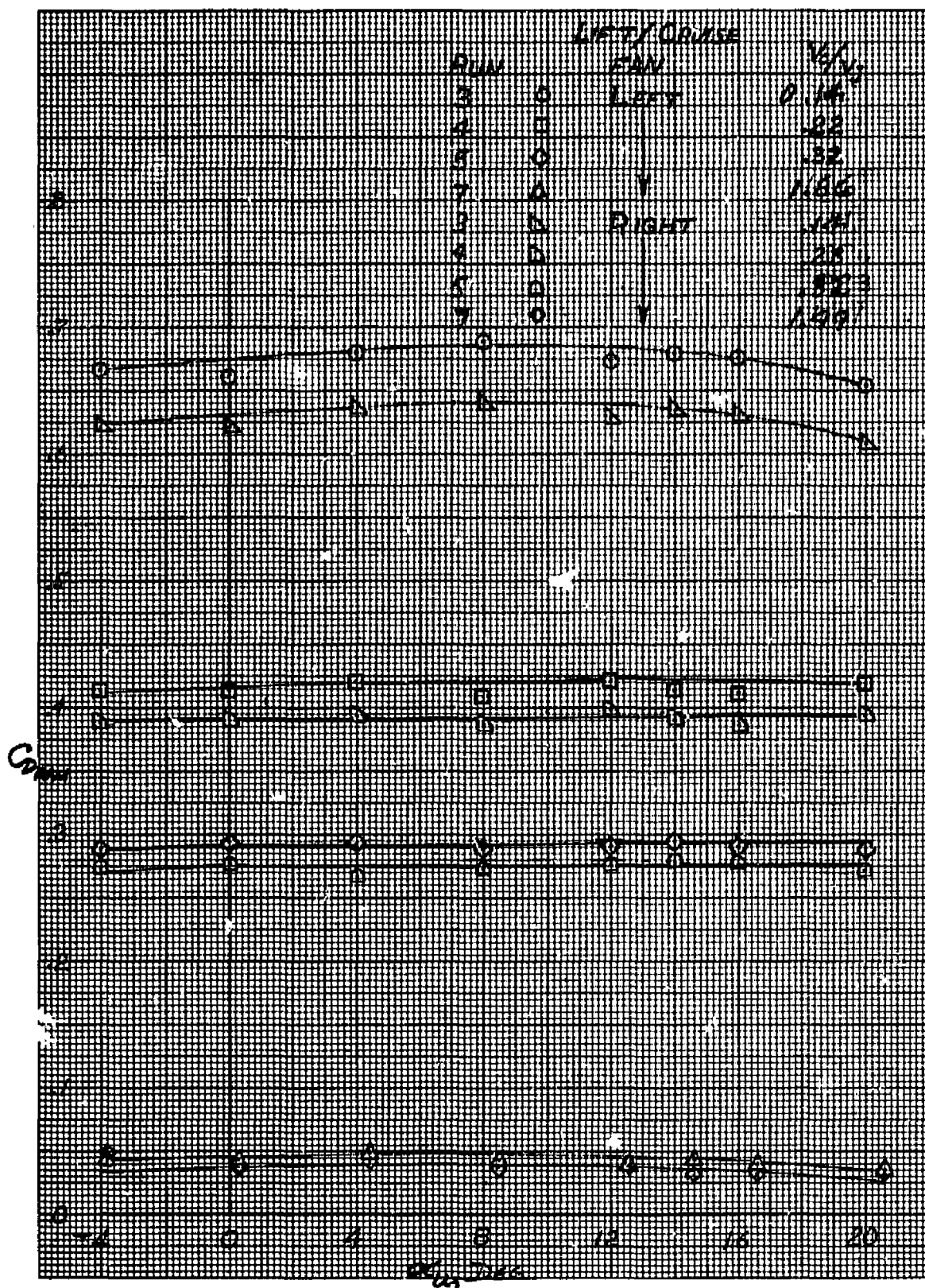
(a) $\delta_{cn} = 90°$

Figure 12.- Variation of ram drag with angle of attack with forward fan and
lift/cruise fan operation.

(b) $\delta_{cn} = 71°$

Figure 12.- Continued.

37
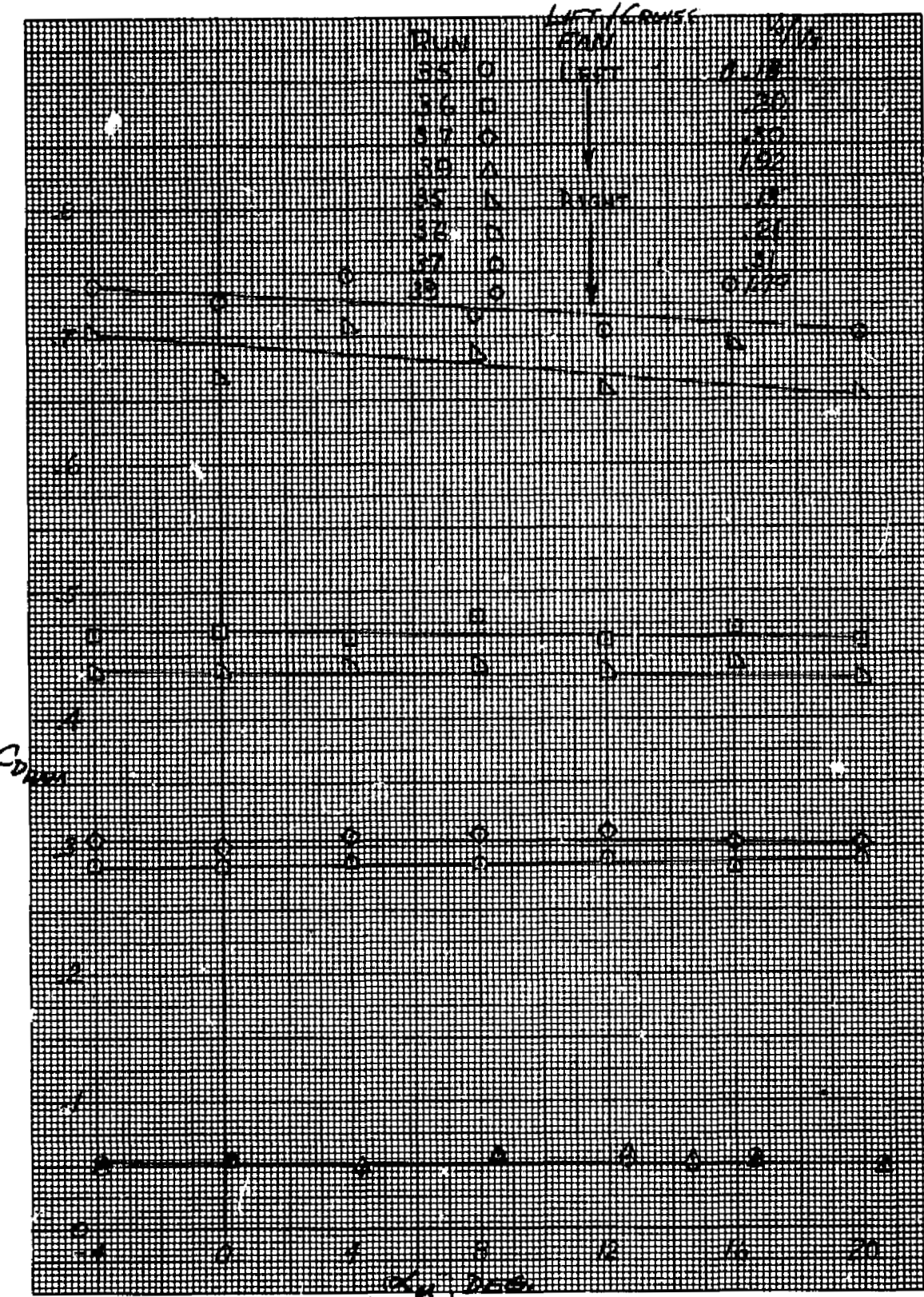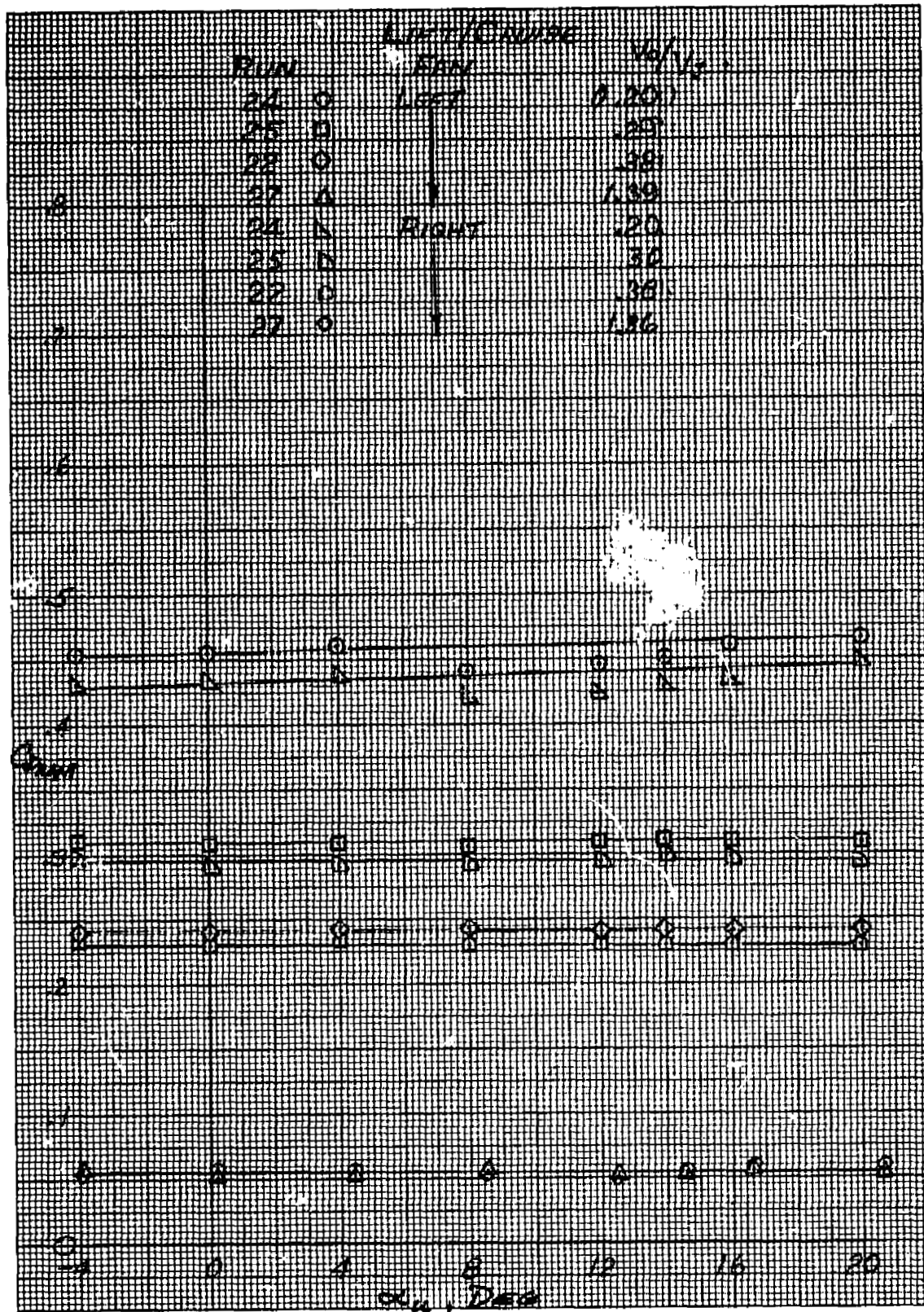
(c) $\delta_{cn} = 56°$

Figure 12.- Continued.
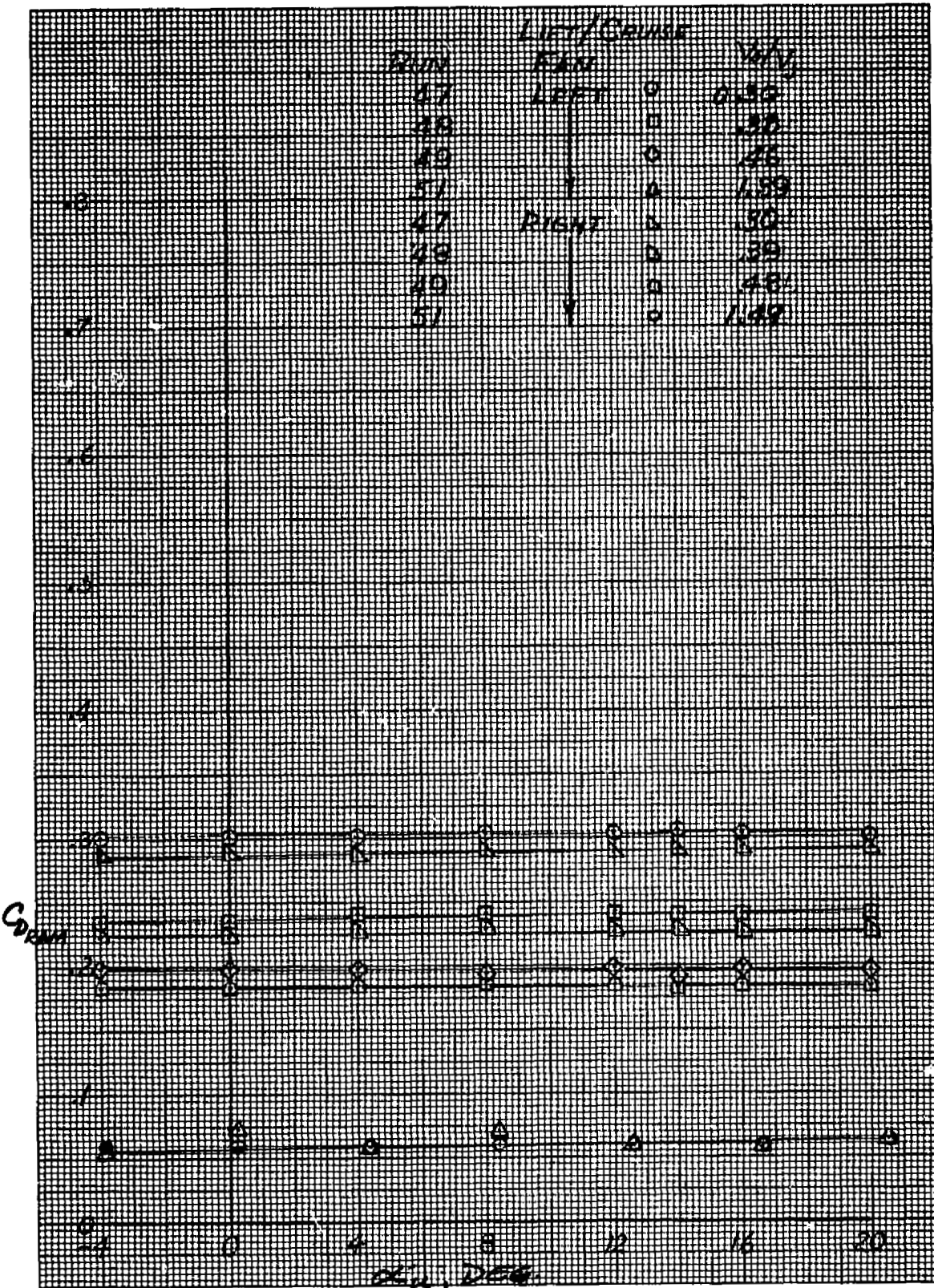
(d) $\delta_{cn} = 38°$

Figure 12.- Continued.

39

(e) $\delta_{cn} = 0°$

Figure 12.- Continued.
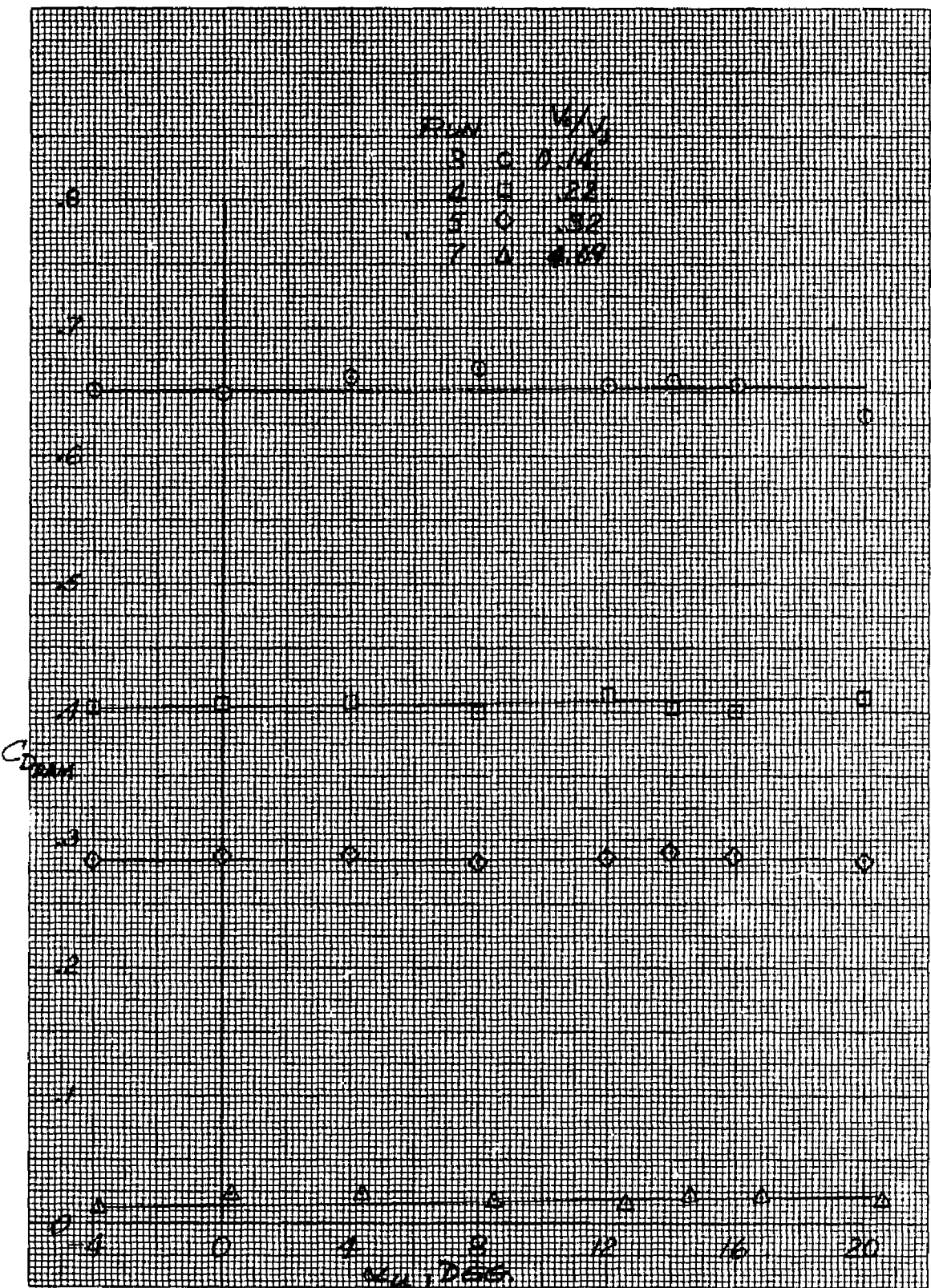
(f) Forward fan, $\beta_v - 90°$

Figure 12.- Continued.

41
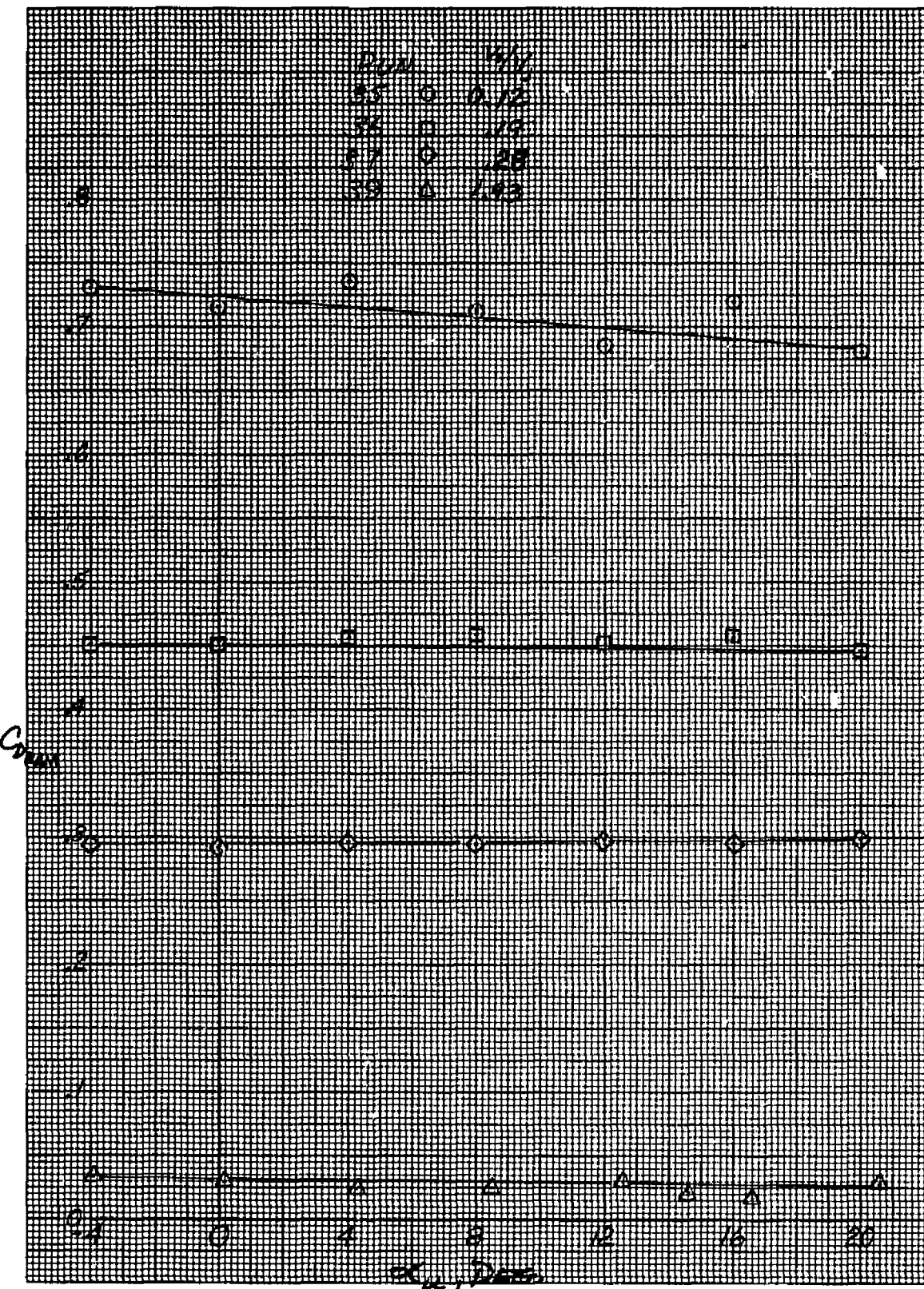
(g) Forward fan, $\beta_v = 55°$

Figure 12.- Continued.
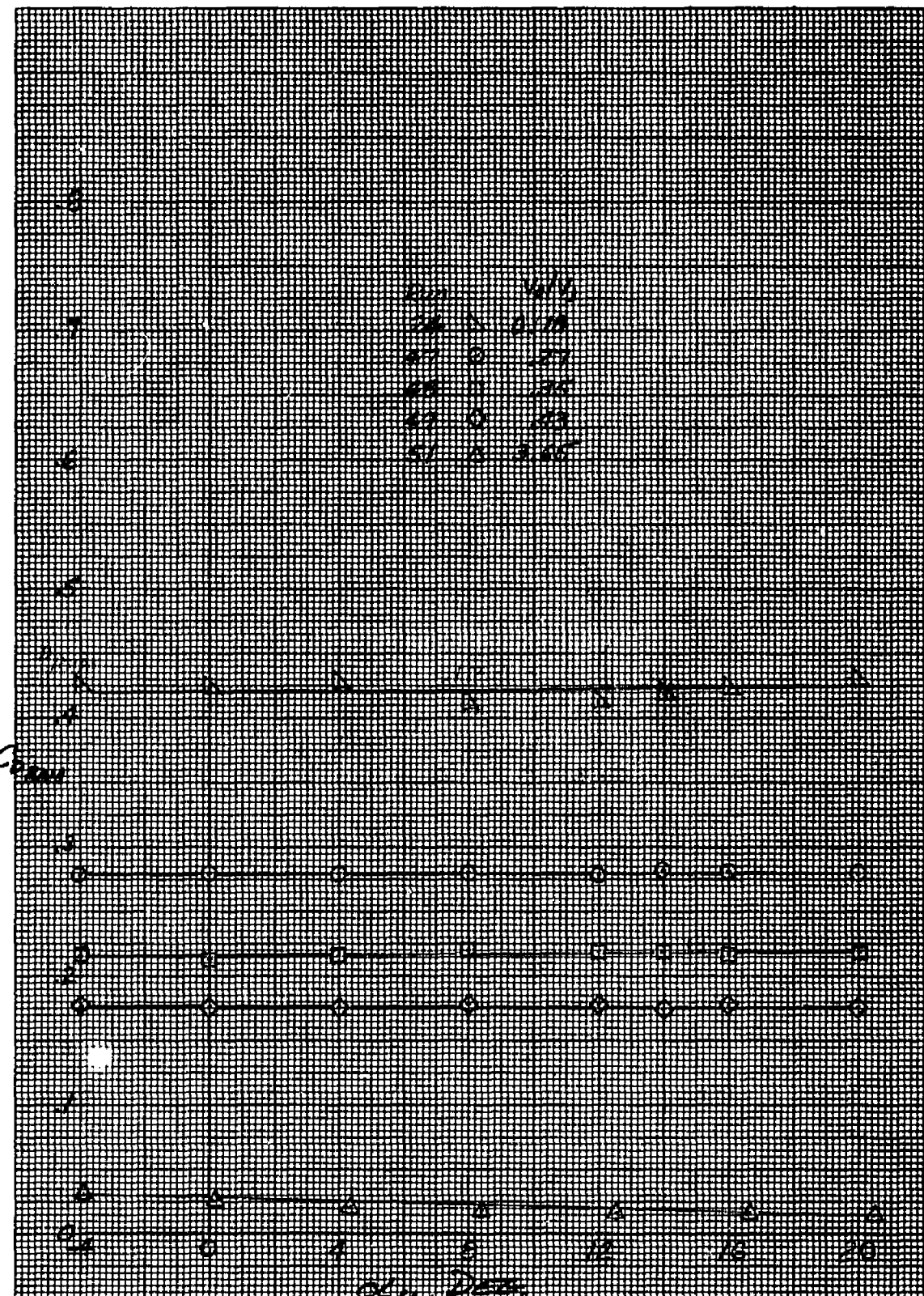
(h) Forward fan, $\beta_v = 43°$

Figure 12.- Concluded.
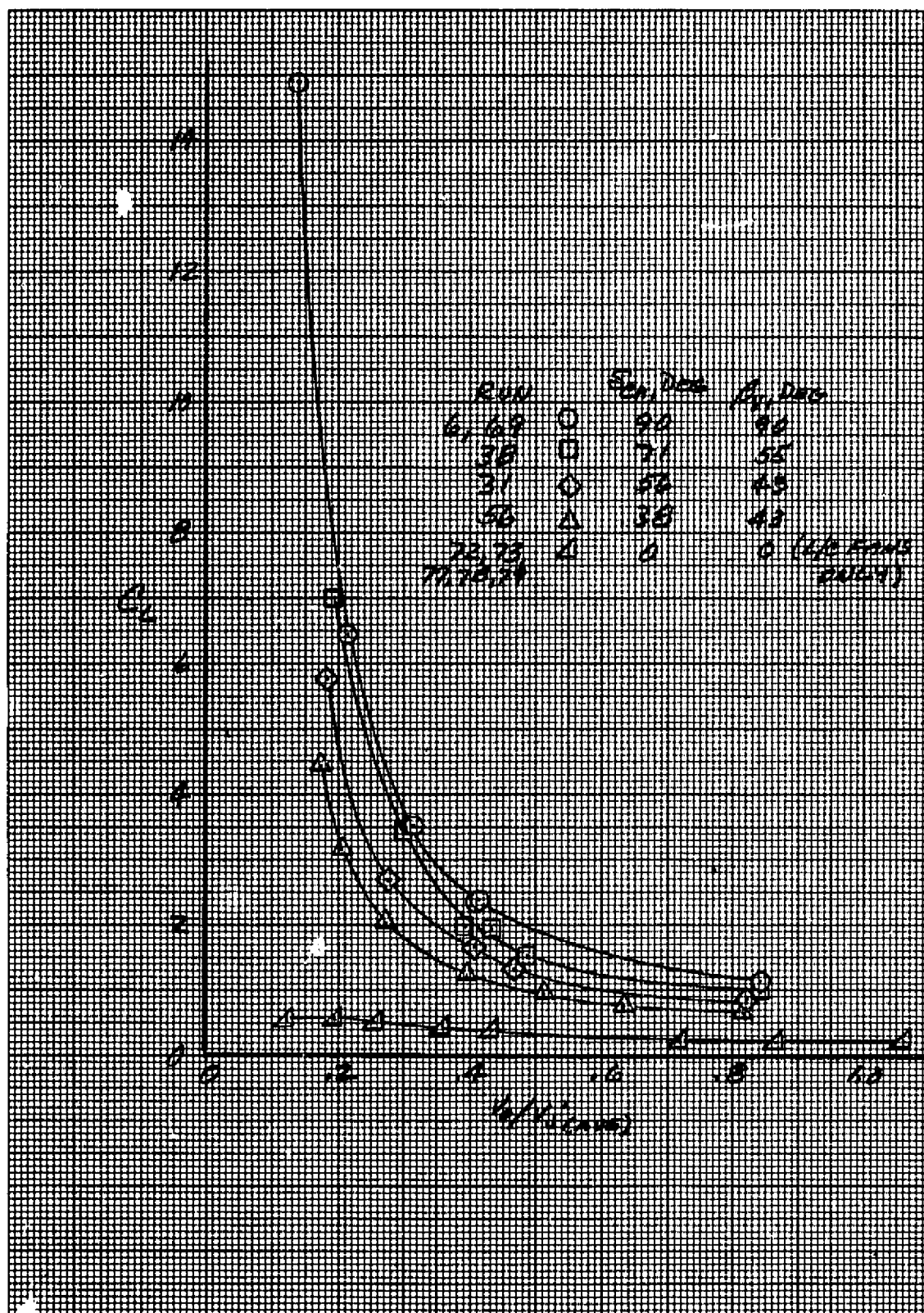
(a) Variation of C_L with V_o/V_j, with three fans operating.

Figure 13.- The effect of jet velocity ratio on longitudinal aerodynamic characteristics; $\alpha_u = 0°$, horizontal tail on, $\delta_f = 15°$, $\delta_{ail} = 10°$, $\beta = 0°$.
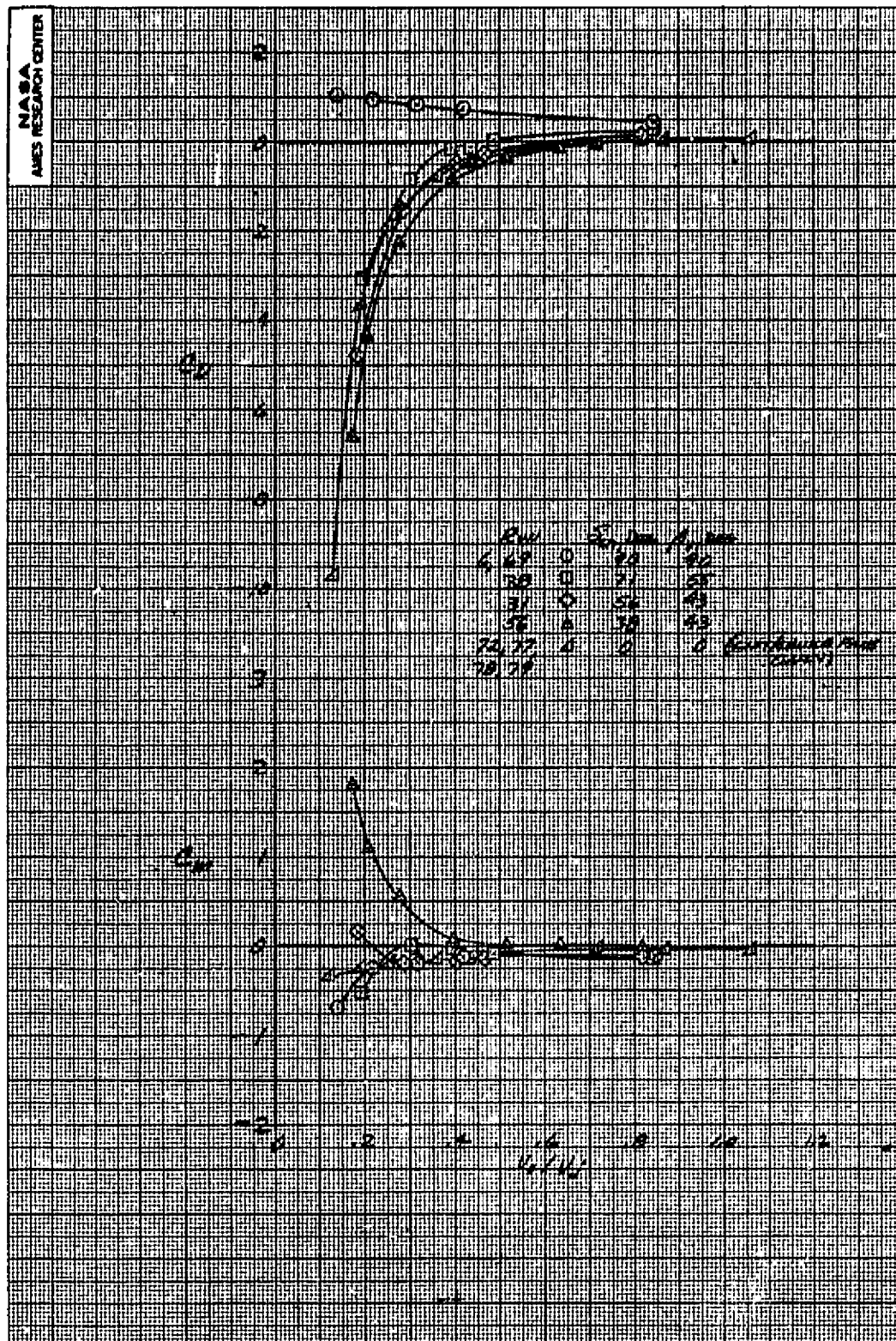
(b) Variation of C_D and C_m with V_o/V_j, with three fans operating.

Figure 13.- Continued.

45
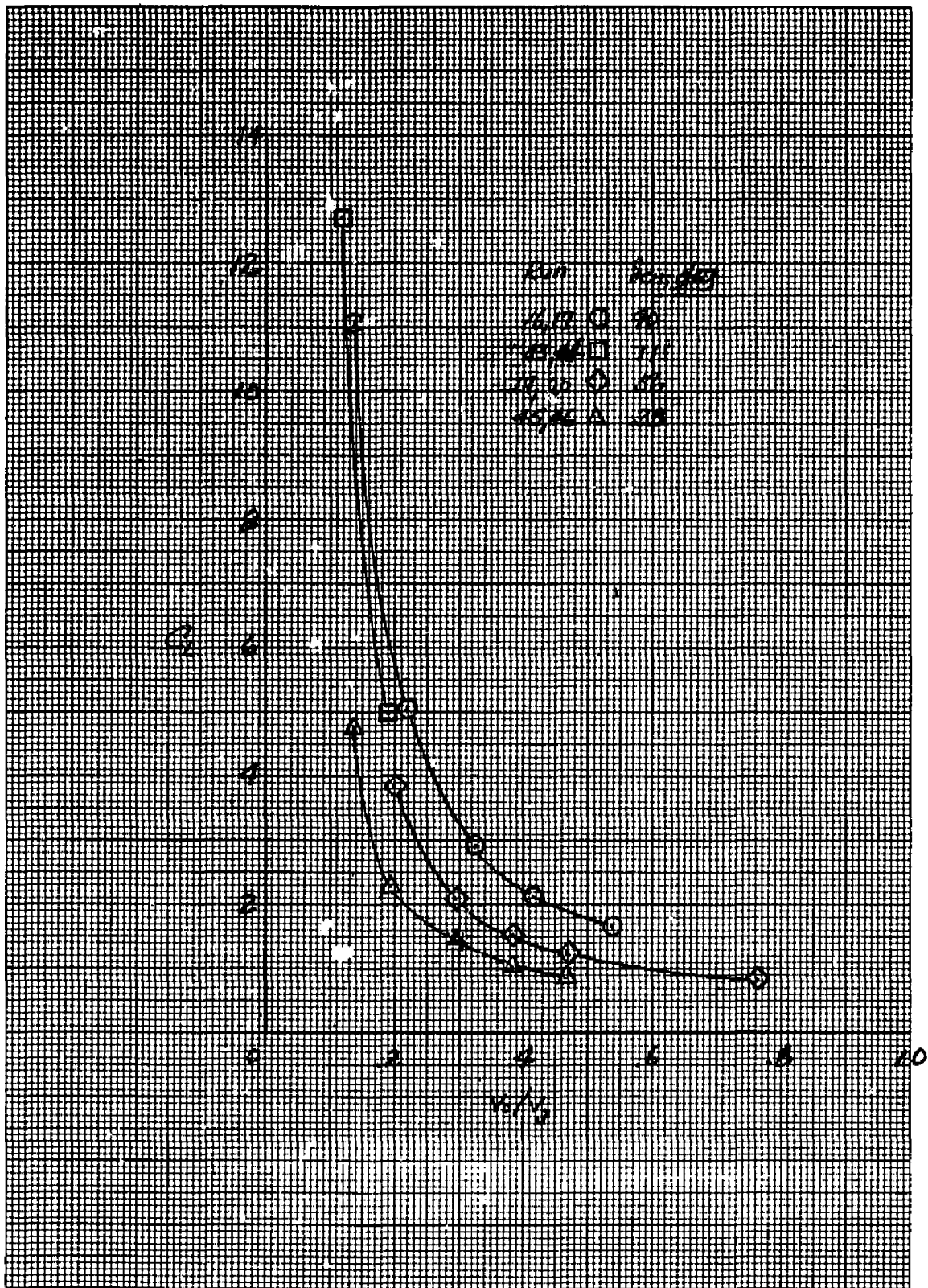
(c) Variation of C_L with V_o/V_j; lift/cruise fans operation only with forward fan inlet covered, $\beta_v = 0°$.

Figure 13.- Continued.

46
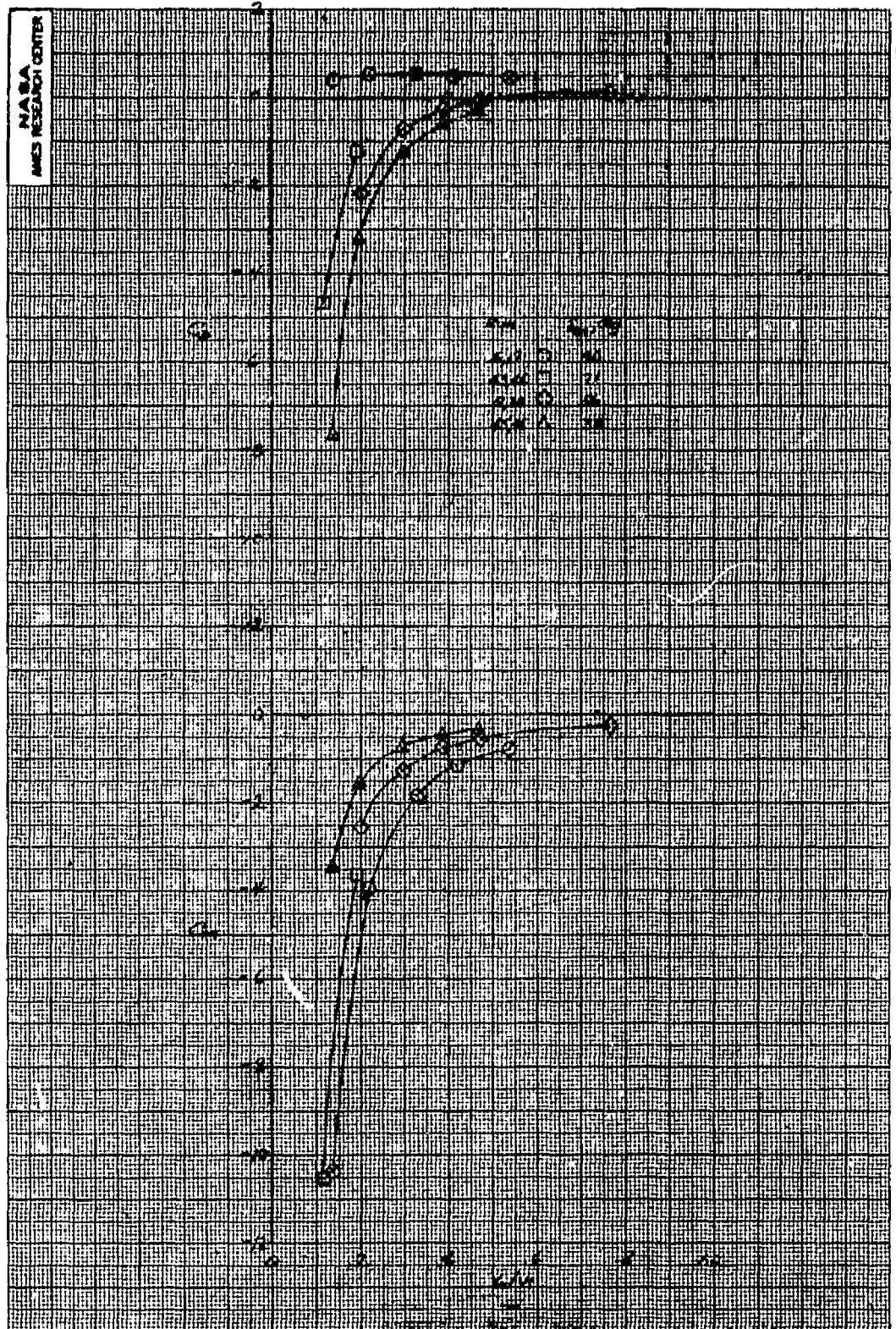
(d) Variation of C_D and C_m with V_o/V_j; lift/cruise fans operation only with forward fan inlet covered, $\beta_v = 0°$.

Figure 13.- Concluded.
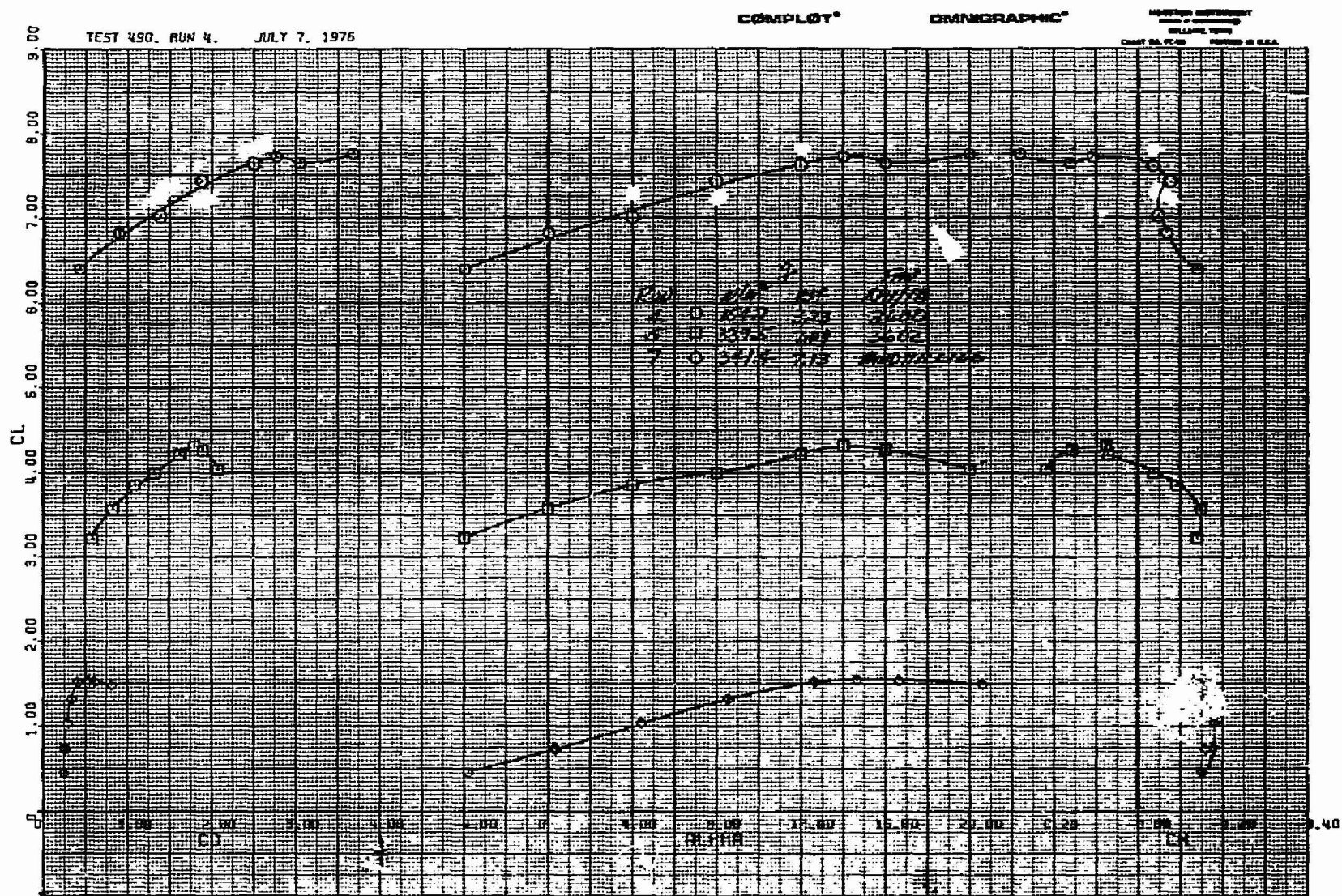
(a) $\delta_{cn} = 90°$, $\beta_v = 90°$

Figure 14.- Longitudinal characteristics of the model with three fans operating and with the horizontal tail installed; $\delta_f = 15°$, $\delta_{ail} = 10°$, $i_t = 0°$, $\beta = 0°$, $\delta_R = 0°$.
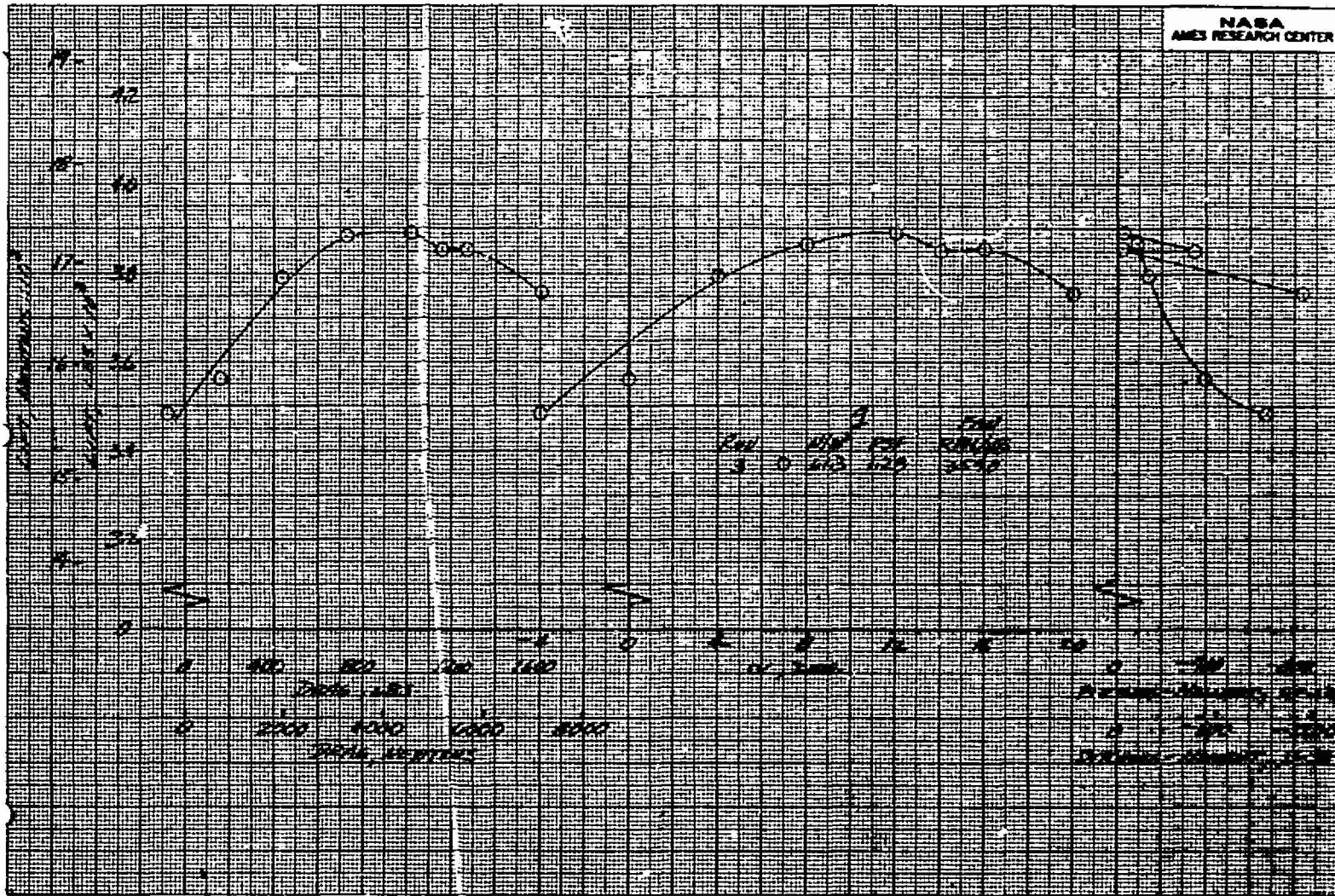
(b) $\delta_{cn} = 90°$, $\beta_v = 90°$

Figure 14.– Continued.
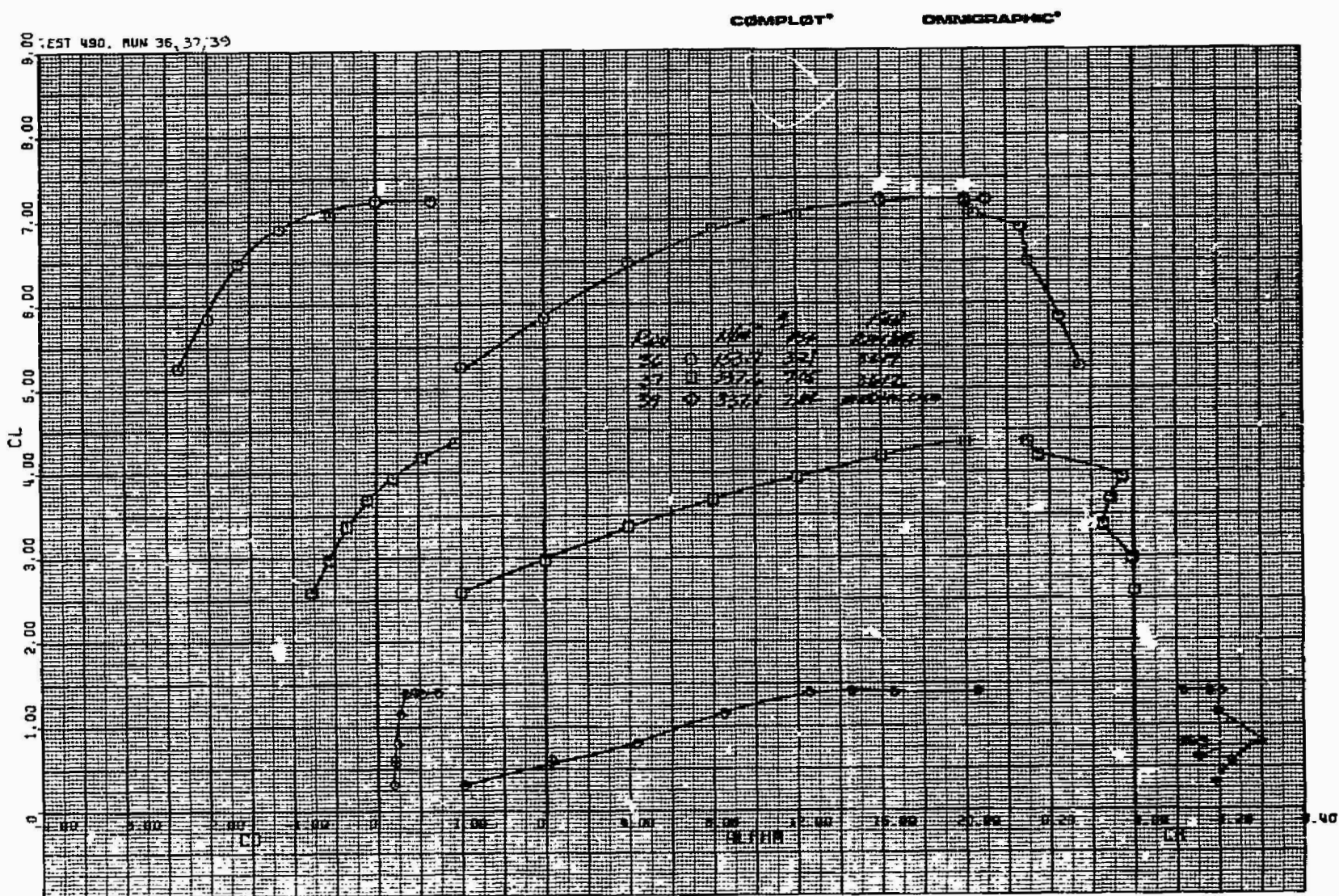
(c) $\delta_{cn} = 71°$, $\beta_v = 55°$

Figure 14.- Continued.
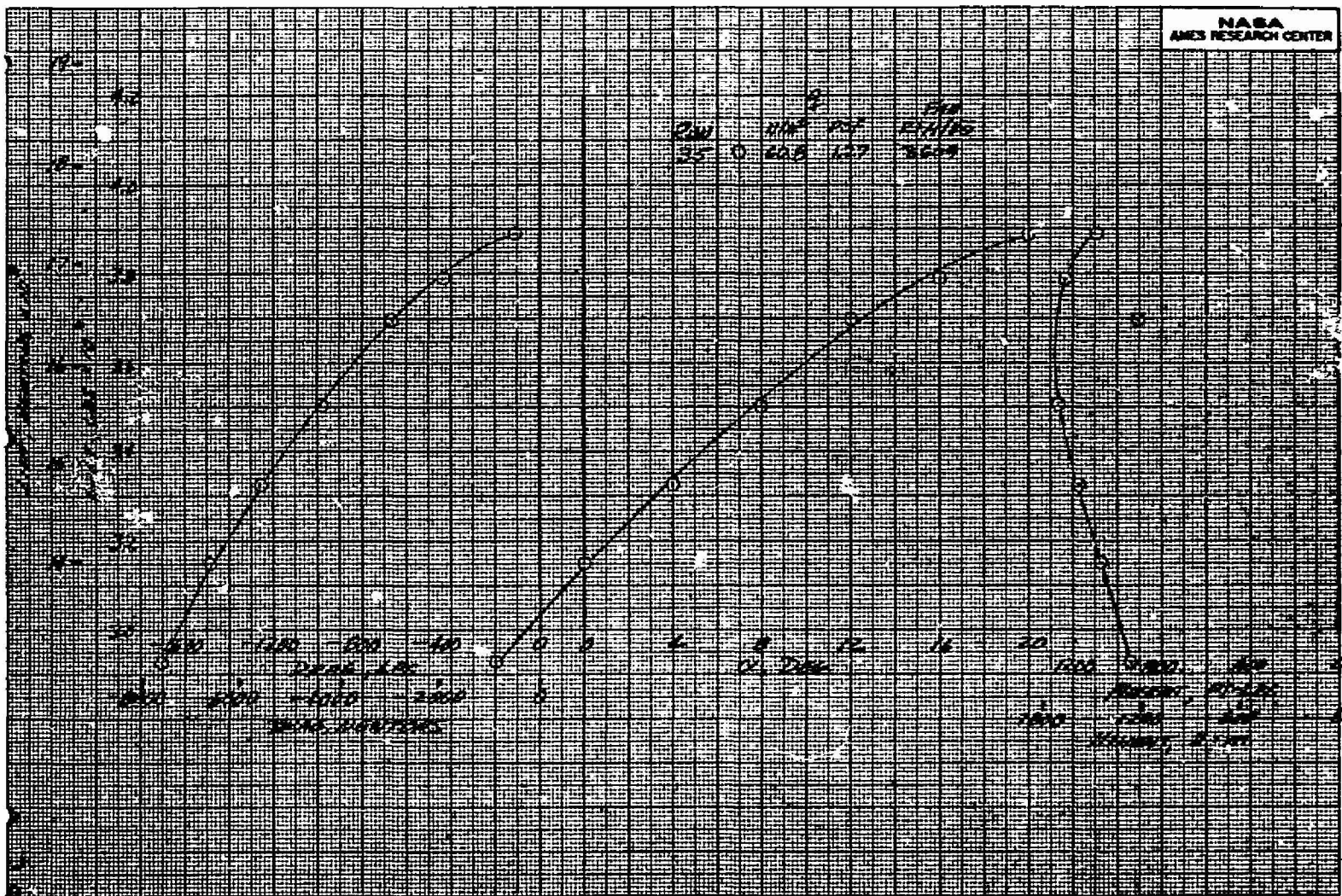
(d) $\delta_{cn} = 71°$, $\beta_v = 55°$

Figure 14.- Continued.
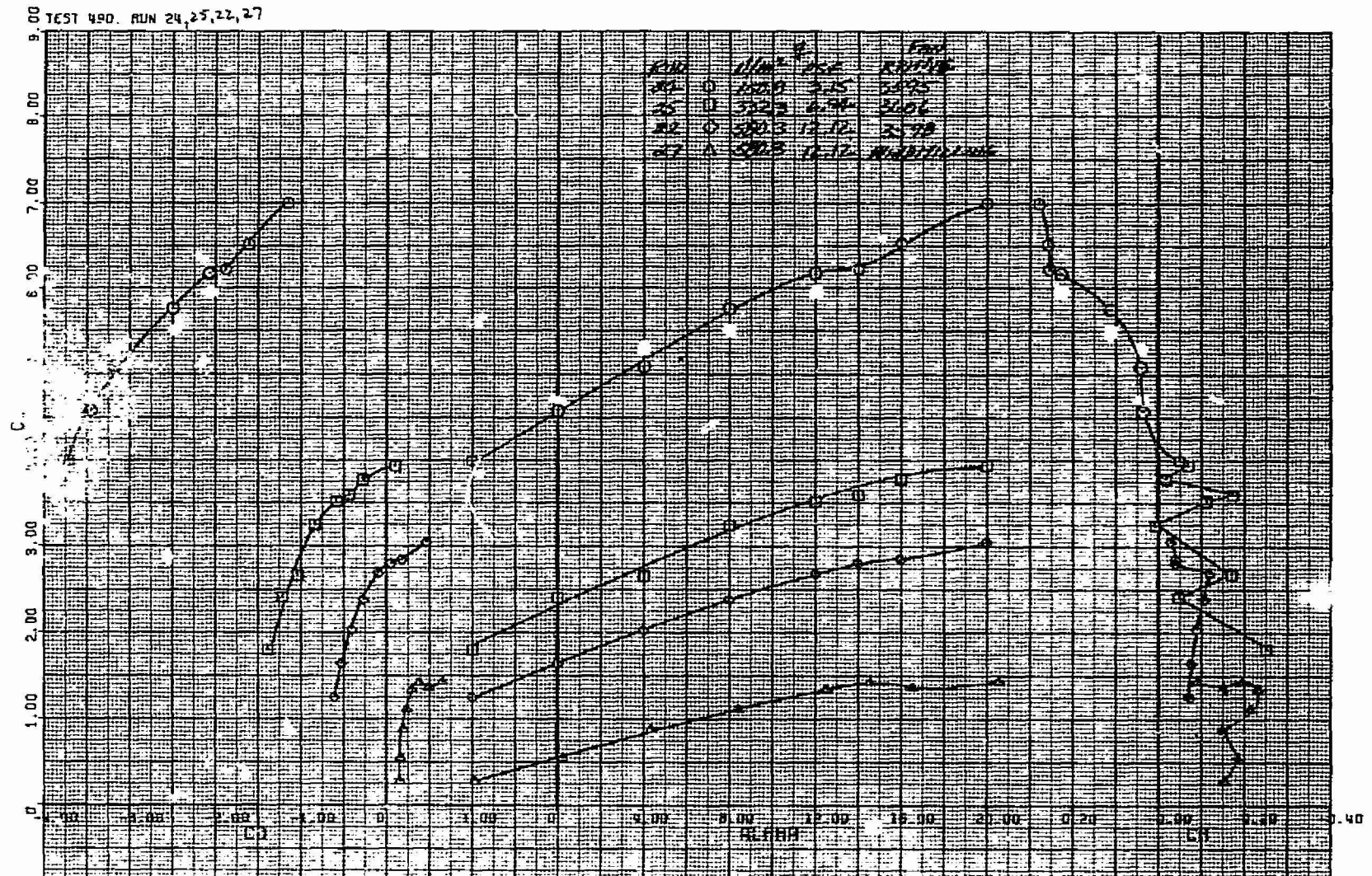
(e) $\delta_{cn} = 56°$, $\beta_v = 43°$

Figure 14.- Continued.

53
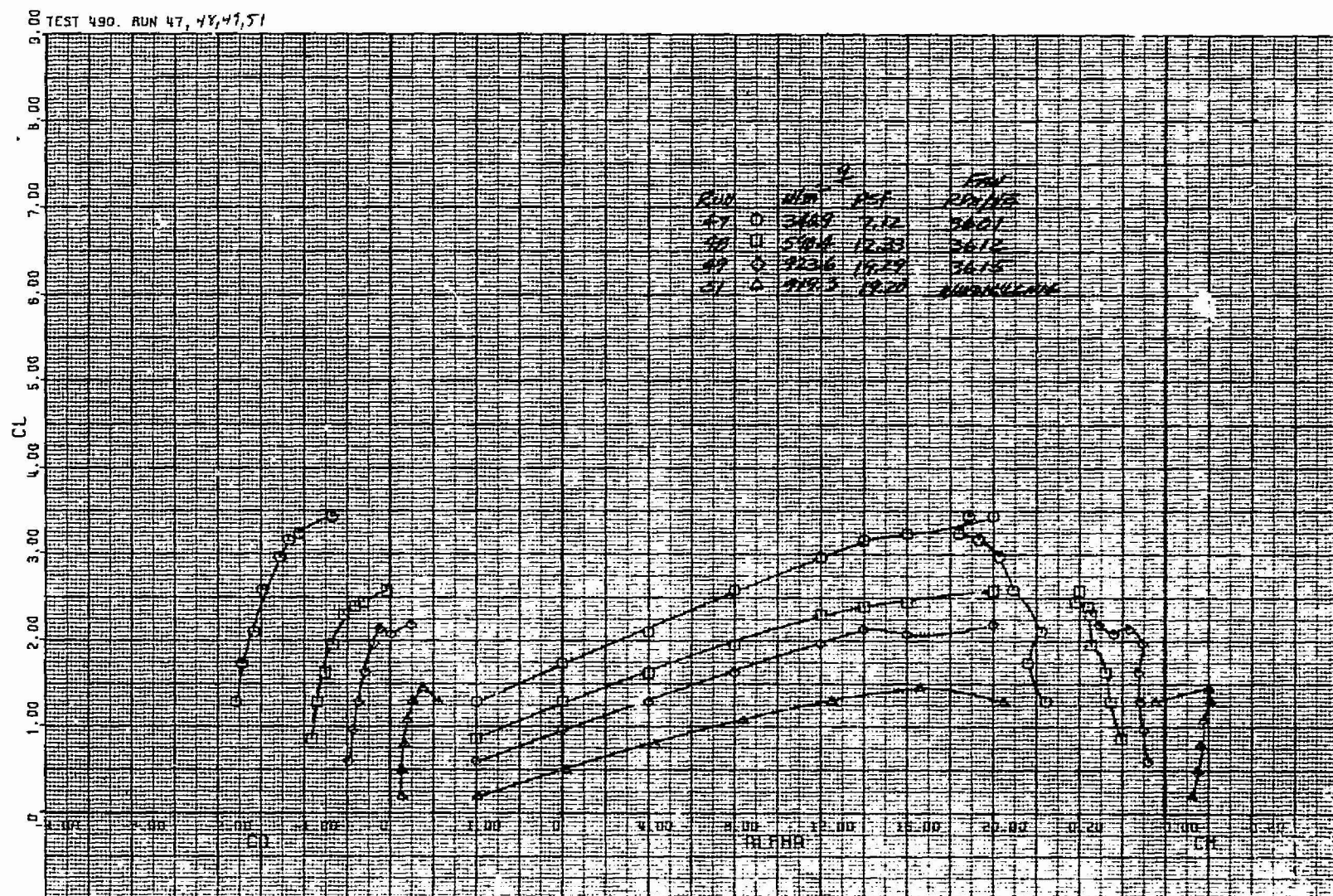
(f) $\delta_{cn} = 38°$, $\beta_v = 43°$

Figure 14.- Concluded.
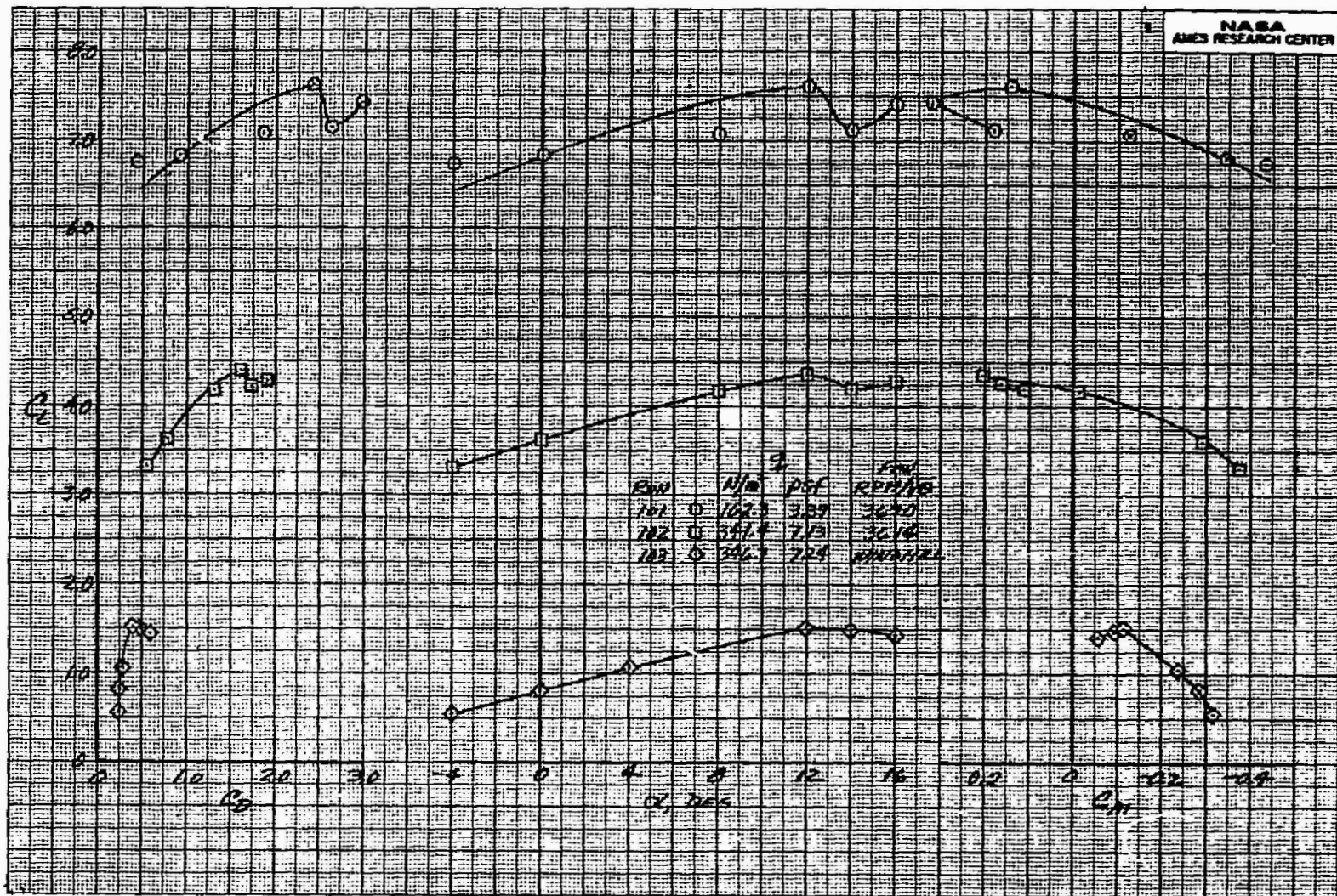
(a) $\delta_{cn} = 90°$, $\beta_v = 90°$

Figure 15.- Longitudinal characteristics of the model with three fans operating; horizontal tail off, $\delta_f = 15°$, $\delta_{ail} = 10°$, $\delta_R = 0°$, $\beta = 0°$.

55
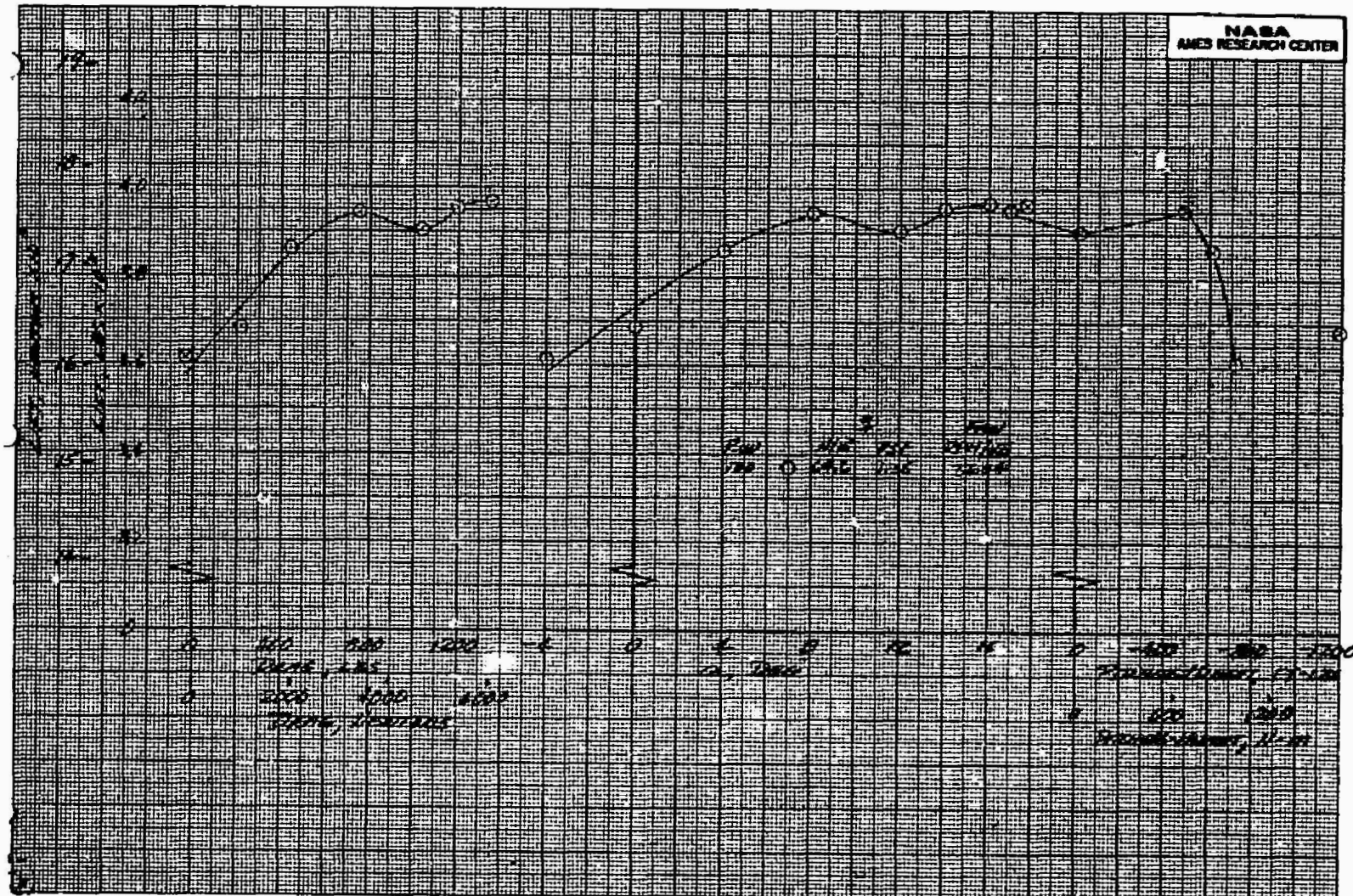
(b) $\delta_{cn} = 90°$, $\beta_v = 90°$

Figure 15.- Continued.
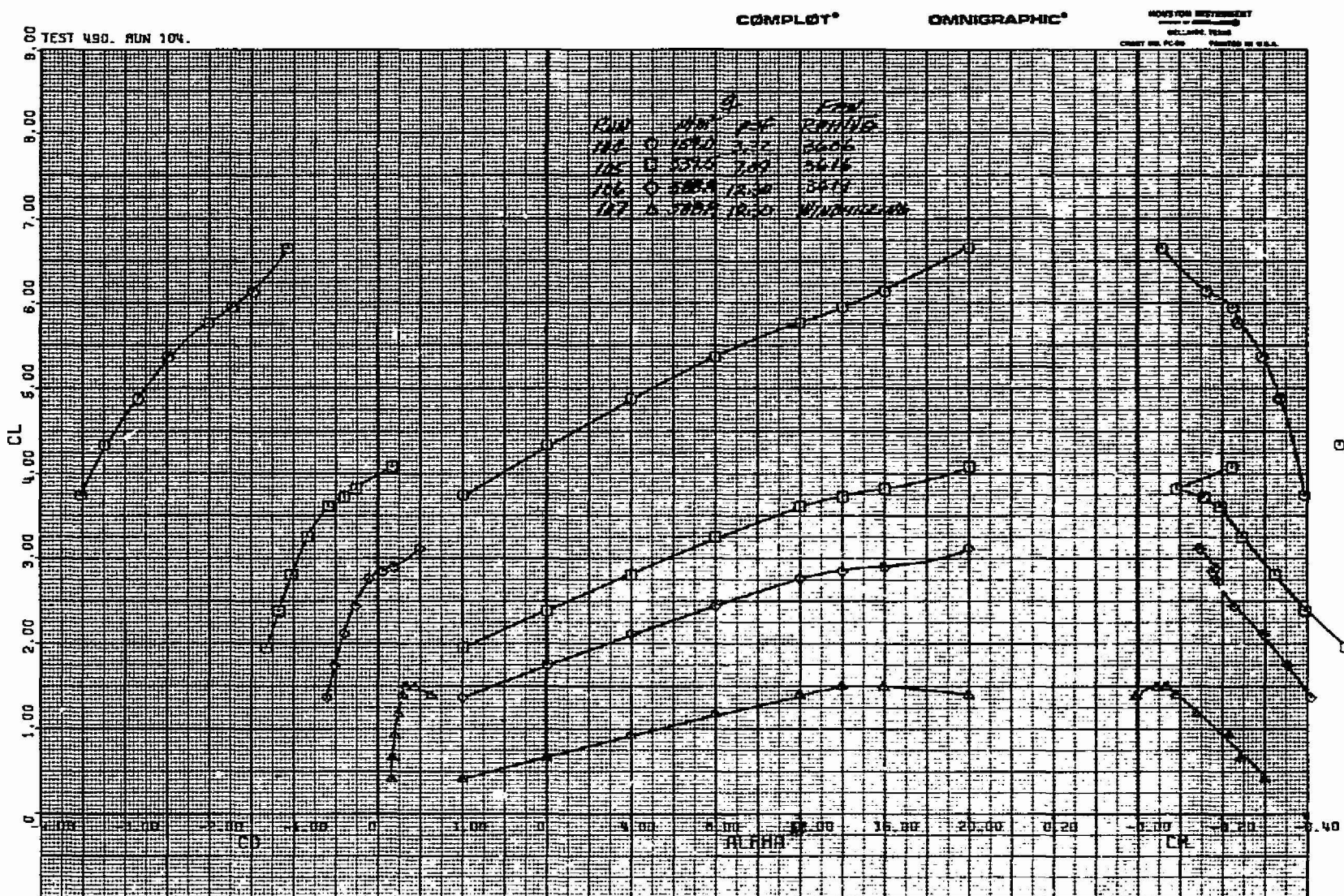
(c) $\delta_{cn} = 56°$, $\beta_v = 43°$

Figure 15.- Concluded.
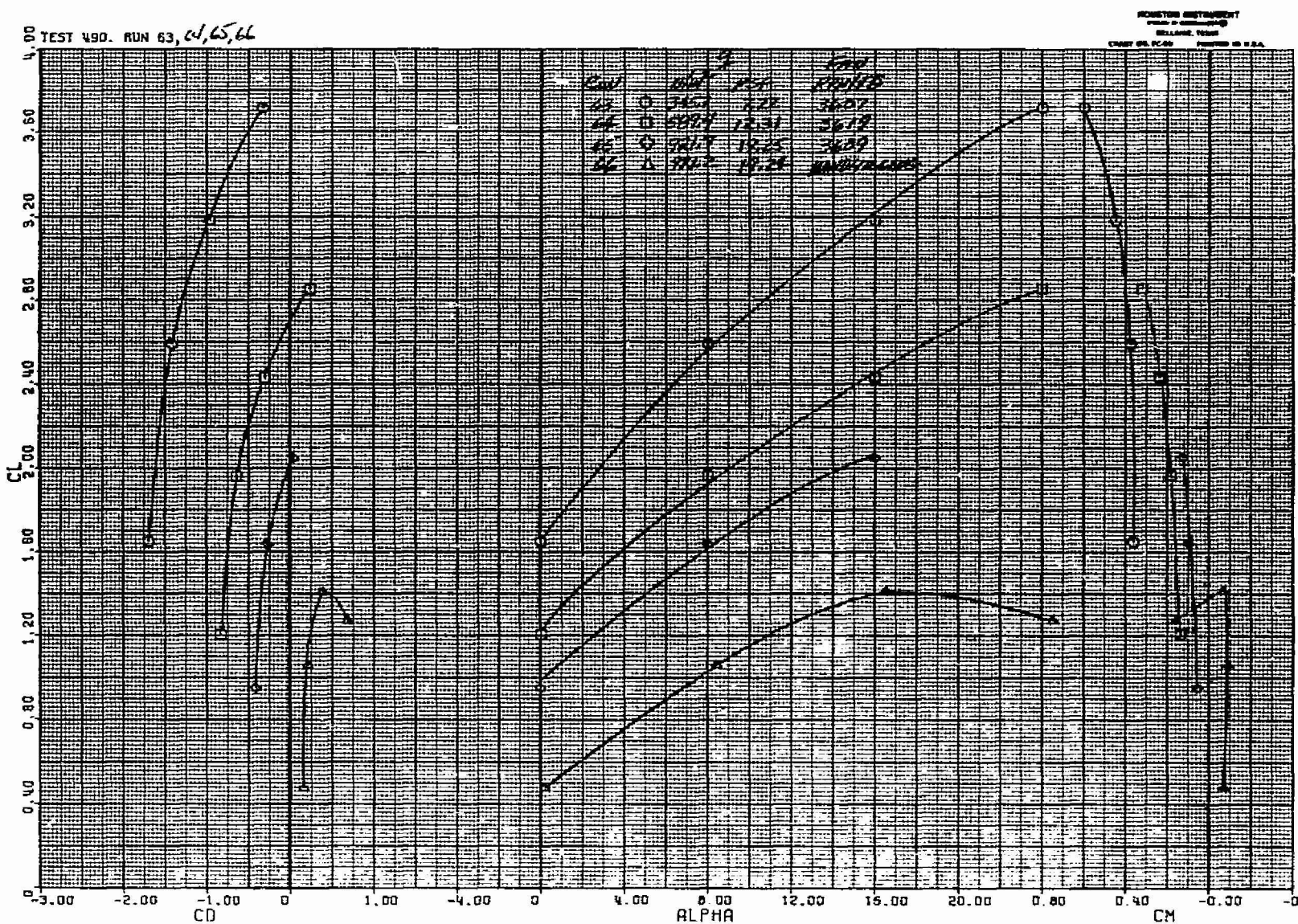
(a) Longitudinal characteristics

Figure 16.- Aerodynamic characteristics of the model with three fans operating and the rudder deflected; $\delta_R = 23°$, $\delta_{cn} = 38°$, $\beta_v = 43°$, $\delta_f = 15°$, $\delta_{ail} = 10°$, $\beta = 0°$, $i_t = 0°$.
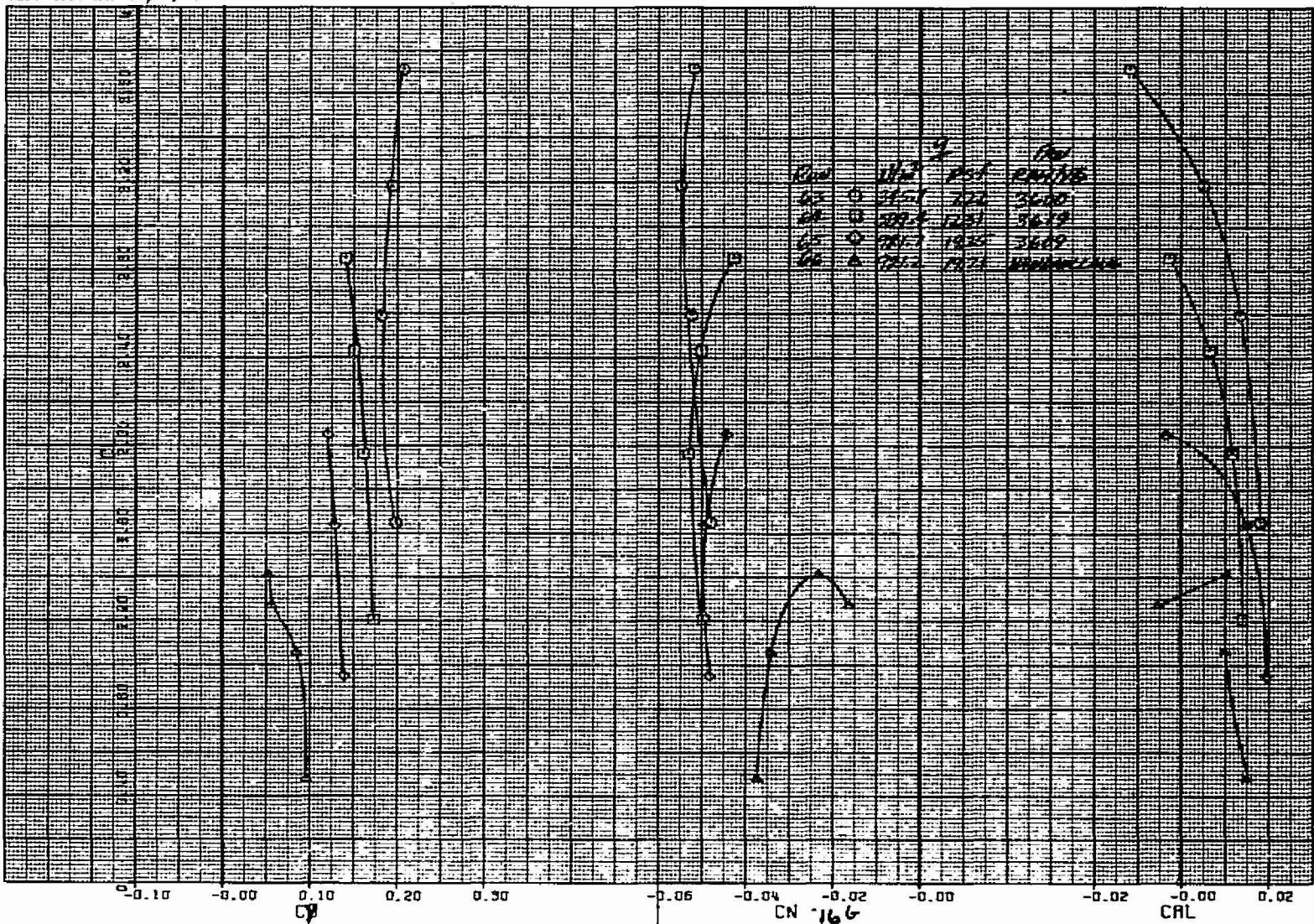
(b) Lateral characteristics

Figure 16.- Concluded.
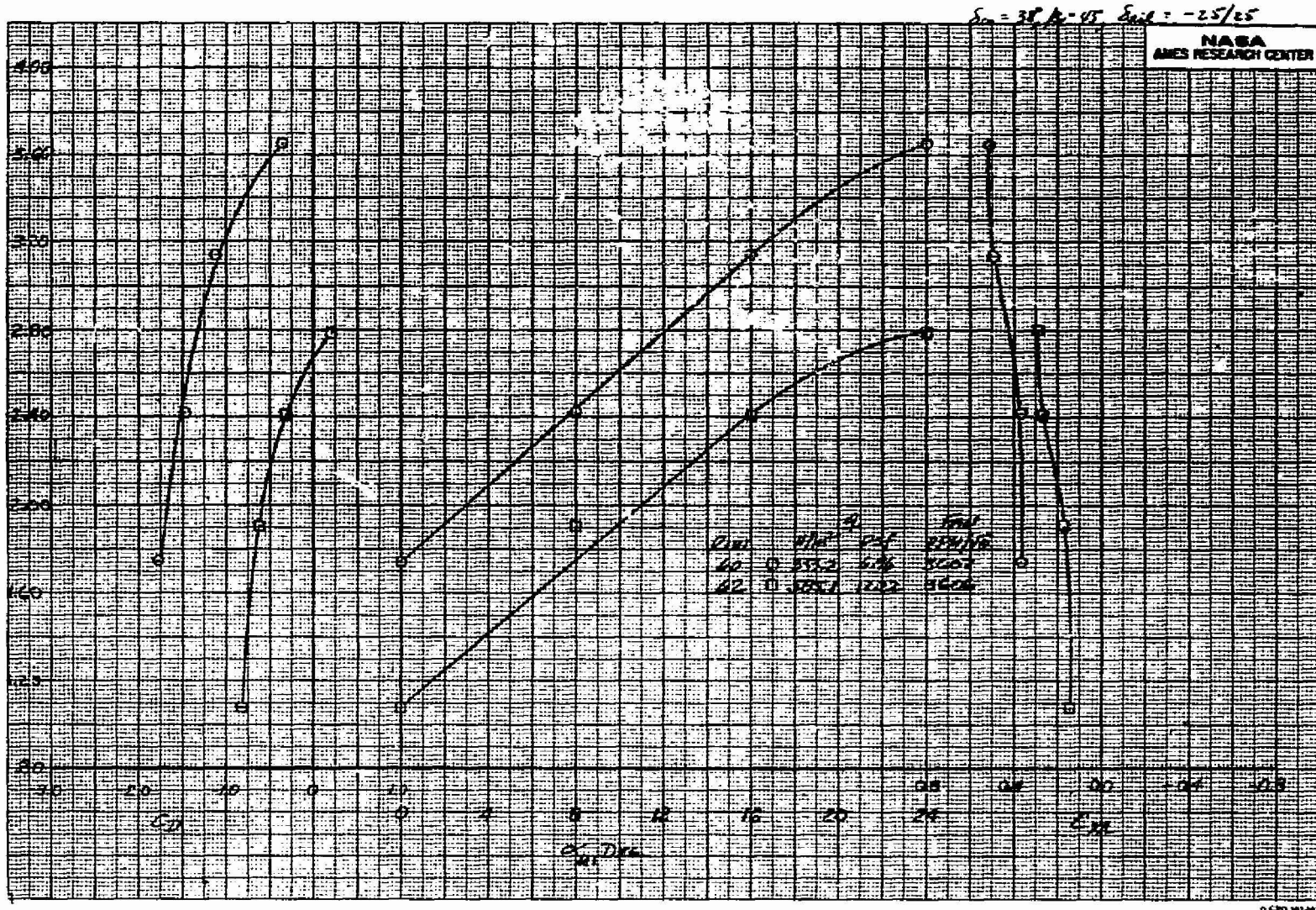
(a) Longitudinal characteristics

Figure 17.- The effect of differential aileron deflection on the model aerodynamic characteristics with three fans operating; $\delta_{ail} = -25°/25°$, $\delta_{cn} = 38°$, $\beta_v = 43°$, $\delta_f = 15°$, $i_t = 0°$, $\beta = 0°$, $\delta_R = 0°$.
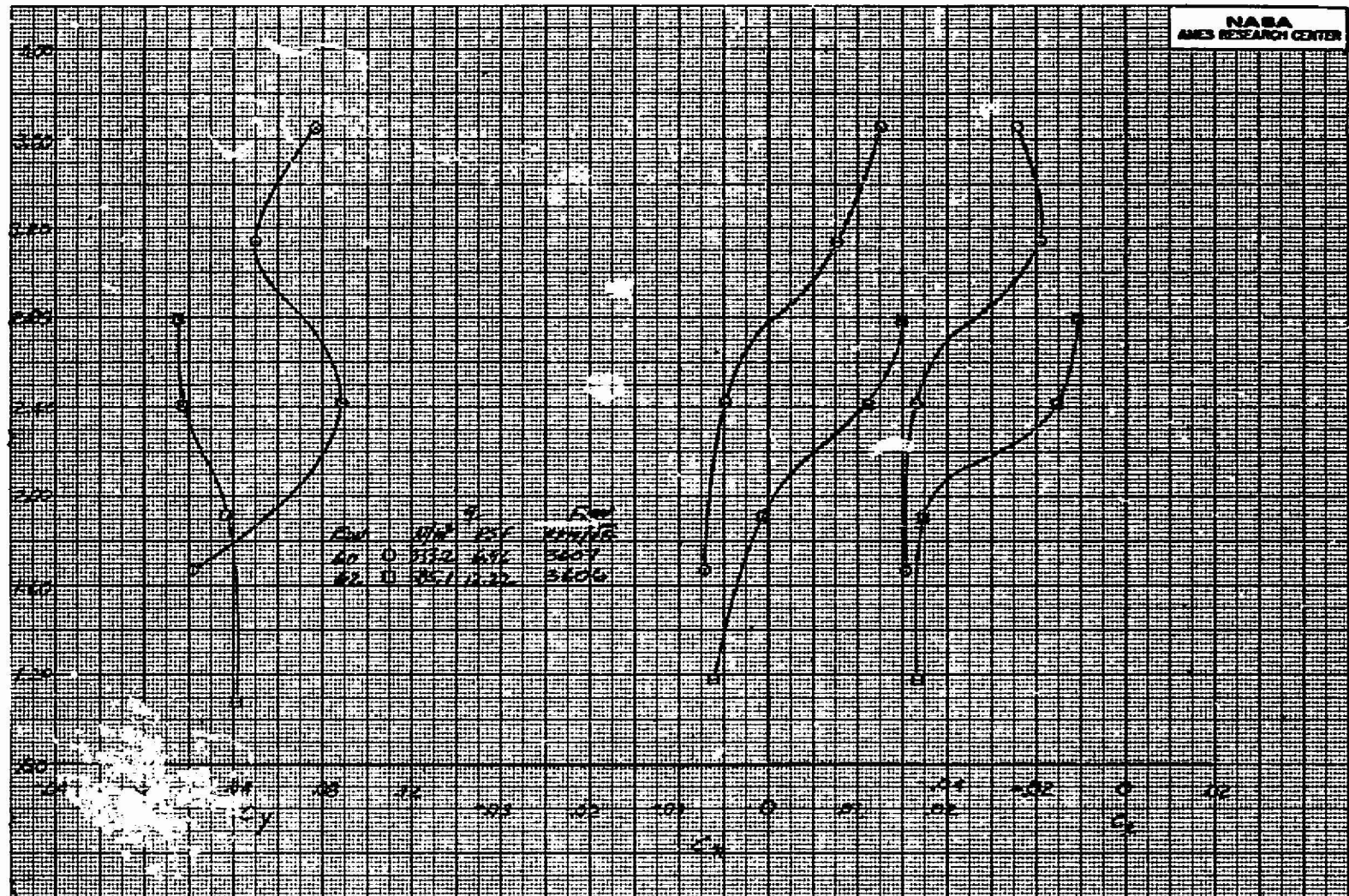
(b) Lateral characteristics

Figure 17.- Concluded.
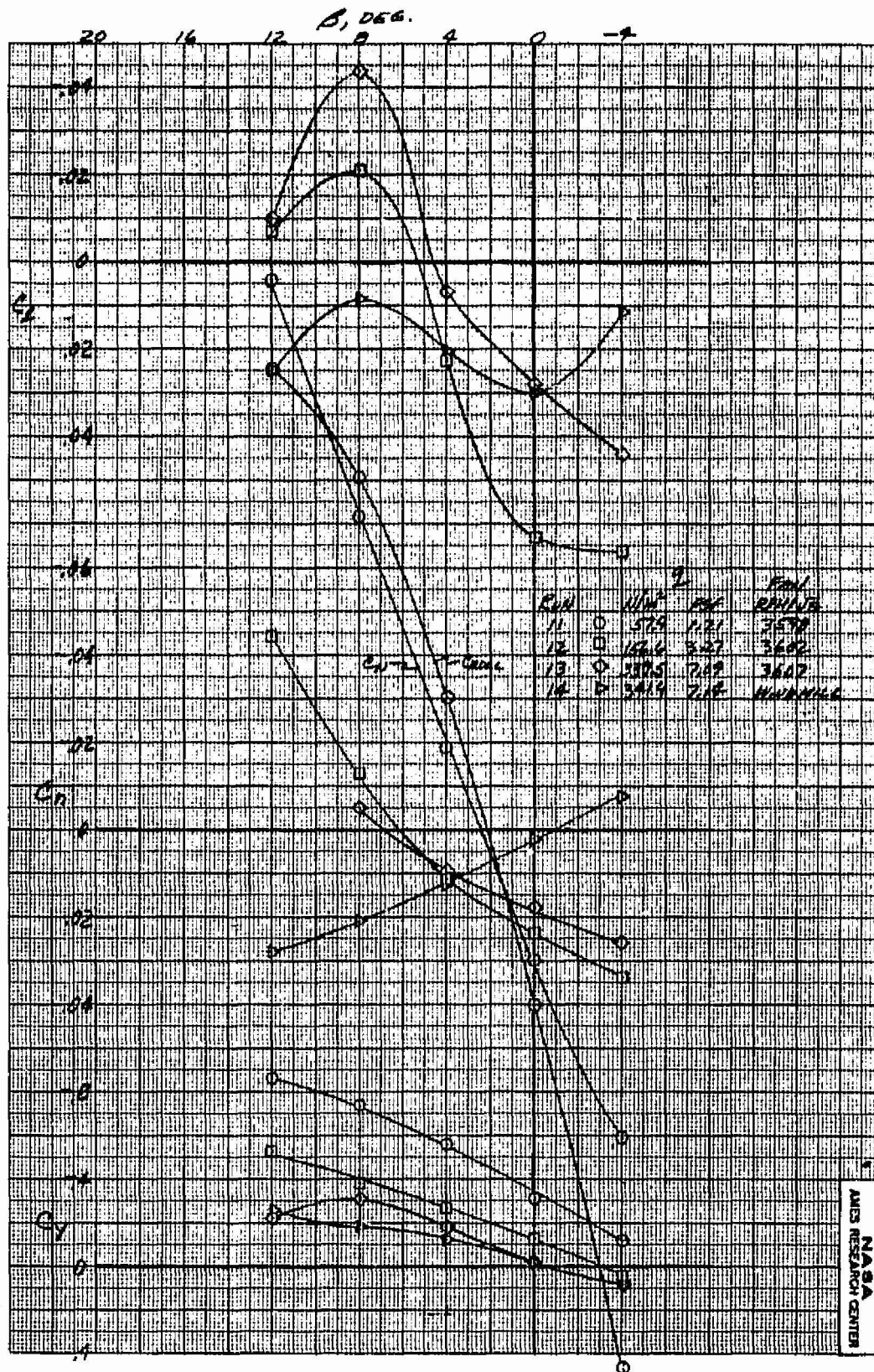
(a) $\delta_{cn} = 90°$, $\beta_v = 90°$, $\alpha_u = 0°$

Figure 18.- Variation of side-force, yawing-moment, and rolling-moment coefficients with sideslip and with three fans operating; $\delta_f = 15°$, $\delta_{ail} = 10°$, $i_t = 0°$, $\delta_R = 0°$.

61
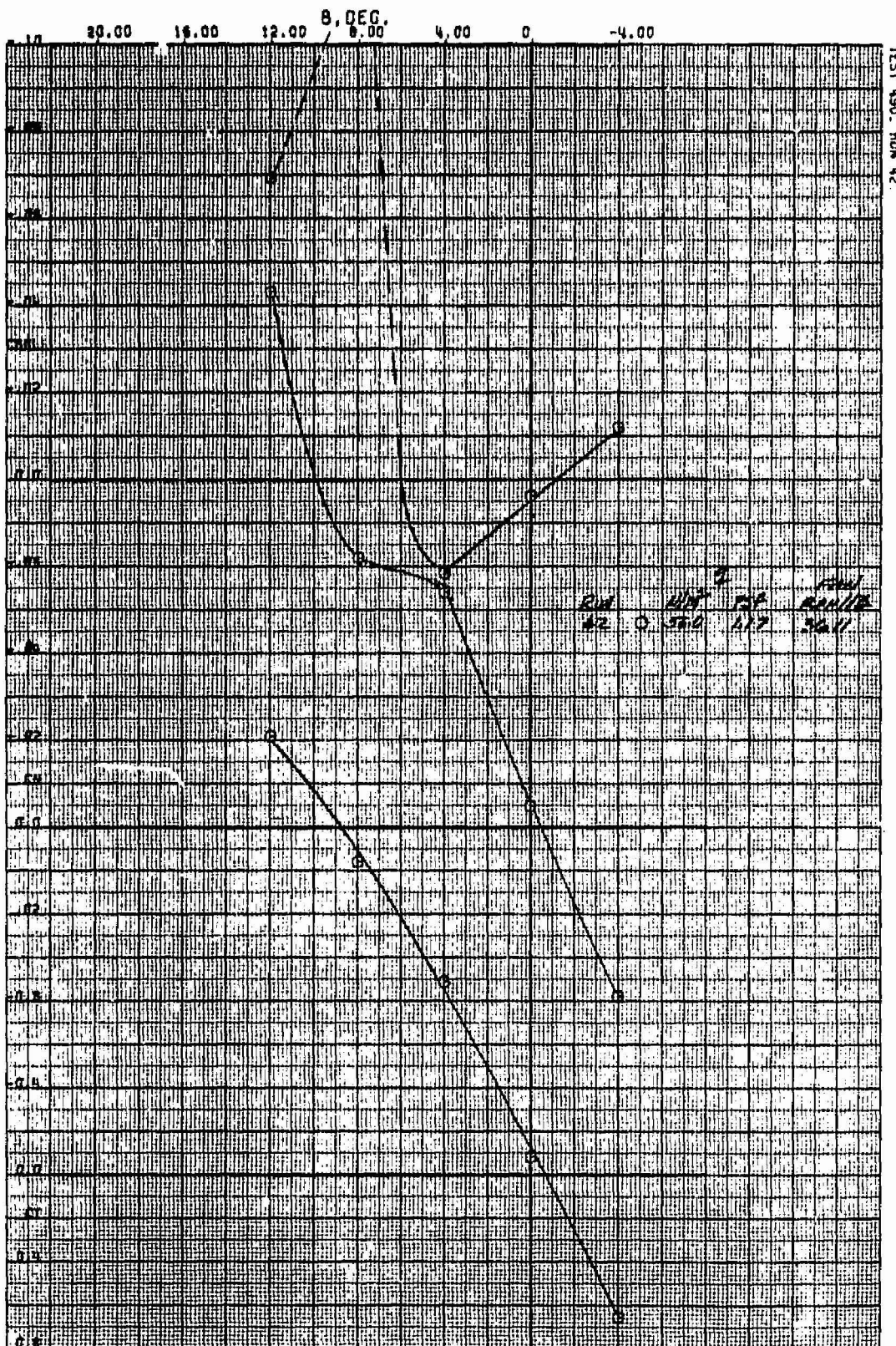
(b) $\delta_{cn} = 71°$, $\beta_v = 55°$, $\alpha_u = 0°$

Figure 18.- Continued.

62
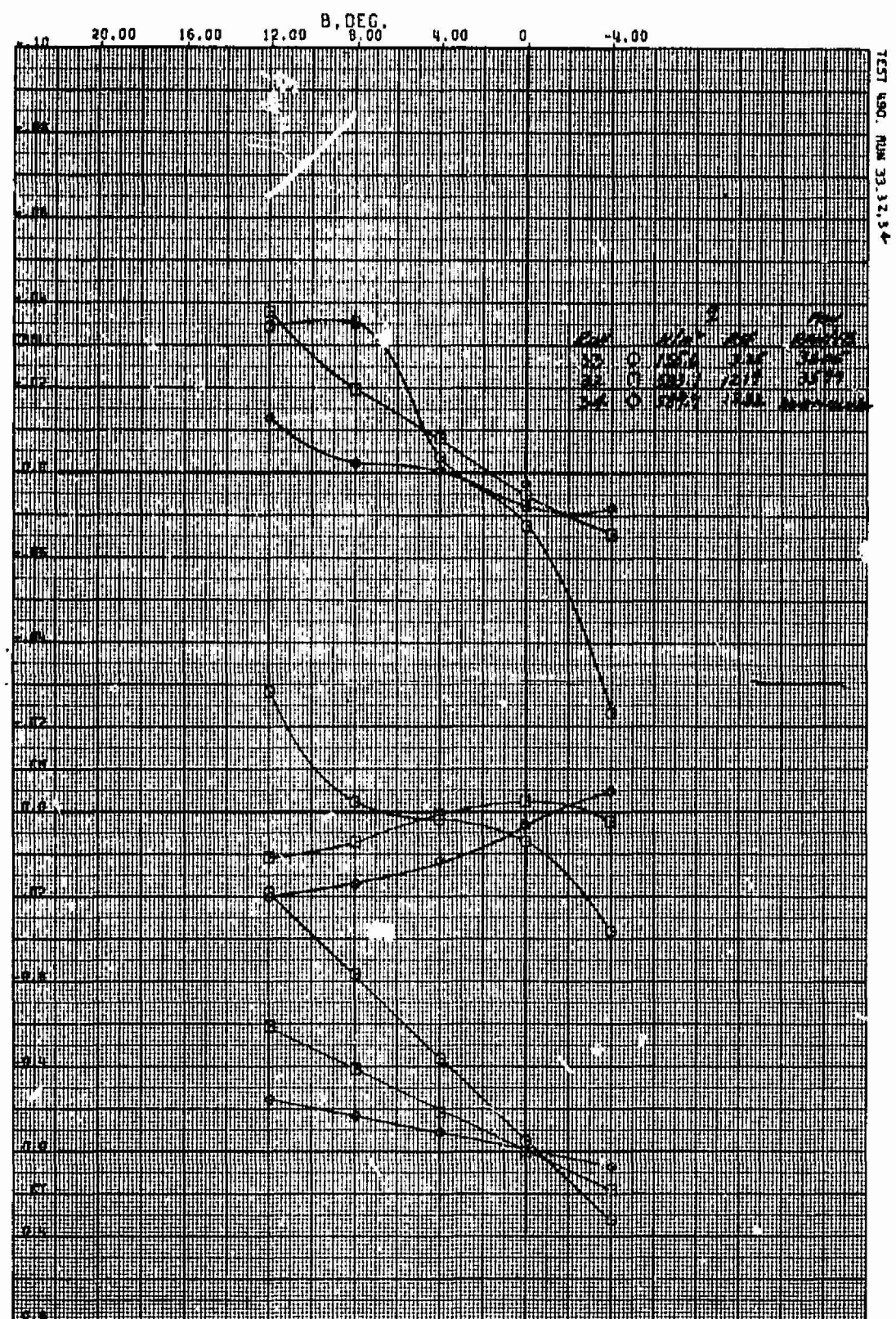
(c) $\delta_{cn} = 56°$, $\beta_v = 43°$. $\alpha_u = 0°$

Figure 18.- Continued.

63
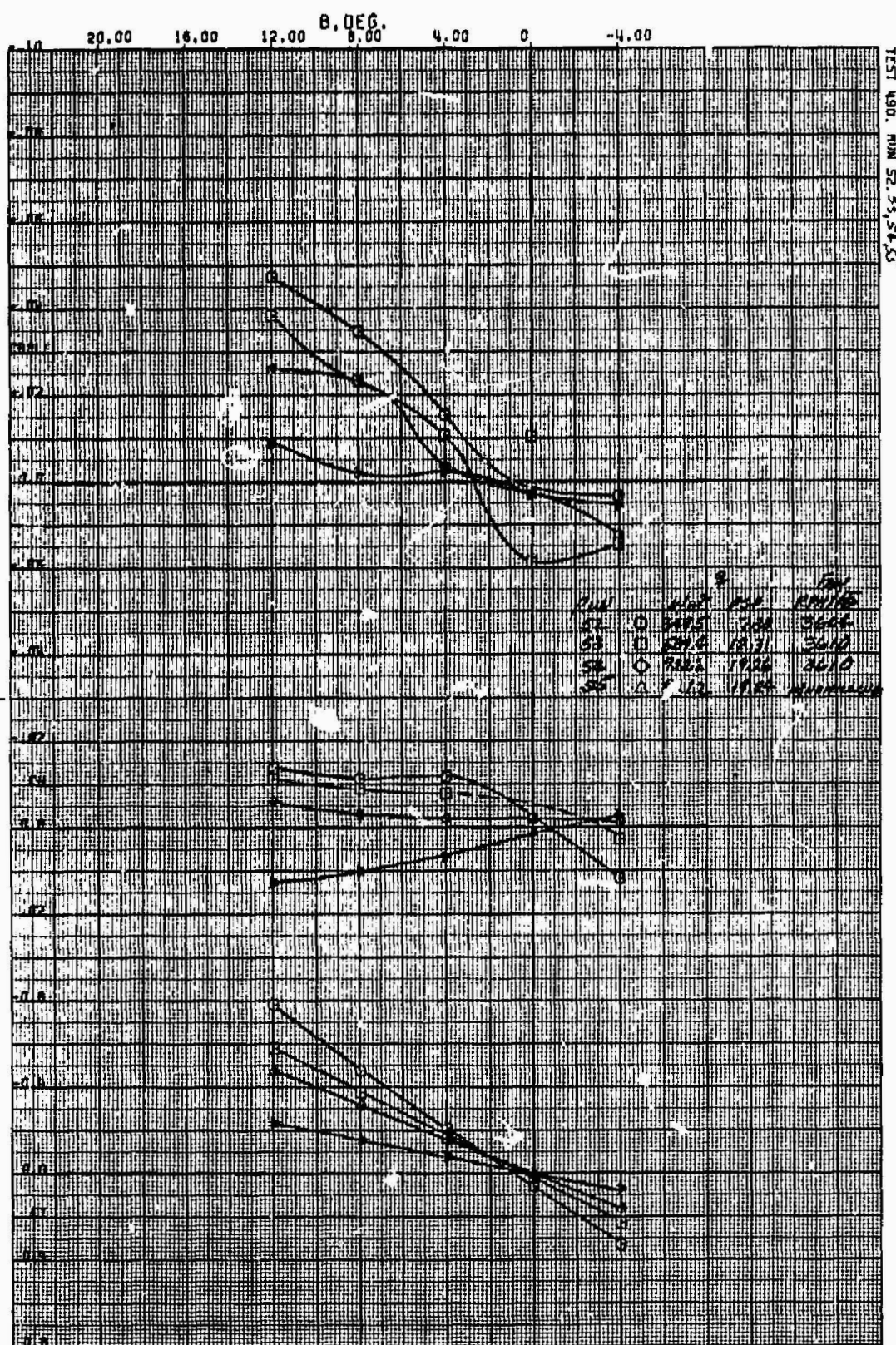
(d) $\delta_{cn} = 38°$, $\beta_v = 43°$, $\alpha_u = 0°$

Figure 18.- Concluded.
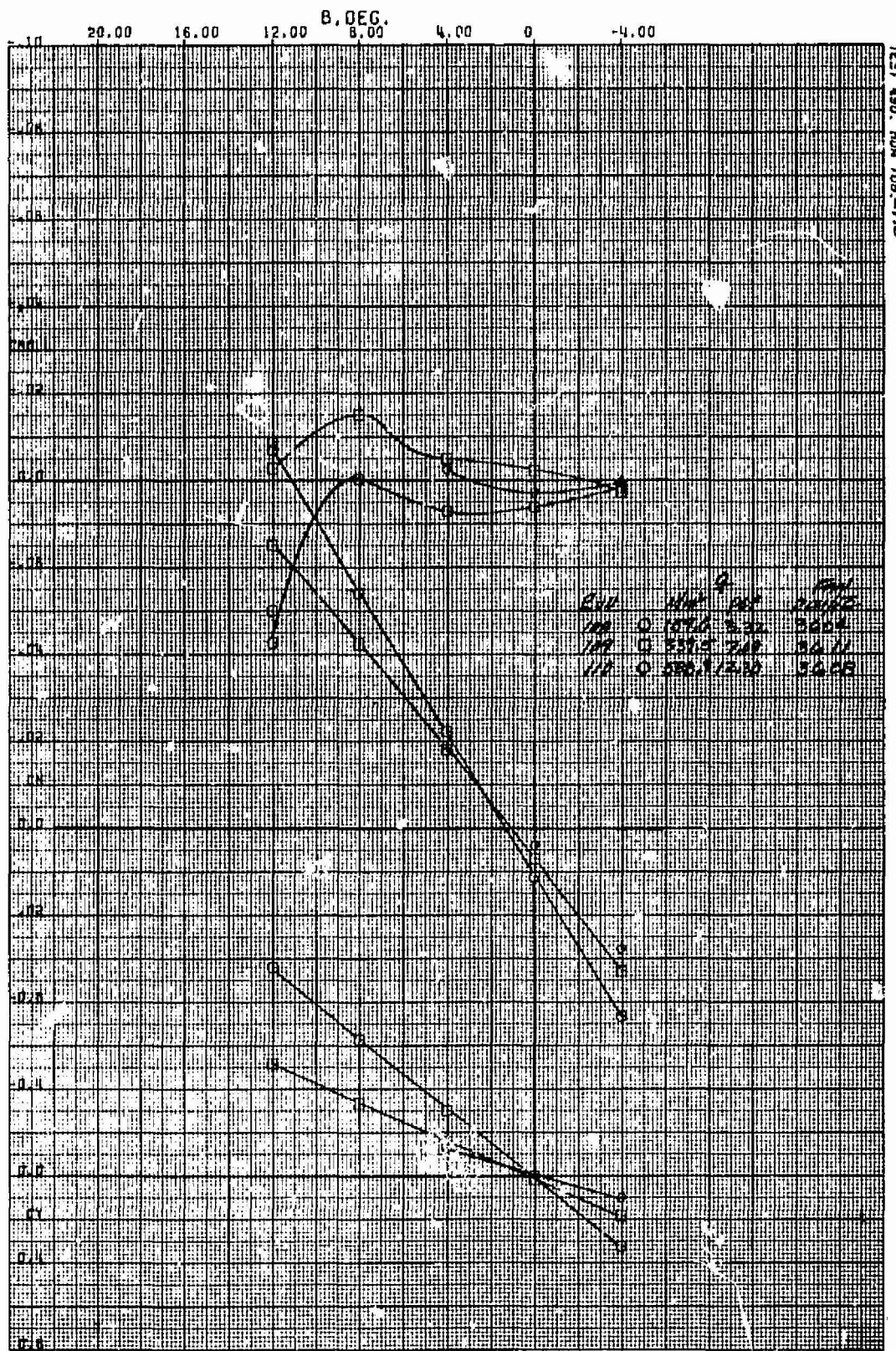
Figure 19.- Variation of side-force, yawing-moment, and rolling-moment coefficients with sideslip, and with three fans operating; horizontal and vertical tails off, $\delta_{cn} = 56°$, $\beta_v = 43°$, $\delta_f = 15°$, $\delta_{ail} = 10°$, $\alpha_u = 0°$.

65
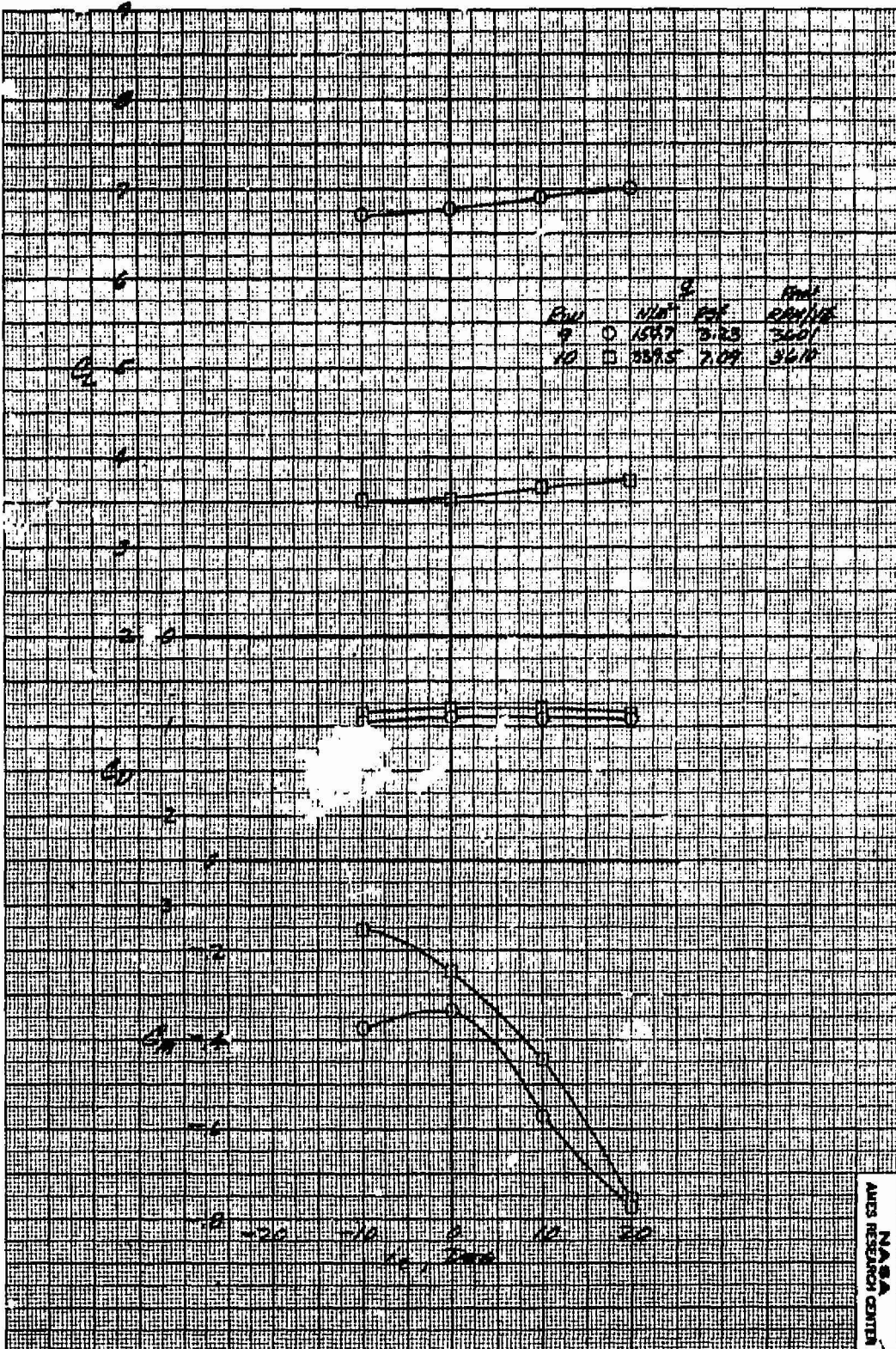
(a) $\alpha_u = 0°$

Figure 20.- The effect of tail incidence on the longitudinal aerodynamic characteristics with three fans operating; $\delta_{cn} = 90°$, $\beta_v = 90°$, $\delta_f = 15°$, $\delta_{ail} = 10°$, $\beta = 0°$, $\delta_R = 0°$.
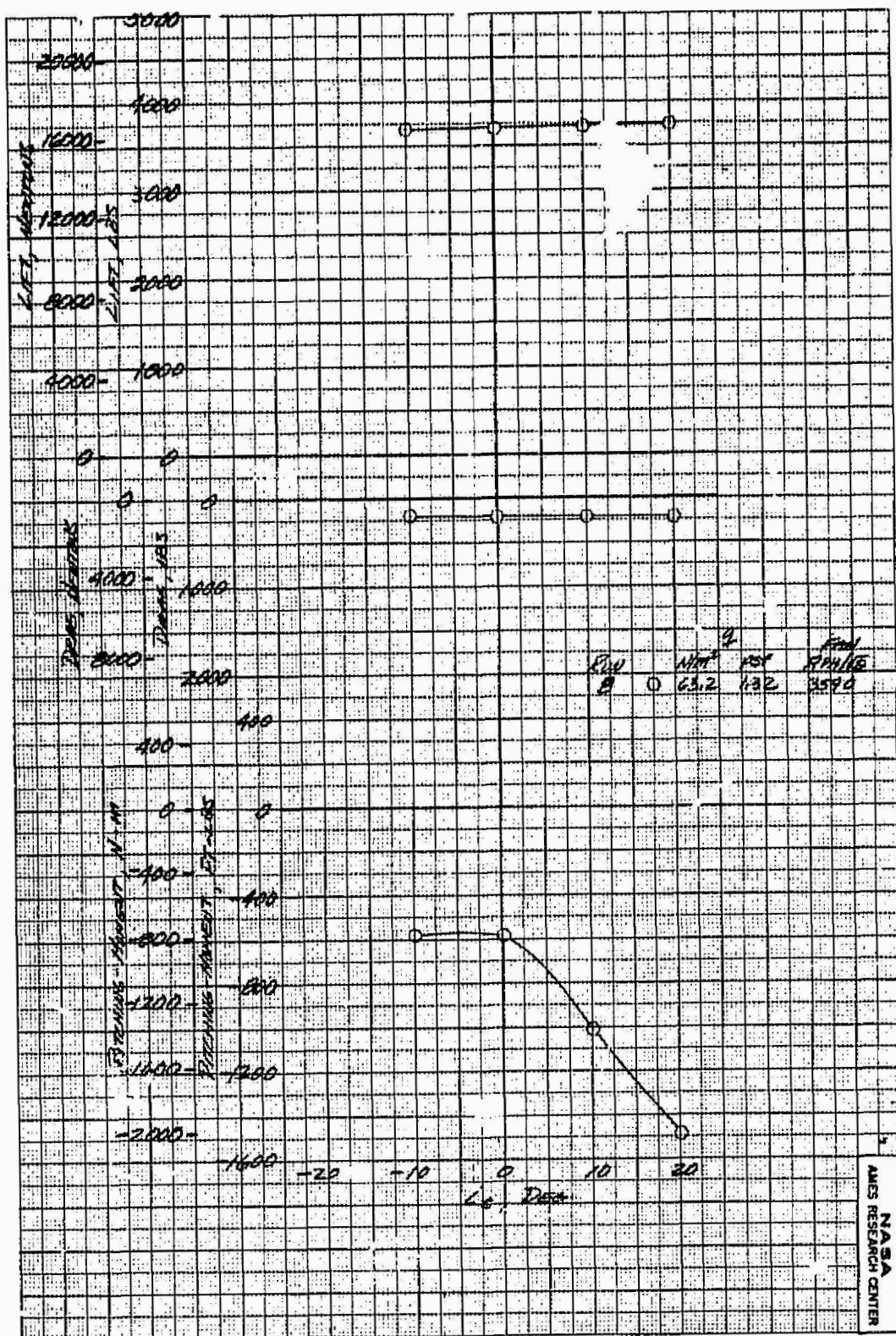
(b) $\alpha_u = 0°$

Figure 20.- Continued.

67

(c) $\alpha_u = 8°$

Figure 20.- Continued.

68

(d) $\alpha_u = 8°$
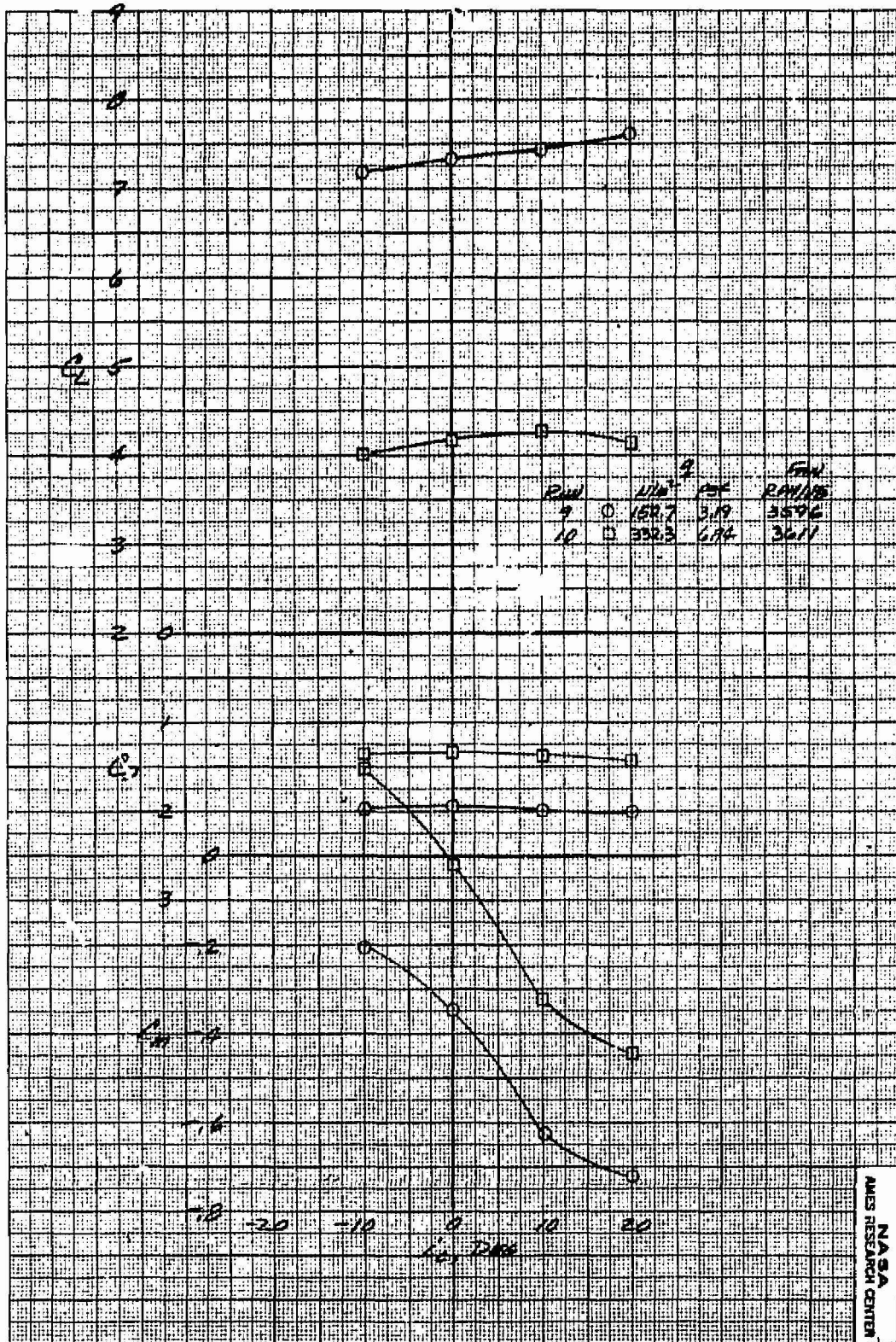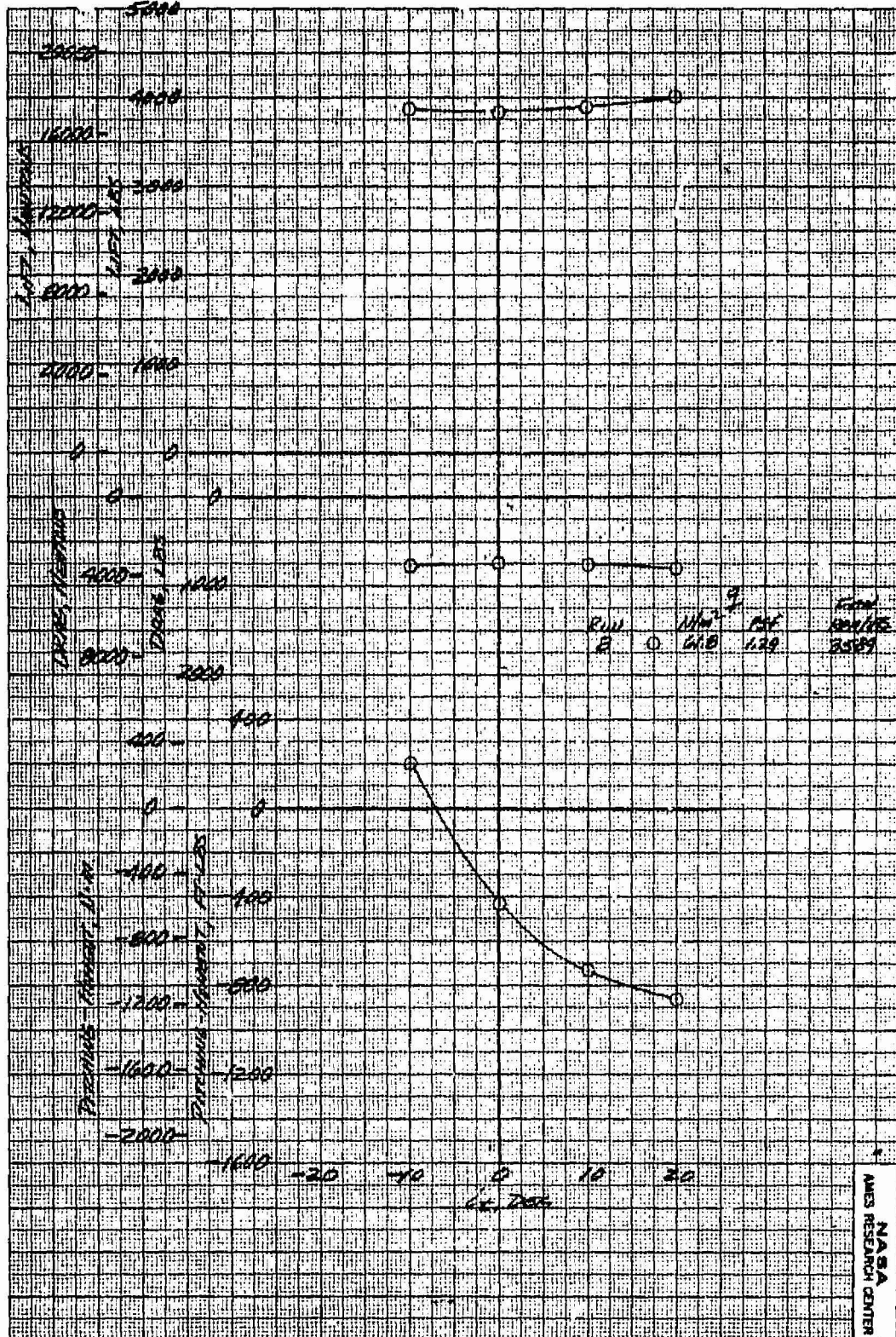
Figure 20.- Continued.
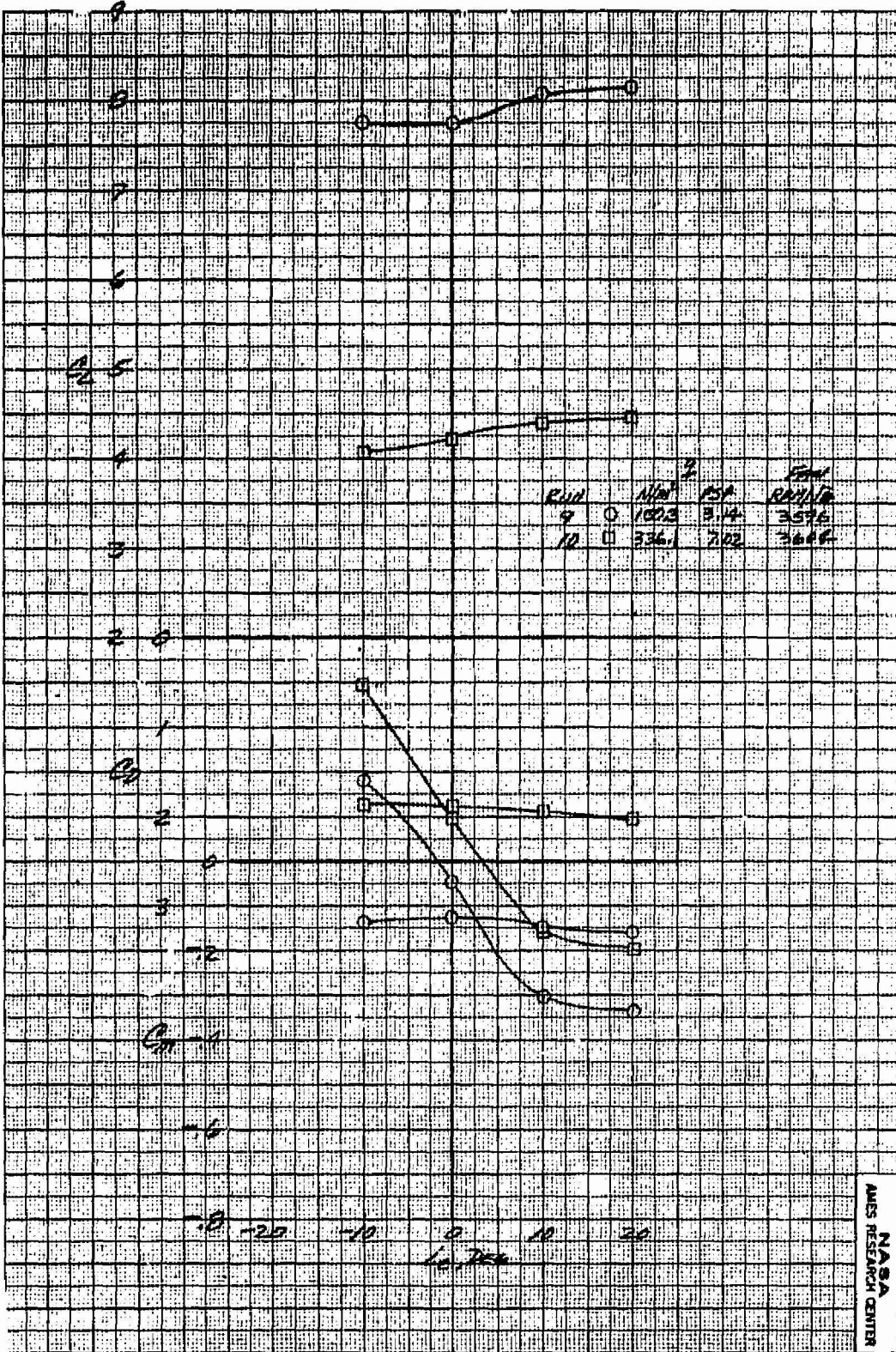
(e) $\alpha_u = 16°$

Figure 20.- Continued.

70
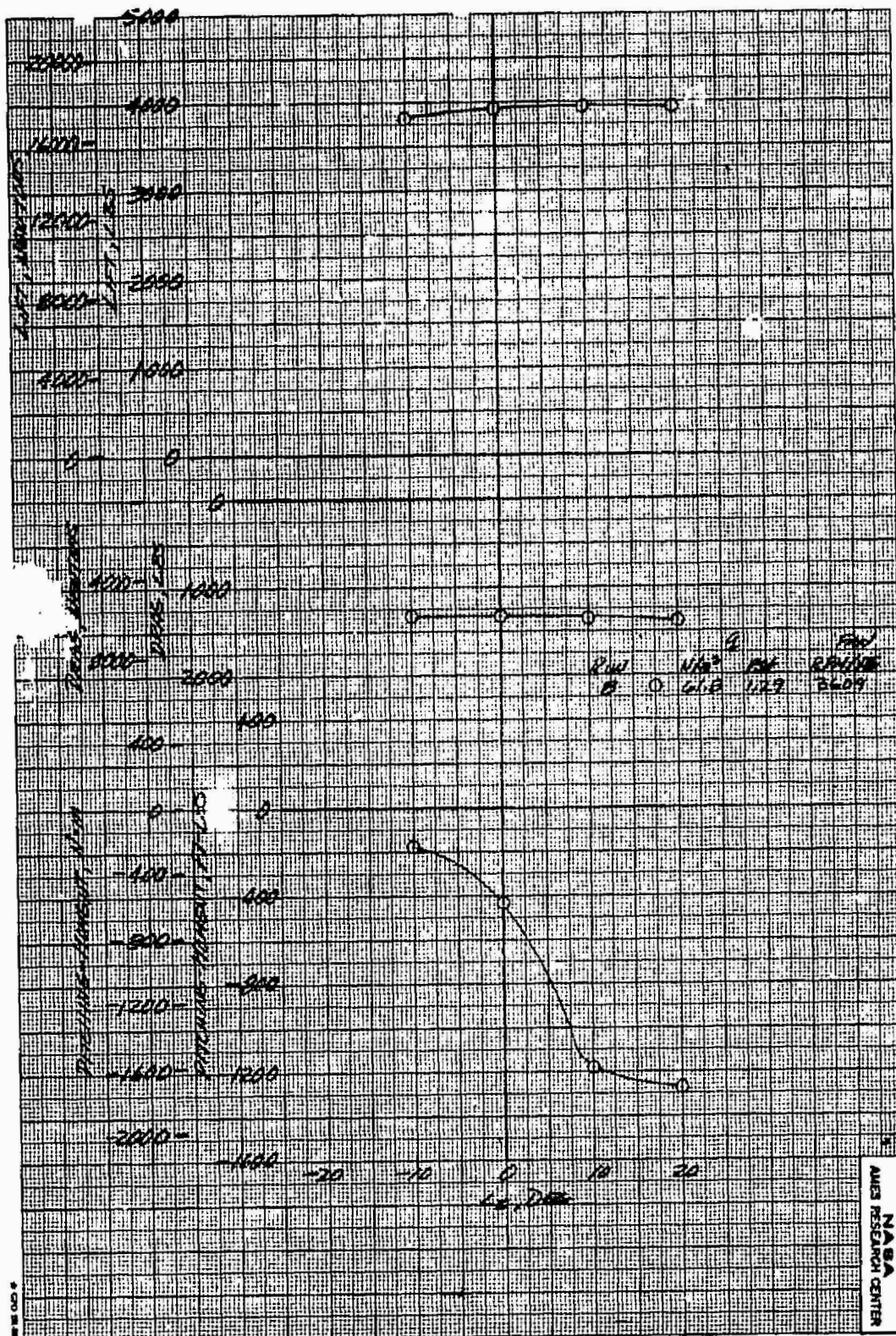
(f) $\alpha_u = 16°$

Figure 20.- Concluded.
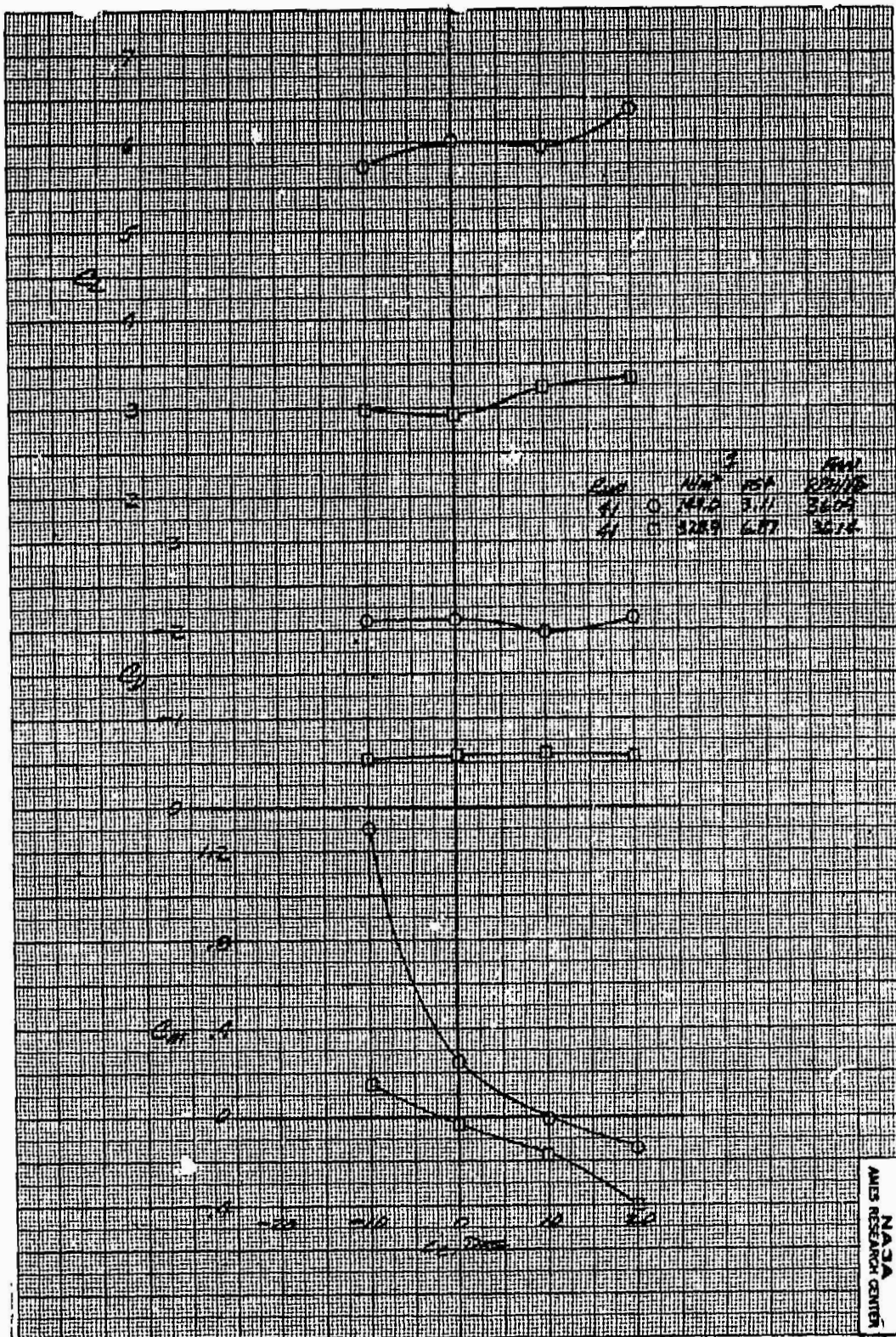
(a) $\alpha_u = 0°$

Figure 21.- The effect of tail incidence on the longitudinal aerodynamic characteristics with three fans operating; $\delta_{cn} = 71°$, $\beta_v = 55°$, $\delta_f = 15°$, $\delta_{ail} = 10°$, $\beta = 0°$, $\delta_R = 0°$.

72
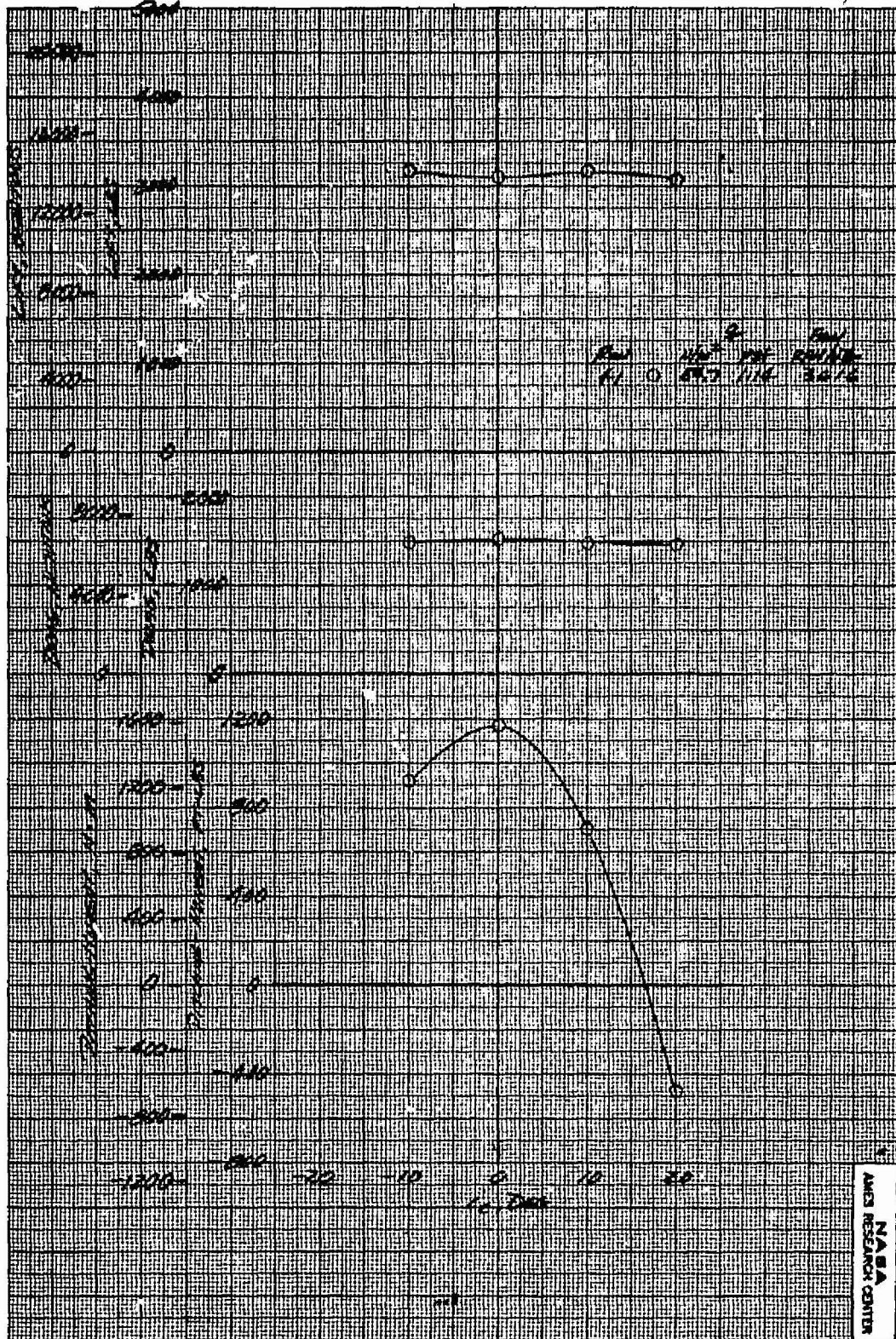
(b) $\alpha_u = 0°$

Figure 21.- Concluded.

73
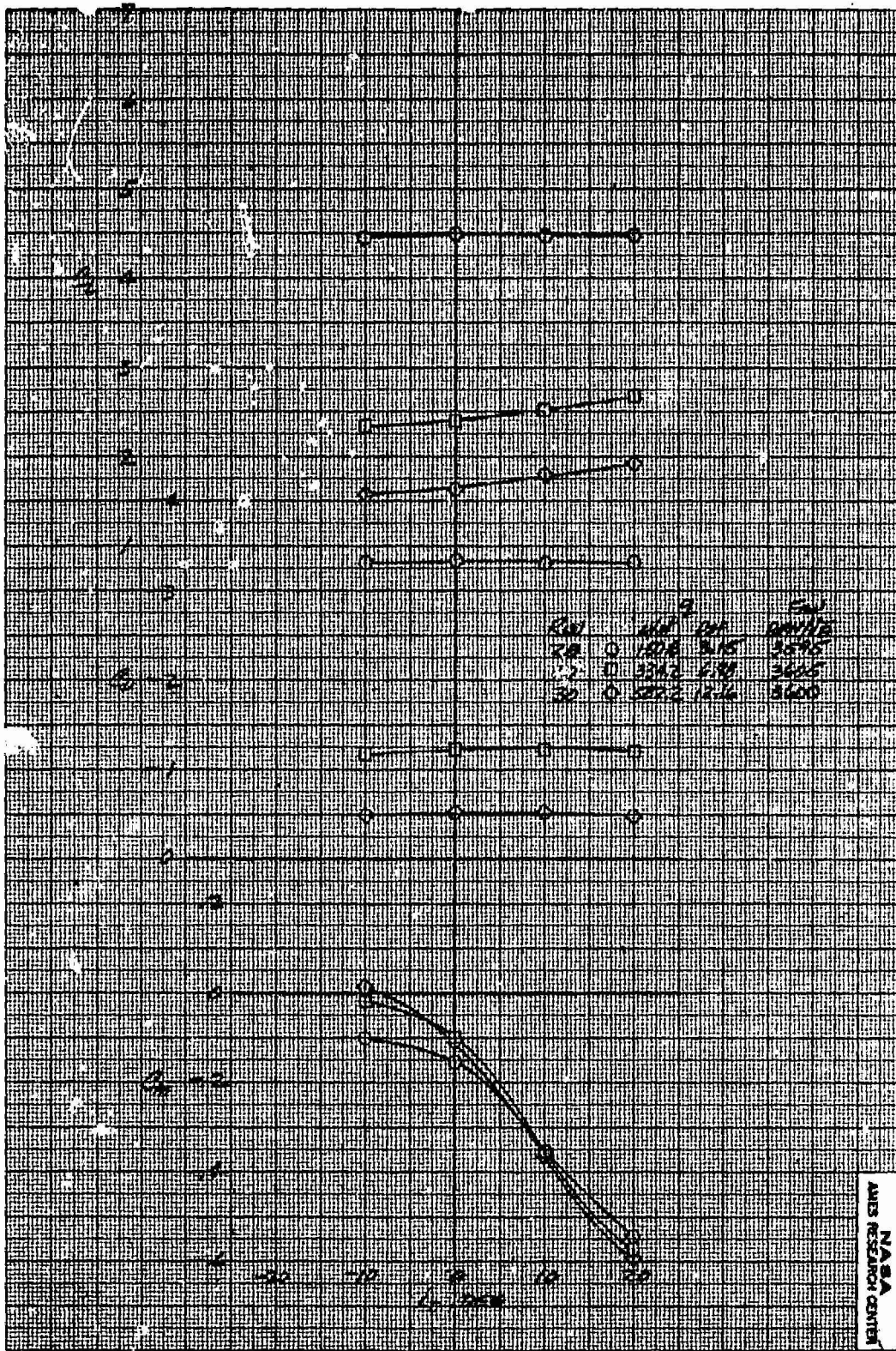
(a) $\alpha_u = 0°$

Figure 22.- The effect of tail incidence on the longitudinal aerodynamic characteristics with three fans operating; $\delta_{cn} = 56°$, $\beta_v = 43°$, $\delta_f = 15°$, $\delta_{ail} = 10°$, $\beta = 0°$, $\delta_R = 0°$.

74
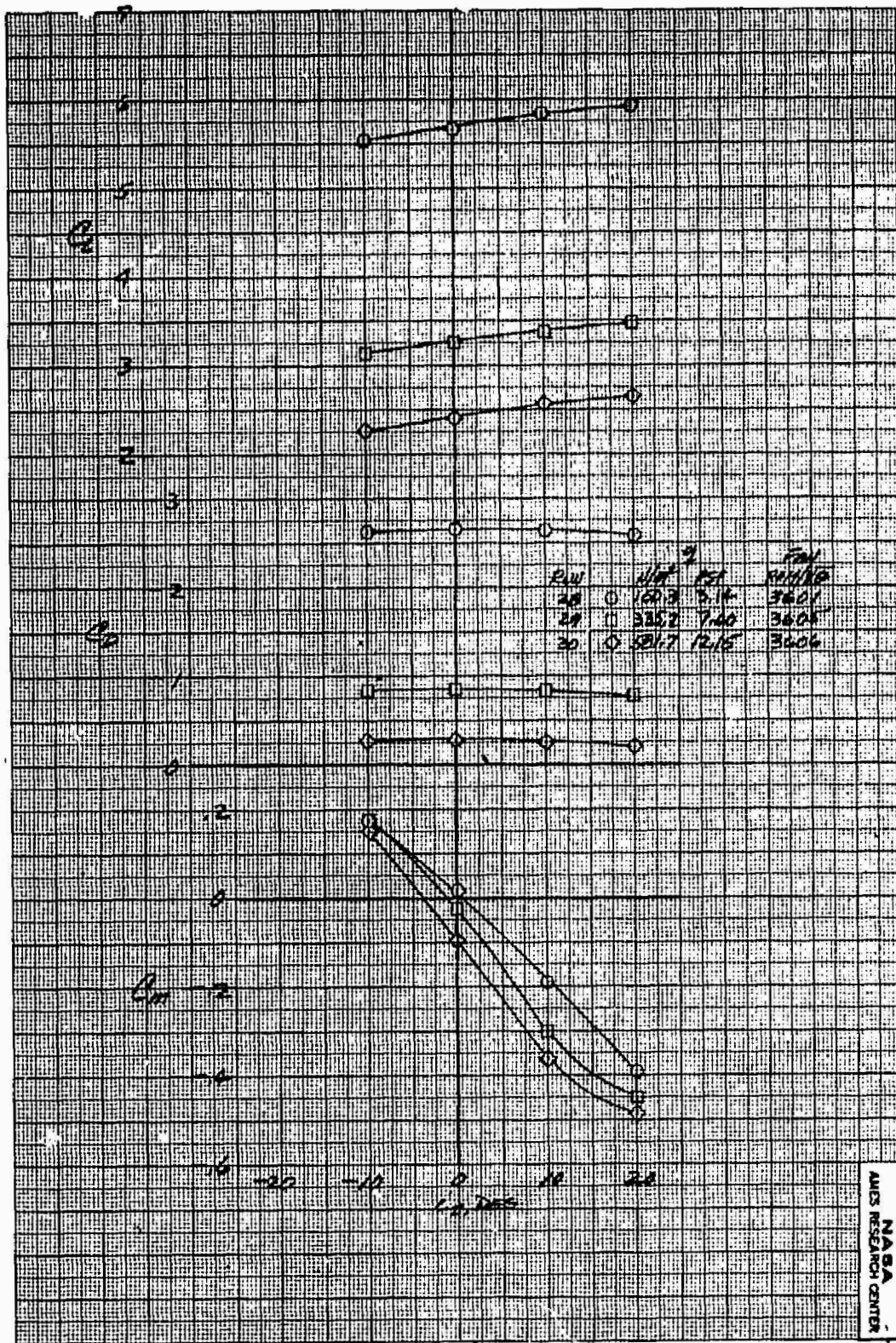
(b) $\alpha_u = 8°$

Figure 22.- Continued.

75
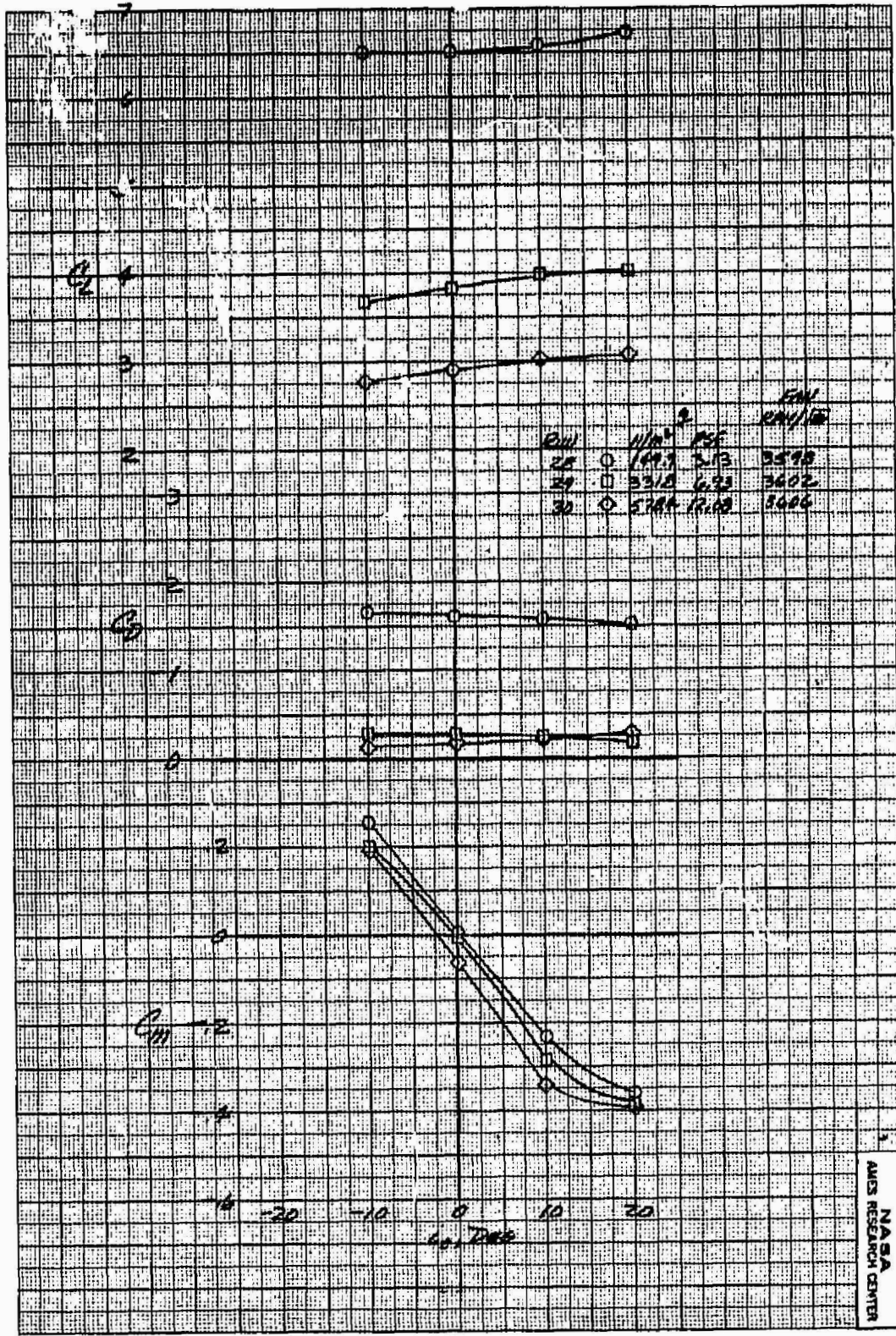
(c) $\alpha_u = 16°$

Figure 22.- Concluded.

76
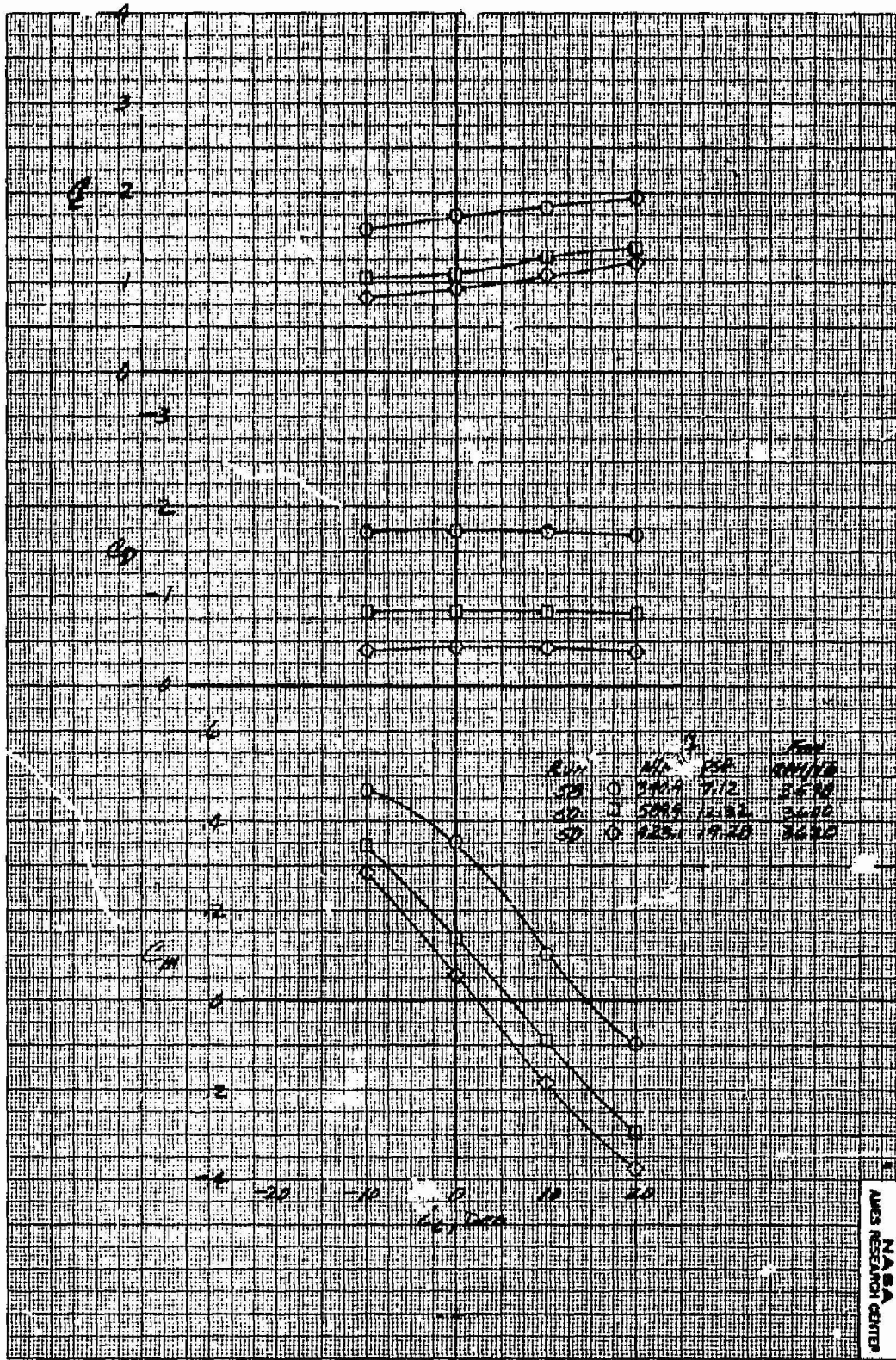
Figure 23.- The effect of tail incidence on the longitudinal aerodynamic char-
acteristics with three fans operating; $\delta_{cn} = 38°$, $\beta_v = 43°$, $\alpha_u = 0°$,
$\delta_f = 15°$, $\delta_{ail} = 10°$, $\beta = 0°$, $\delta_R = 0°$.
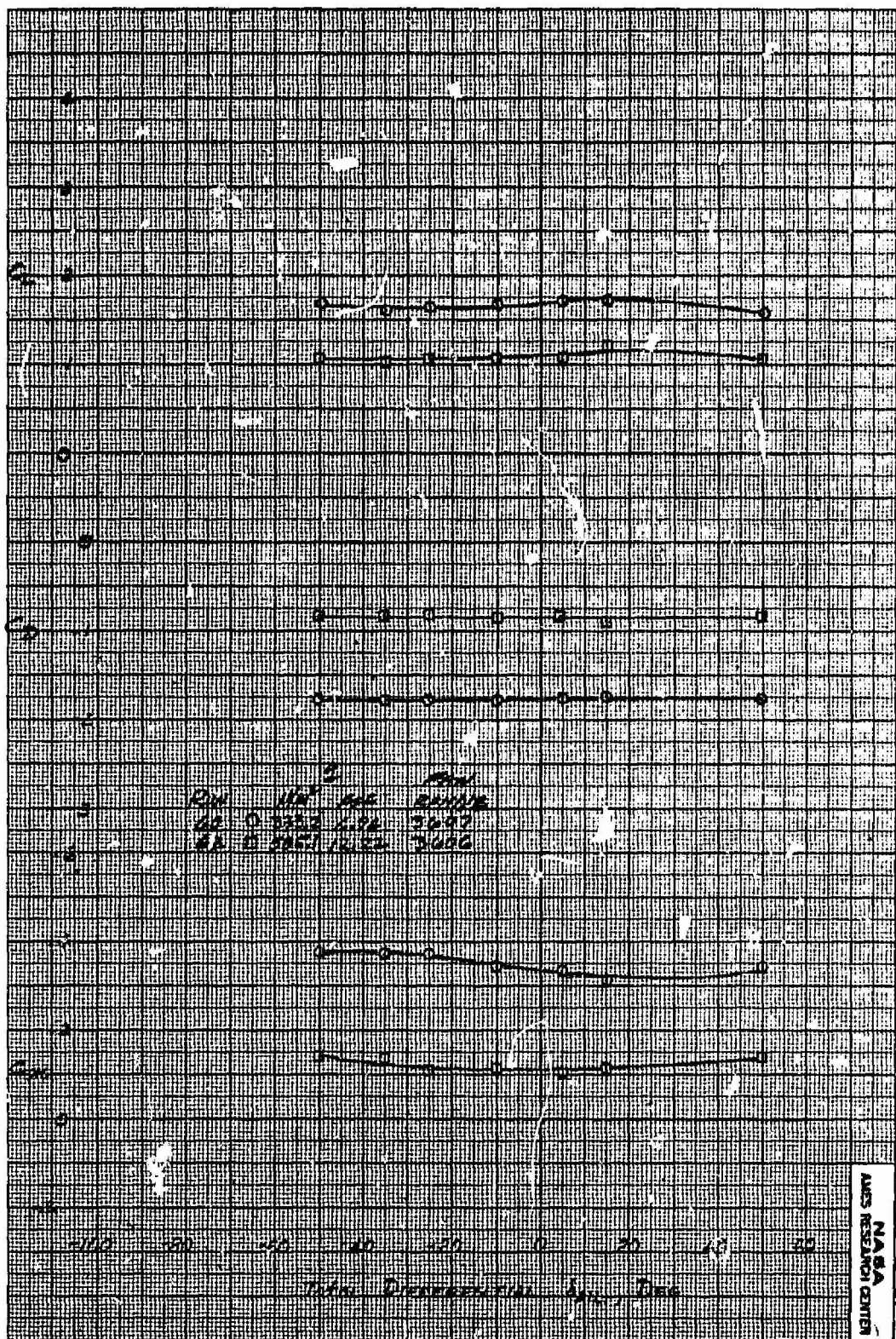
(a) Longitudinal characteristics

Figure 24.- The effect of total differential aileron deflection on the model aerodynamic characteristics with three fans operating; $\delta_{cn} = 38°$, $\beta_v = 43°$, $\delta_f = 15°$, $i_t = 0°$, $\beta = 0°$, $\delta_R = 0°$, $\alpha_u = 0°$.
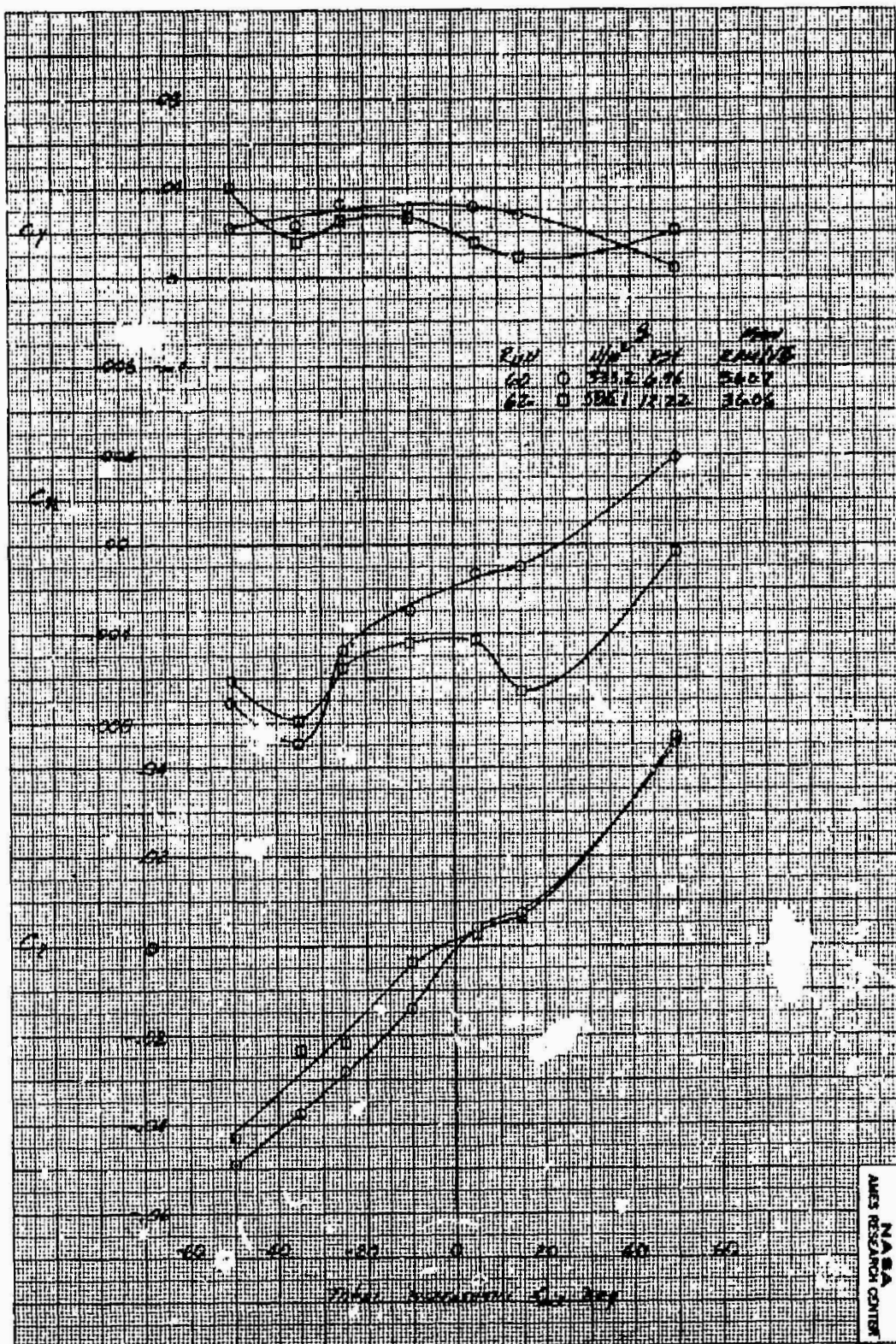
(b) Lateral characteristics

Figure 24.- Concluded.
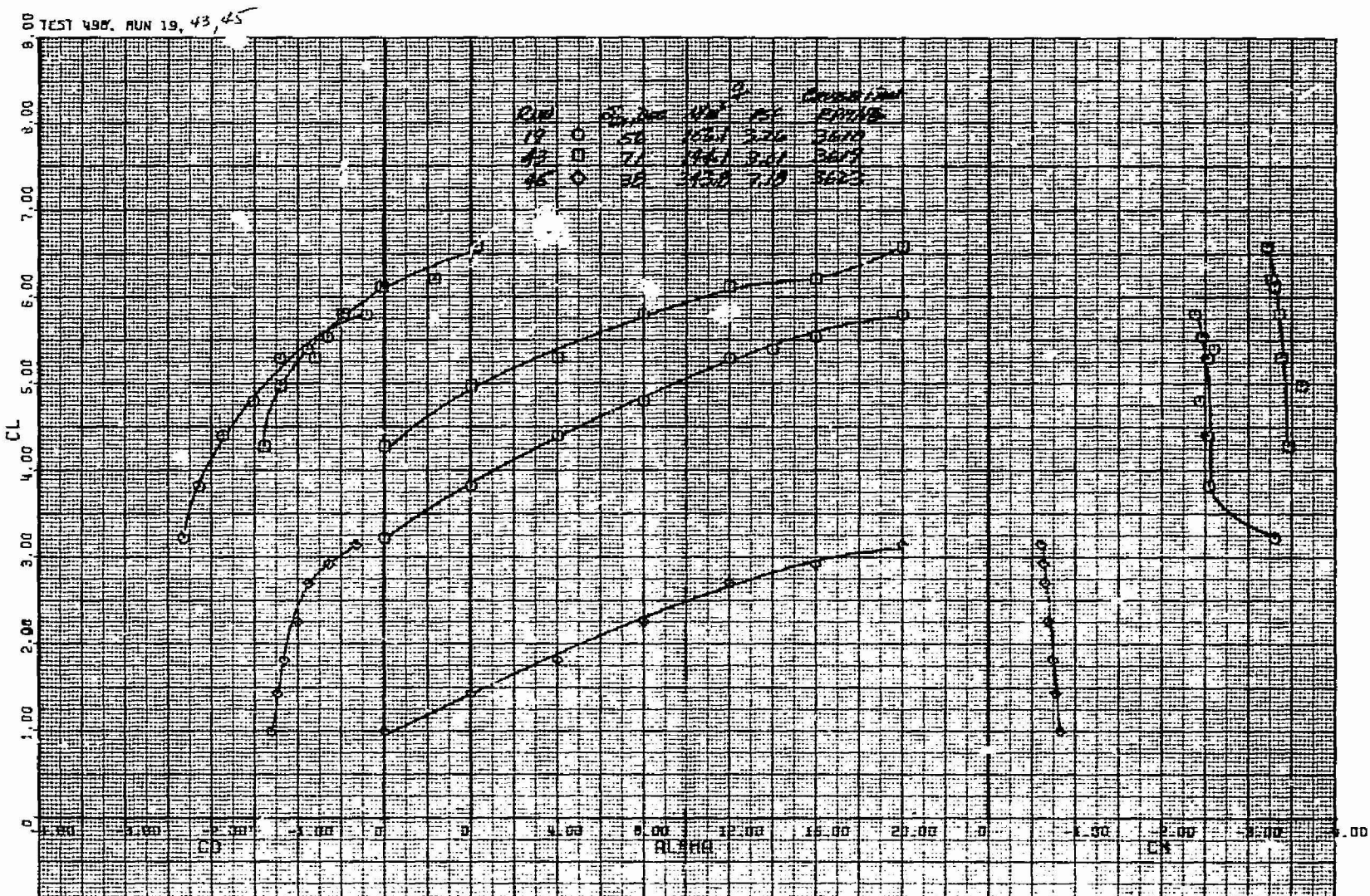
(a) δ_{cn} = variable

Figure 25.- Longitudinal characteristics of the model with the lift/cruise fan exit nozzles deflected to discrete positions, forward fan inlet covered and exit louvers at $\beta_v = 0°$, $\delta_f = 15°$, $\delta_{ail} = 10°$, $\beta = 0°$

81
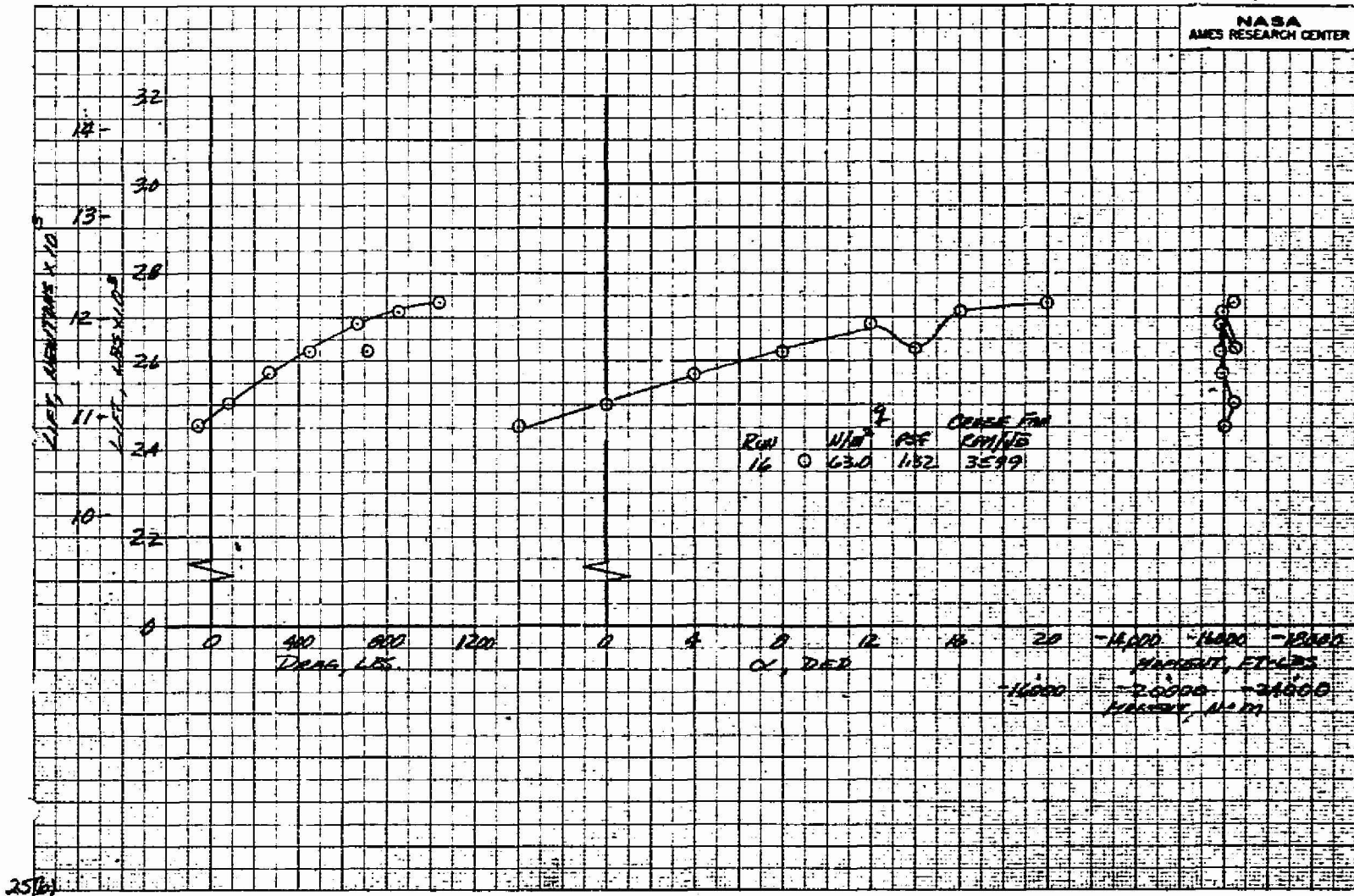
(b) $\delta_{cn} = 90°$

Figure 25.- Concluded.
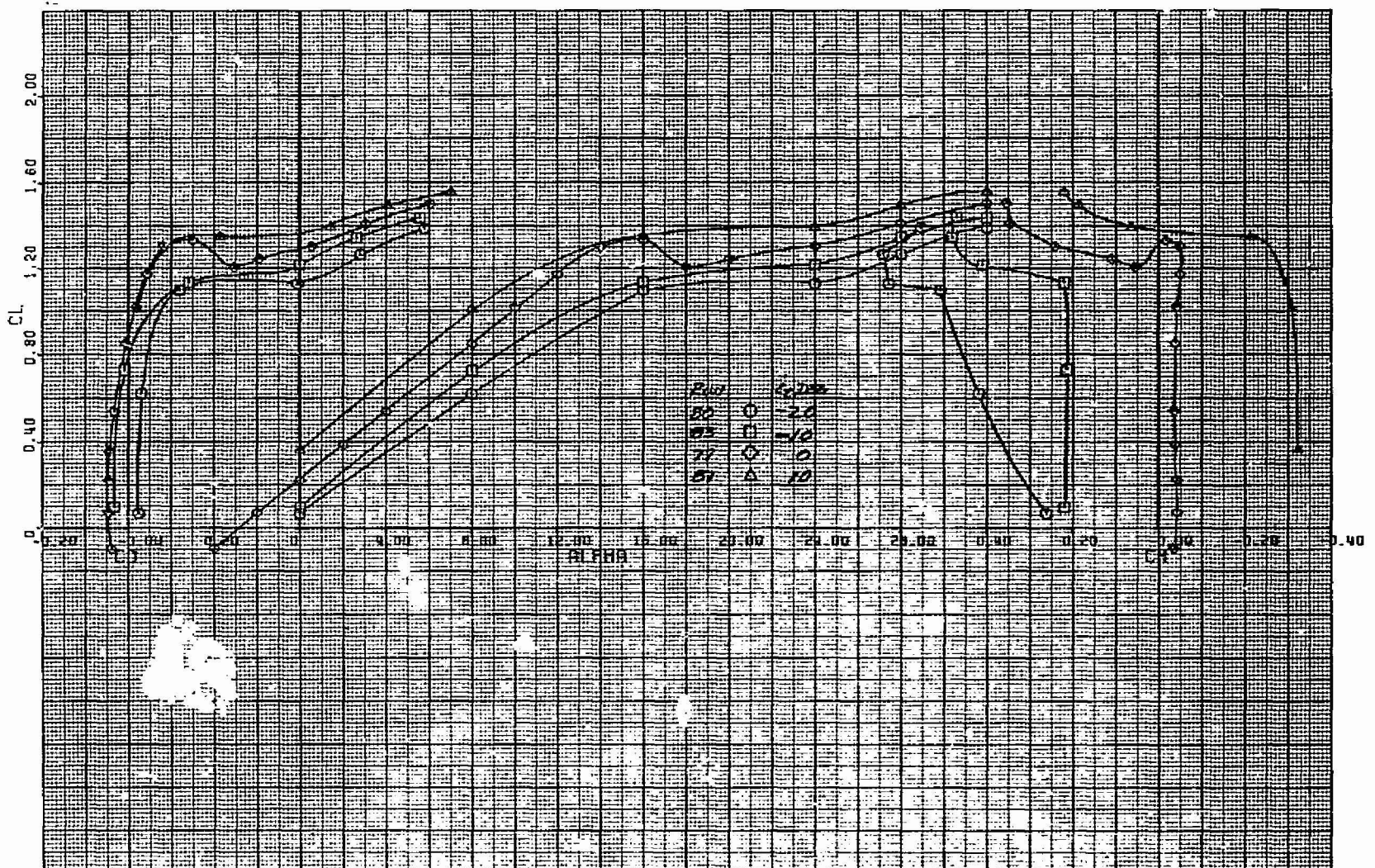
(a) Cruise fan rpm/$\sqrt{\theta}$ = 2717

Figure 26.- Longitudinal characteristics of the model in the cruise configuration; forward fan inlet and exit covered, $\delta_{cn} = 0°$, $\delta_f = 0°$, $\delta_{ail} = 0°$, $\beta = 0°$, $\delta_R = 0°$, q = 1638.5 N/m^2 (34.22 psf).

83

(b) Cruise fan rpm/$\sqrt{\theta}$ = 2158

Figure 26.- Continued.
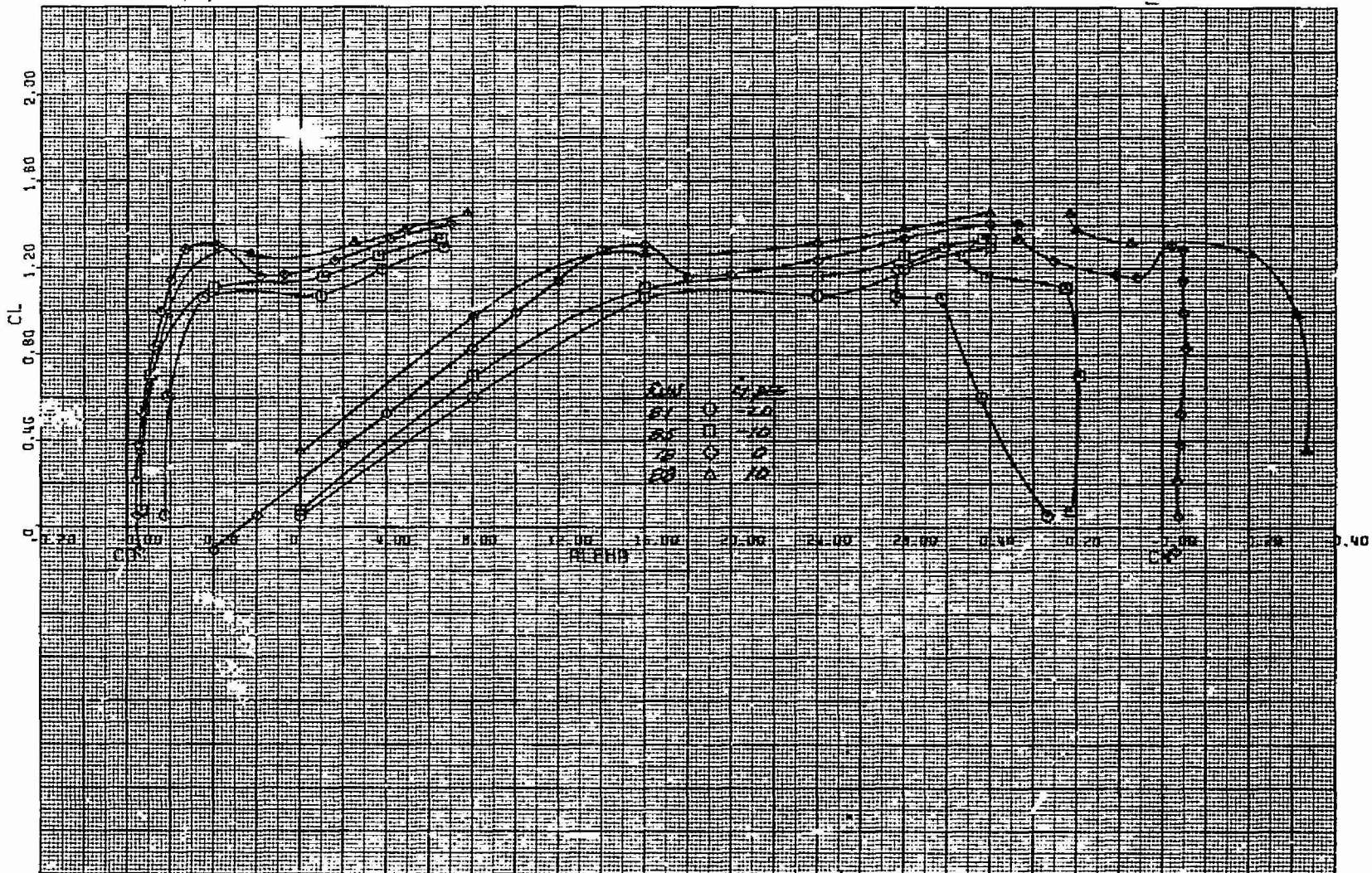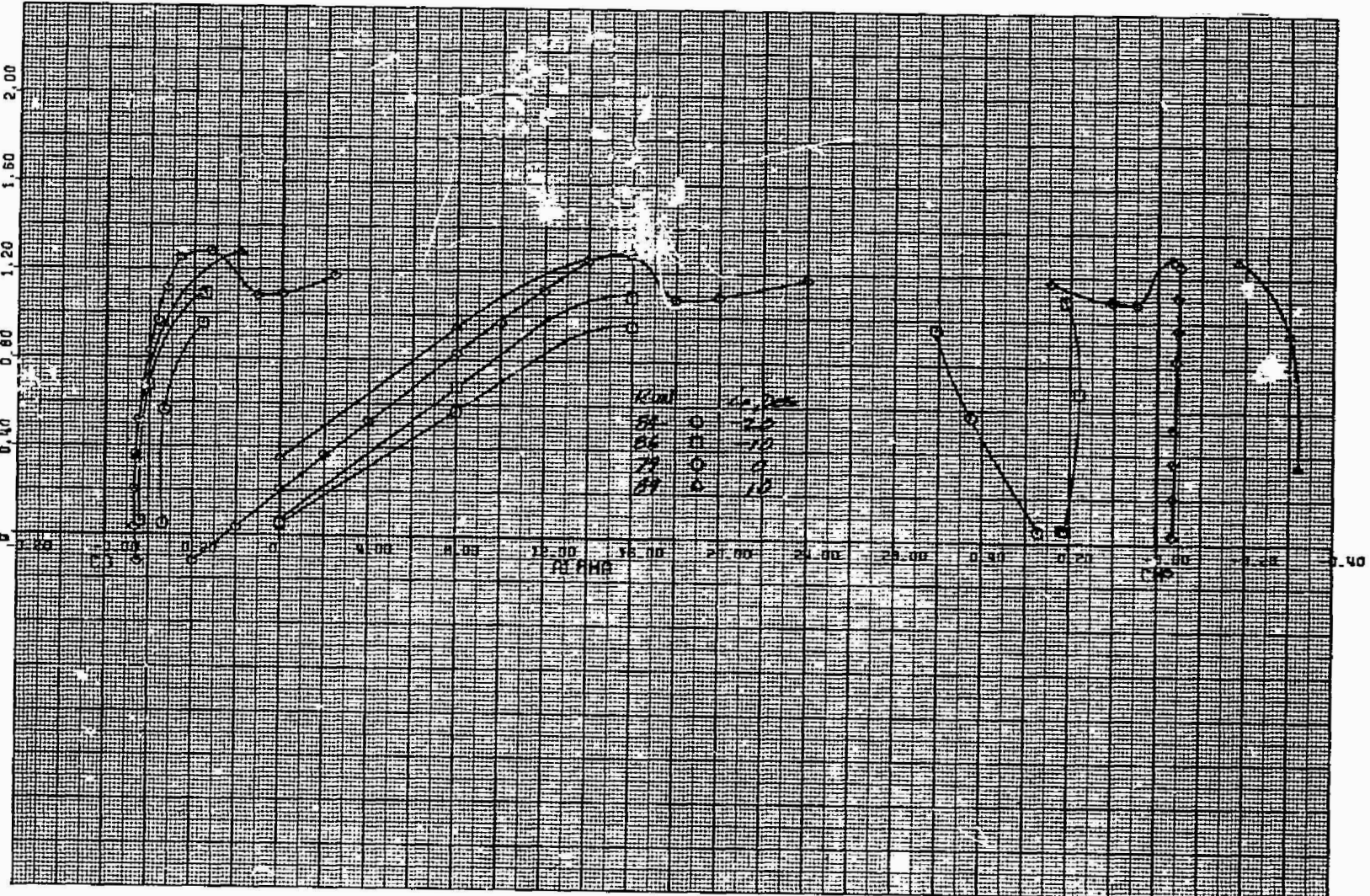
(c) Cruise fan rpm/$\sqrt{\theta}$ = 1599

Figure 26.- Concluded.
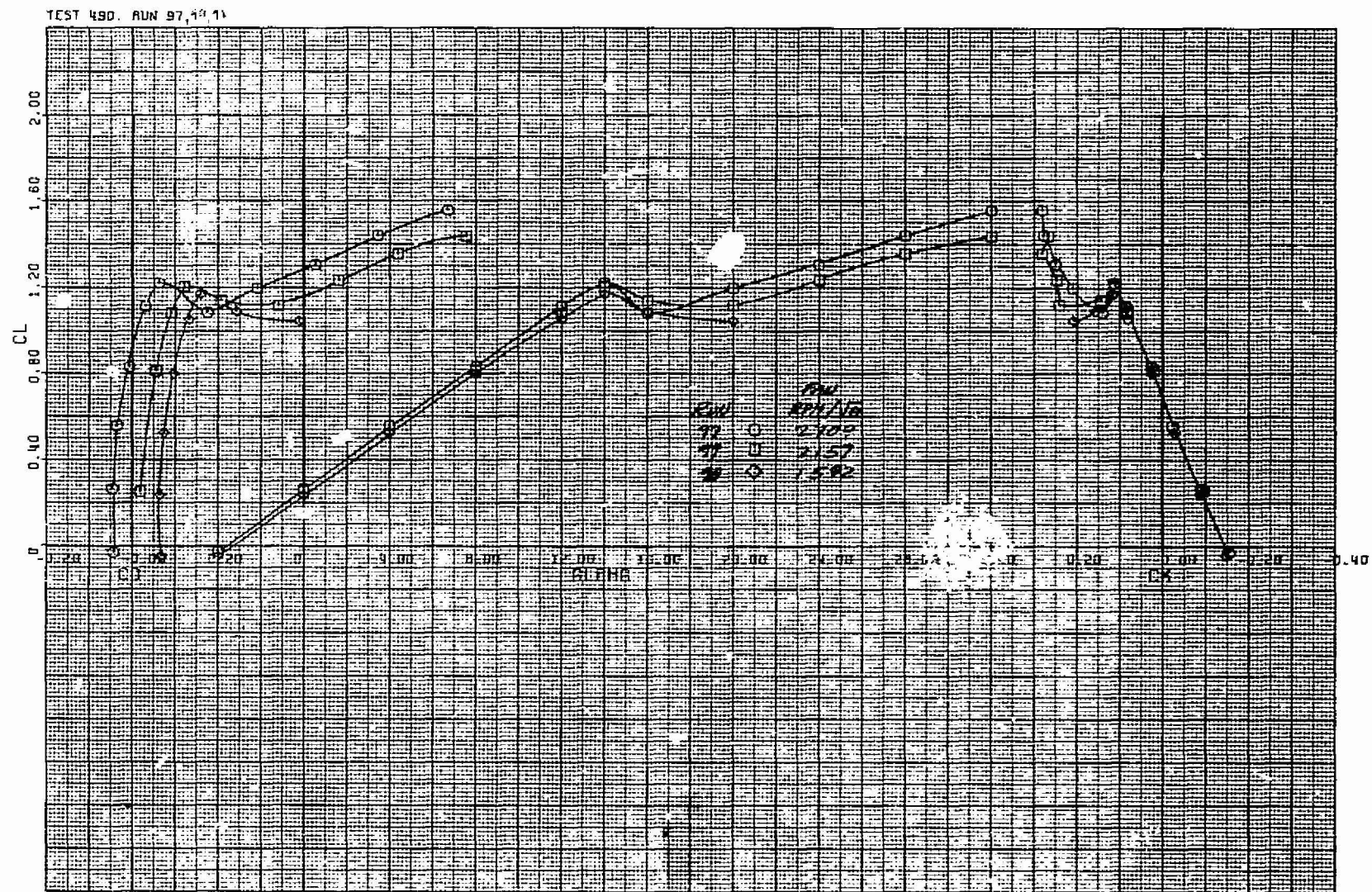
Figure 27.– Longitudinal characteristics of the model in the cruise configuration with the horizontal tail off; forward fan inlet and exit covered, $\delta_{cn} = 0°$, $\delta_f = 0°$, $\delta_{ail} = 0°$, $\beta = 0°$, $\delta_R = 0°$, $q = 1638.0$ N/m^2 (34.21 psf).
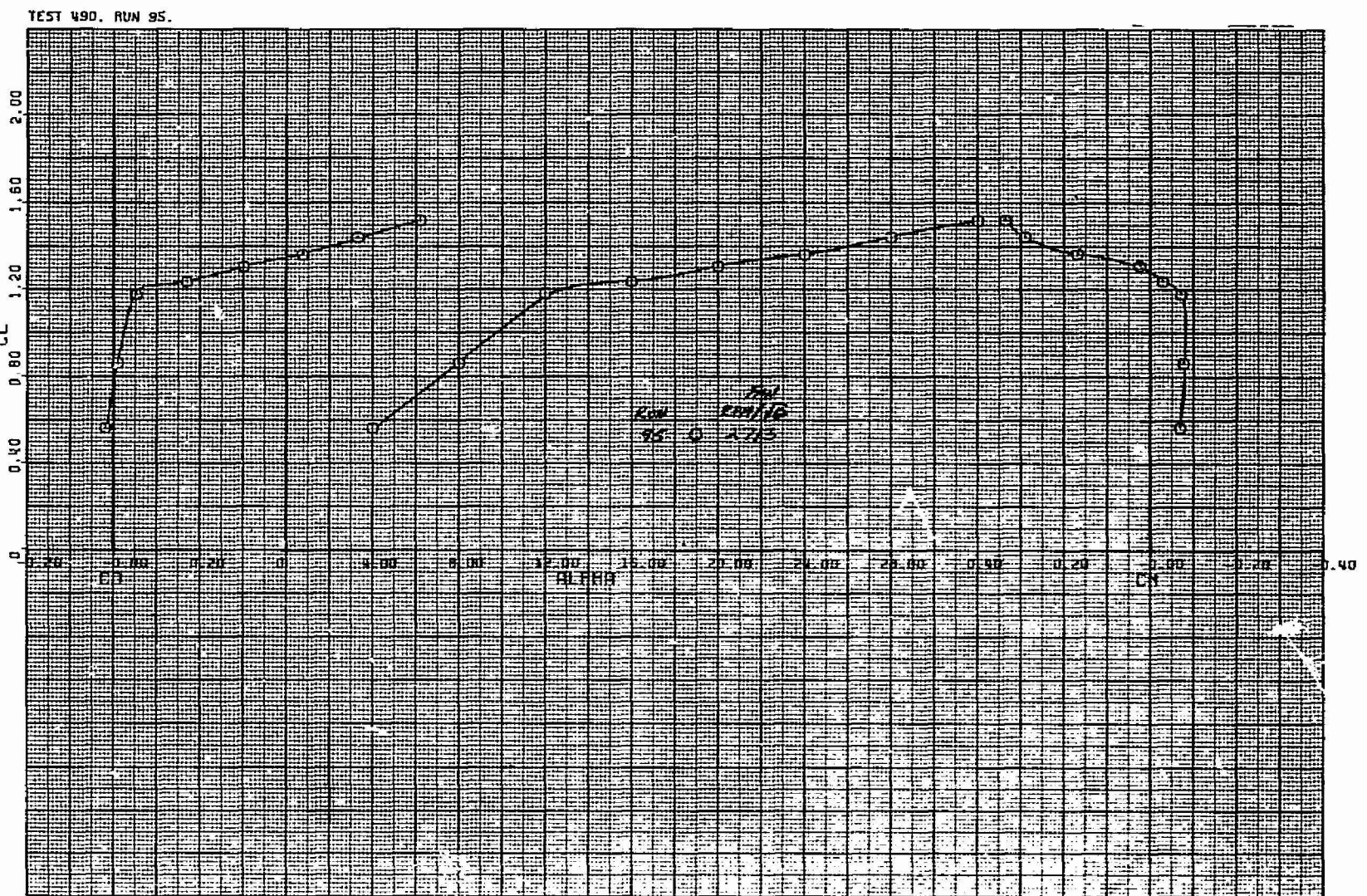
(a) Longitudinal characteristics

Figure 28.— Aerodynamic characteristics of the model with sideslip of 8°; forward fan inlet and exit covered, $\delta_{cn} = 0°$, $\delta_f = 0°$, $\delta_{ail} = 0°$, $i_t = 0°$, $\delta_R = 0°$, $q = 1638.9$ N/m^2 (er.23 psf).
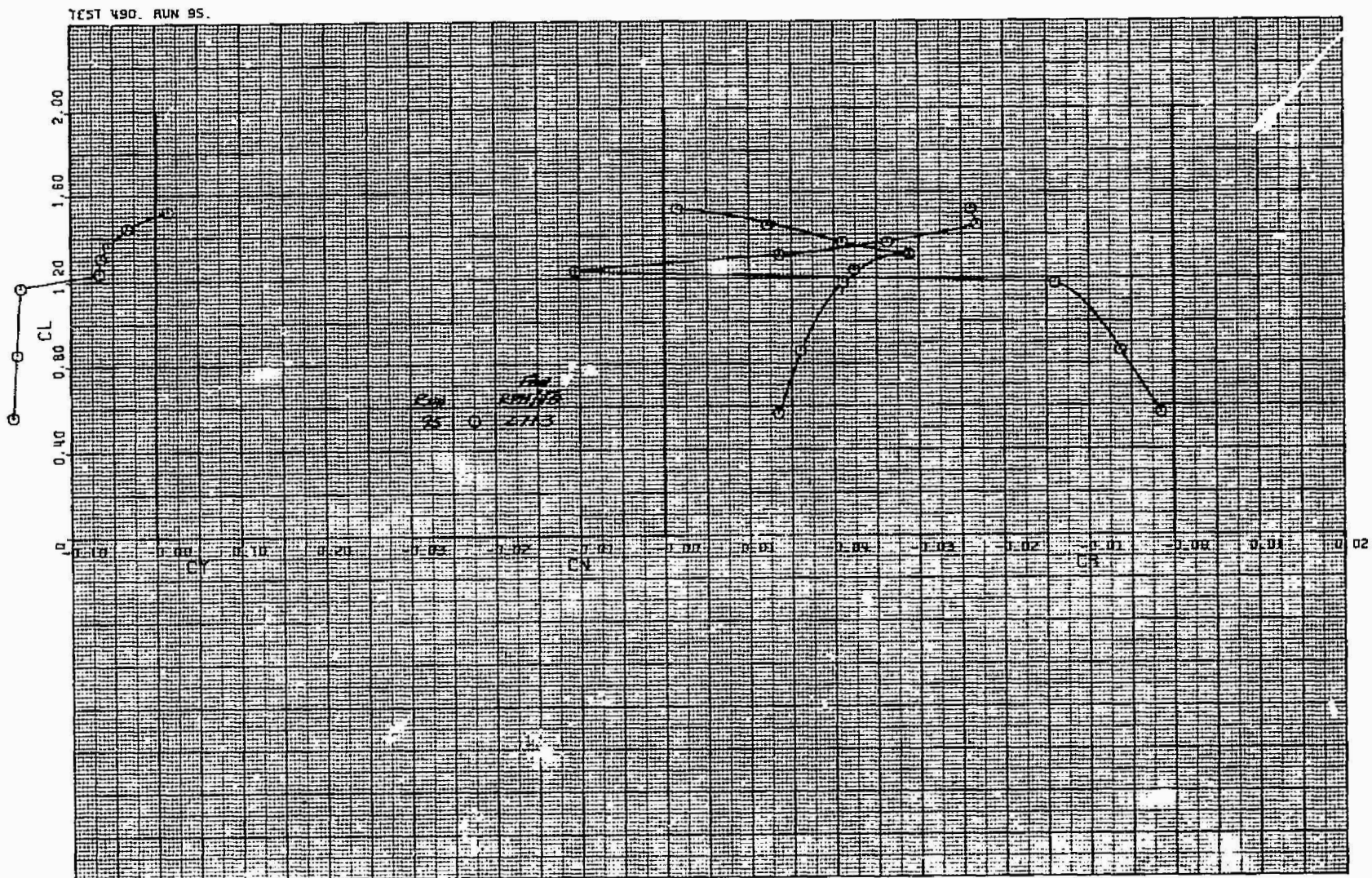
(b) Lateral characteristics

Figure 28.- Concluded.

87
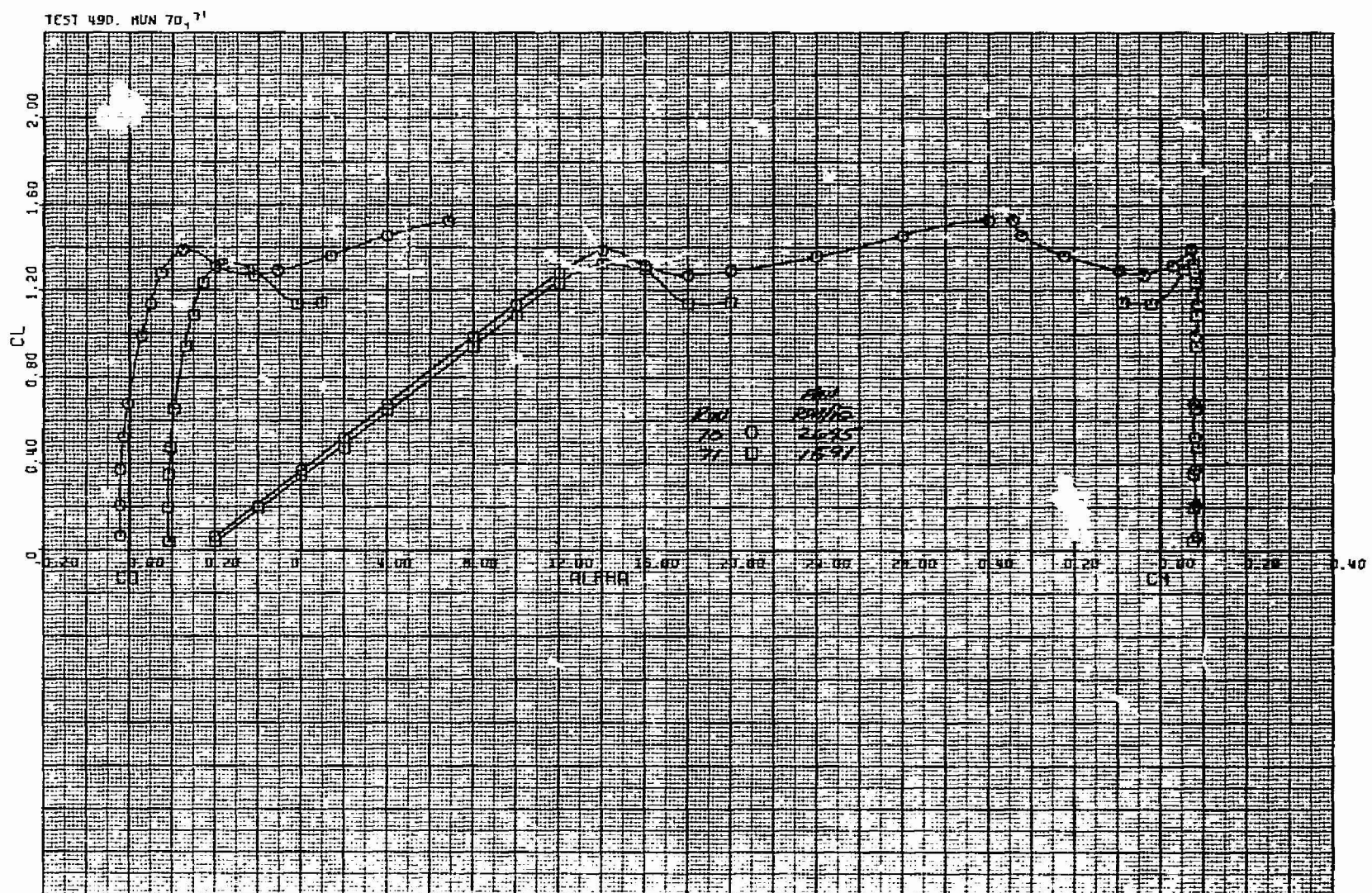
Figure 29.— Longitudinal characteristics of the model with the flaps and ailerons deflected; δ_f = 15°, δ_{ail} = 10°, forward fan inlet covered and with the exit louvers at ℓ_v = 0°, δ_{cn} = 0°, β = 0°, i_t = 0°, δ_R = 0°, q = 1639.5 N/m² (34.24 psf).
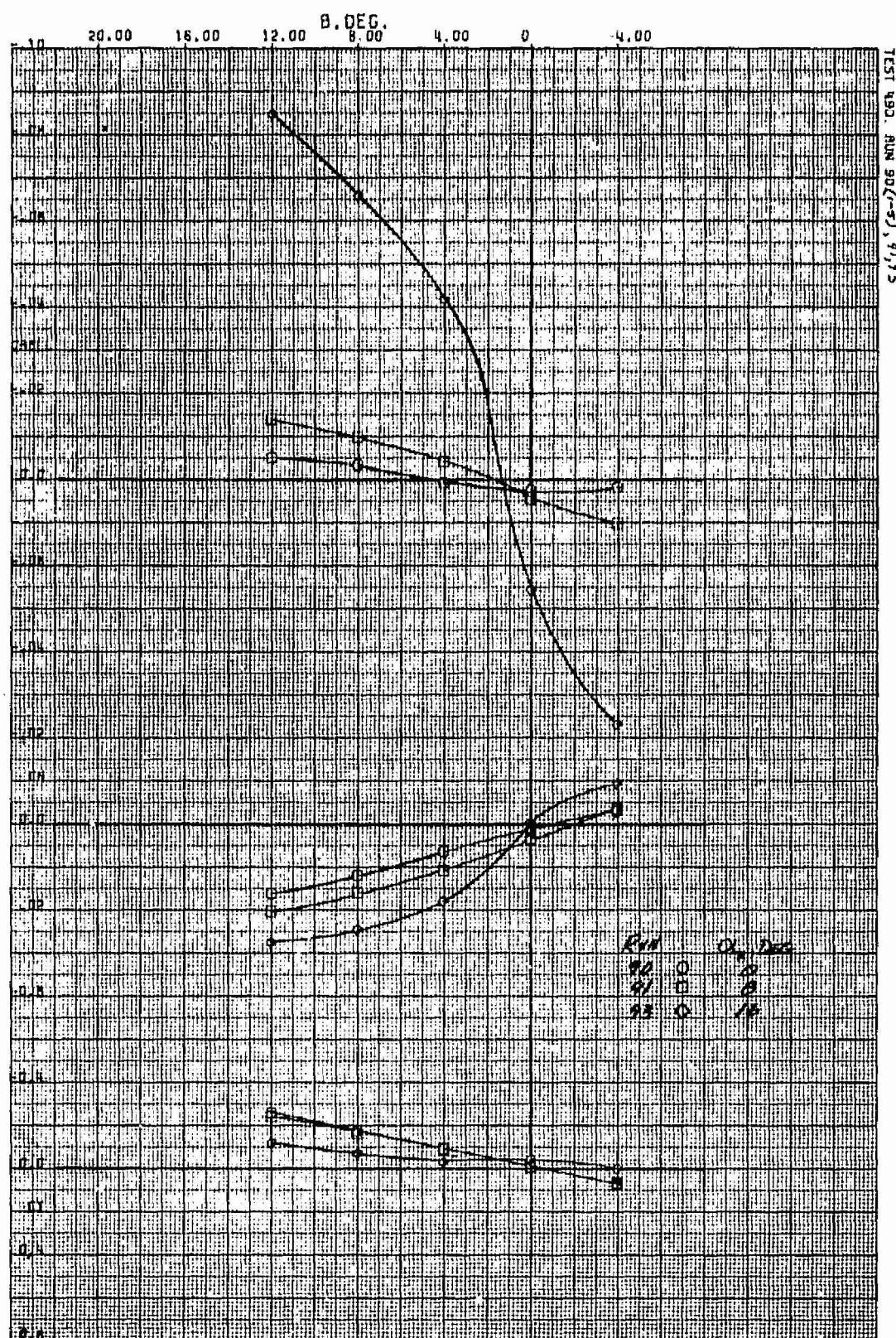
(a) Cruise fan rpm/$\sqrt{\theta}$ = 2712

Figure 30.- Variation of side-force, yawing-moment, and rolling-moment coeffi-
cients with sideslip; forward fan inlet and exit covered, $\delta_{cn} = 0°$, $\delta_f = 0°$,
$\delta_{ail} = 0°$, $i_t = 0°$, $\delta_R = 0°$, q = 1640.4 N/m² (34.26 psf).
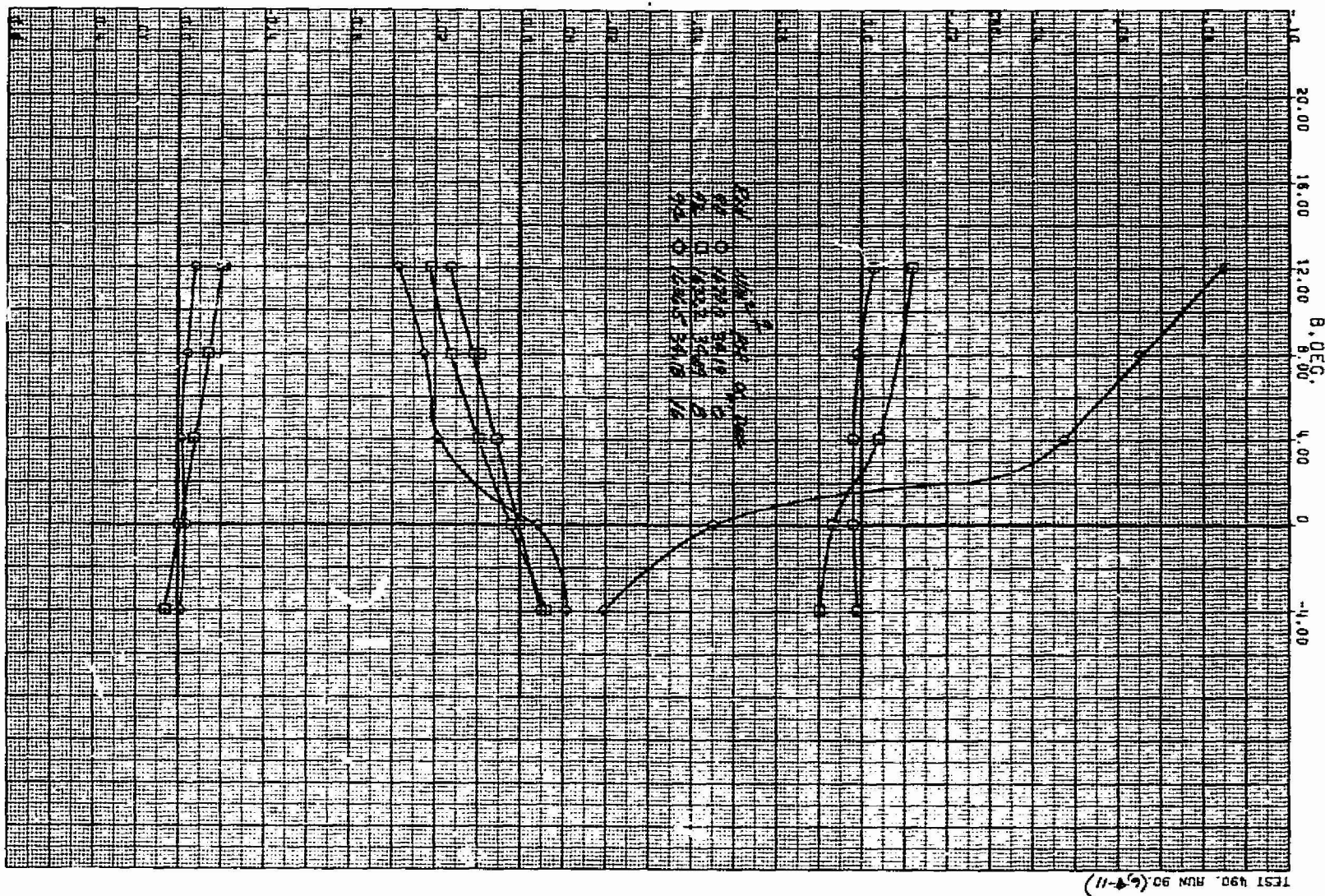
(b) Cruise fan rpm/$\sqrt{\theta}$ = 1615

Figure 30.- Concluded.